

INVESTIGATION OF SWEAT BIOMARKERS FOR REAL-TIME REPORTING OF  
INFECTION AND INFLAMMATION USING WEARABLE SWEAT SENSOR

by

Badrinath Jagannath

APPROVED BY SUPERVISORY COMMITTEE:

---

Shalini Prasad, Chair

---

Sriram Muthukumar

---

Shashank Sirsi

---

Soudeh Khoubrouy

Copyright 2021

Badrinath Jagannath

All Rights Reserved

To my parents, my brother, and my late grandmother

INVESTIGATION OF SWEAT BIOMARKERS FOR REAL-TIME REPORTING OF  
INFECTION AND INFLAMMATION USING WEARABLE SWEAT SENSOR

by

BADRINATH JAGANNATH, BTECH, MS

DISSERTATION

Presented to the Faculty of  
The University of Texas at Dallas  
in Partial Fulfillment  
of the Requirements  
for the Degree of

DOCTOR OF PHILOSOPHY IN  
BIOMEDICAL ENGINEERING

THE UNIVERSITY OF TEXAS AT DALLAS

December 2021

## ACKNOWLEDGMENTS

I would like to thank my advisor, Dr. Shalini Prasad, for supporting me throughout my PhD program. I am extremely grateful to her for giving me opportunities to work on several sponsored projects that made me an integral part of the Biomedical Microdevices and Nanotechnology lab (BMNL). I have received immense support from her and I am very grateful to her for always reminding me that there is light at the end of the tunnel. I would like to express my gratitude to Dr. Sriram Muthukumar for being a fascinating mentor. I thoroughly enjoyed having very strong technical discussions with him. He has always encouraged me to perform better.

I am thankful to my committee members, Dr. Shashank Sirsi and Dr. Soudeh Khoubrouy, for being a part of my committee. I would like to acknowledge the sponsors from Texas Instruments, BARDA, and Crohn's & Colitis Foundation for funding and supporting the projects I have worked on at BMNL. I would like to thank Dr. Sita Bopanna for her support with the clinical studies. I would like to thank all my co-authors for collaborating on various projects. I have thoroughly enjoyed working with them. I would like to specially thank Dr. Rujuta Munje and Dr. Kai-Chun Lin for all the technical discussions. I am extremely grateful to my best buddies in the lab, Ambalika Tanak and Ashlesha Bhide, for being my sounding board in the lab always. It has truly been an honor to work with them.

I would like to express my sincere gratitude to all my teachers for creating a lasting impact on science. I am sincerely thankful to three people, my grandmother, Krishna and Harini for motivating me to pursue a career in Biomedical Engineering. I would like to thank my best

friends, Bindu Bandlamudi, Akshay Pallerla, and Shravan Kumar for always being patient with me. I would like to thank Gulvaiz Khan for being so supportive during my stay here in Dallas.

I am extremely grateful to my brother, Dwaraka, for inculcating the value of pursuing Science. It was his constant support, interactions and conversations that made me aspire higher. Finally, I am eternally grateful to my parents for all their sacrifices, patience, and encouragement. I couldn't have reached this far without their support. I am extremely grateful to them for all the values and being a true inspiration.

November 2021

INVESTIGATION OF SWEAT BIOMARKERS FOR REAL-TIME REPORTING OF  
INFECTION AND INFLAMMATION USING WEARABLE SWEAT SENSOR

Badrinath Jagannath, PhD  
The University of Texas at Dallas, 2021

Supervising Professor: Shalini Prasad

Inflammatory biomarkers are modulated due to an infection or inflammatory trigger. Cytokines are inflammatory biomarkers that orchestrate the manifestation and progression of an infection/inflammatory event. Hence, non-invasive, real-time monitoring of cytokines can be pivotal in assessing the progression of infection/inflammatory event. However, real-time monitoring of biomarkers is not feasible with the current technology as most of them rely on blood-based detection. Continuous monitoring of host immune markers in sweat can aid in real-time monitoring of the immune status. This dissertation demonstrates a wearable SWEATSENSOR device that can track the levels of immune cytokine markers in real-time from passively expressed sweat. The developed device is of a watch form-factor that can be worn on the arm to reliably track the biomarker response from low volumes of sweat ( $\sim 1 \mu\text{L}$ ) and the biomarker levels can be monitored in real-time. The developed SWEATSENSOR device was validated for reliably reporting the levels of several cytokines and chemokines. Additionally, this work presents a thorough validation on the presence of certain critical infection and inflammatory markers such as interferon-inducible protein (IP-10) and tumor necrosis factor-

related apoptosis-inducing ligand (TRAIL), C-reactive protein that make it feasible for using sweat as a biofluid for actively monitoring the health status. Additionally, human subject clinical studies demonstrate the feasibility of non-invasively tracking infections such as influenza from sweat. Such a wearable device can offer significant strides in improving prognosis and provide personalized therapeutic treatment for several inflammatory/infectious diseases.

## TABLE OF CONTENTS

ACKNOWLEDGMENTS .....	v
ABSTRACT.....	vii
LIST OF FIGURES .....	xii
CHAPTER 1 INTRODUCTION .....	1
1.1    Wearable Biosensors for point-of-care applications.....	1
1.2    Sweat as biofluid for wearable biosensing.....	2
1.3    Innovation and Novelty.....	3
CHAPTER 2 DESCRIPTION AND CHARACTERIZATION SWEATSENSER DEVICE .....	5
2.1    Prior Publication .....	5
2.2    Description of SWEATSENSER .....	5
2.3    SWEATSENSER electronic reader design.....	7
2.4    Material Characterization of SWEATSENSER.....	8
2.5    SWEATSENSER functional electrode characterization .....	10
2.6    Electrochemical Characterization of SWEATSENSER .....	11
2.7    Detection modality of SWEATSENSER.....	12
2.8    Analytical algorithm for real-time detection of biomarker levels .....	13
CHAPTER 3 DETECTION OF INFECTION FROM SWEAT USING SWEATSENSER DEVICE .....	15
3.1    Prior Publication .....	15
3.2    Abstract.....	15
3.3    Introduction.....	16
3.4    Materials & Methods .....	19
3.5    Results and Discussion .....	23
3.5.1    Characterization of SWEATSENSER .....	23
3.5.2    Evaluation of SWEATSENSER analytical performance metrics.....	27
3.5.3    Pre-Clinical utility of SWEATSENSER on healthy subjects .....	30
3.5.4    On-body testing of cytokines in passive eccrine sweat .....	32

3.5.5 Clinical utility of SWEATSENSE for infection detection from eccrine sweat	36
3.6 Conclusion .....	39
3.7 Acknowledgments.....	40
<b>CHAPTER 4 NOVEL APPROACH TO TRACK THE LIFECYCLE OF INFLAMMATION FROM CHEMOKINE EXPRESSION TO INFLAMMATORY PROTEINS IN SWEAT .....</b>	<b>41</b>
4.1 Abstract.....	41
4.2 Introduction.....	41
4.3 Pathway of IP-10 and TRAIL .....	43
4.4 Materials and Methods.....	45
4.5 Results and Discussion .....	47
4.5.1 Characterization of Capture probe antibodies.....	47
4.5.2 SWEATSENSE device metrics for IP-10, TRAIL, CRP measurements.	48
4.5.3 Validation of IP-10, TRAIL and CRP in eccrine sweat of healthy cohort	54
4.5.4 On-body measurements in healthy human subjects using SWEATSENSE	57
4.6 Conclusion .....	59
4.7 Acknowledgements.....	60
<b>CHAPTER 5 SWEAT-BASED WEARABLE ENABLING TECHNOLOGY FOR REAL-TIME MONITORING OF IL-1B AND CRP AS POTENTIAL MARKERS FOR IBD.....</b>	<b>61</b>
5.1 Prior Publication .....	61
5.2 Abstract .....	61
5.3 Introduction.....	62
5.4 Materials and Methods.....	65
5.5 Results and Discussions .....	69
5.5.1 Demonstration of SWEATSENSE device for detection of IL-1 $\beta$ and CRP in passive sweat.....	69
5.5.2 Evaluation of sensor performance: repeatability and reproducibility studies	70
5.5.3 Comparison of performance of SWEATSENSE device with reference methods to report biomarker levels in sweat .....	73
5.5.4 Pre-clinical utility and continuous on-body measurements of IBD biomarkers in healthy human subjects.....	76
5.6 Conclusion .....	81

5.7	Acknowledgement .....	82
REFERENCES .....	86	
BIOGRAPHICAL SKETCH .....	94	

CURRICULUM VITAE

## LIST OF FIGURES

Figure 2.1. Schematic of sensing layers. Schematic was created in Biorender.....	5
Figure 2.2. Skin-SWEATSENSOR device interface, where, SWEATSENSOR is functionalized with specific antibodies to capture the study biomarkers. Schematic was created in Biorender.....	7
Figure 2.3. Architecture of the SWEATSENSOR electronic reader indicating various components used for transduction and processing of the biochemical interaction.....	8
Figure 2.4. A) EDX spectra of patch membrane and ZnO deposited on patch membrane. Carbon and oxygen peaks at 0.27 and 0.5 KeV respectively are observed due to the polymeric structure of porous patch. Upon deposition of Zinc oxide, a peak at 1 KeV corresponding to L-shell of Zinc with an increase in oxygen peak intensity and decrease of carbon peak is observed. B) SEM image of uniform deposition of ZnO on patch membrane. ....	8
Figure 2.5. XPS characterization of ZnO sensor surface pre- and post-functionalization of cross-linker. Zn and O peak-shifts from 1022.4 eV to 1023.9 eV and 532.2 eV to 534.2 eV respectively are observed due to Zn-S bonds. ....	9
Figure 2.6. Finite element analysis characterization of sensor. Electrode potential distribution between working and reference electrode signifying the uniform distribution of voltage across working electrode. Electrical current density distribution between working and reference electrode showing peaks at working electrode. ....	11
Figure 2.7. Stable electrochemical equilibrium potential between working and reference electrode.....	12
Figure 2.8. Schematic of the methodology implemented for training and prediction of levels of the biomarkers.....	13
Figure 3.1. Schematic of immunological cascading effects of inflammatory response. ....	17
Figure 3.2. FTIR spectra confirming conjugation of the antibodies on the sensor surface. ....	23

Figure 3.3. Characterization of SWEATSENSOR. (A-D) Binding efficiency determined through Kd values for cytokines (A: IL-6, B: IL-8, C: IL-10, D: TNF-a). (E-H) Spike and Recovery plots demonstrating ability to report concentrations reliably for cytokines in sweat (E: IL-6, F: IL-8, G: IL-10, H: TNF-a); Linear regression analysis was performed between ‘Actual’ and ‘Reported’ concentration and  $R^2 > 0.95$  was achieved for  $n \geq 3$  measures. (I-L) Selectivity and Specificity of SWEATSENSOR for target cytokine marker in sweat (I: IL-6, J: IL-8, K: IL-10, L: TNF-a); SWEATSENSOR demonstrates minimal (<2%) or no response to non-specific molecules, while is highly specific (>97%) to target biomarker. Data is represented as mean  $\pm$  SEM.....25

Figure 3.4. Analytical metrics of SWEATSENSOR. (A-E) Ability of SWEATSENSOR to reliably track biomarker levels during various stages of infection from early-stage pathogen attack to recovery. Temporal profiles of biomarkers during various stages of infection (Top part) and the corresponding levels reported by SWEATSENSOR is represented as whisker plot. The band with double-sided arrow (indicated in the top half of the graph) indicates time snapshot of cytokine profile during various stages of infection. Specifically, (A-C) demonstrates the SWEATSENSOR response tracking of cytokine markers during wellness to illness phase and (D, E) demonstrate the recovery phase which is illness to wellness. (F,G) Reproducibility of SWEATSENSOR demonstrated with Pro-inflammatory (F: IL-8) and Anti-inflammatory (G: IL-10) cytokines for  $n \geq 4$  sensors. (H, I) Time stability of SWEATSENSOR for (H: IL-8) and (I: IL-10) cytokines. RT refers to sensor incubated in room temperature without lyophilization and FD refers to freeze-dry (i.e. lyophilized sensor) for  $n=2$  measures. (J) Accuracy of SWEATSENSOR in reporting cytokine markers in sweat. Data is represented as mean  $\pm$  SEM Note: Lyophilized SWEATSENSERs were used for reproducibility and stability studies.....28

Figure 3.5. Validation of SWEATSENSOR with standard reference method for human subject samples. (A) PharmChek sweat patch worn by subject on arm. (B) Schematic of sweat sample collection using patch for correlation of SWEATSENSOR with ELISA. (C-F) Pearson’s Correlation between SWEATSENSOR and reference ELISA method with Pearson’s correlation coefficient  $r = 0.99$  for all biomarkers from  $n = 26$  healthy human subject measures. (G-J) Bland-Altman analysis between SWEATSENSOR and ELISA from  $n=26$  healthy human subject measures with a mean bias  $-1.99 \text{ pg mL}^{-1}$  IL-6 (G),  $-9.43 \text{ pg mL}^{-1}$  IL-8 (H),  $-0.5 \text{ pg mL}^{-1}$  IL-10 (I),  $0.55 \text{ pg mL}^{-1}$  TNF- $\alpha$  (J).....32

Figure 3.6. A. Temperature measured in three healthy subjects across varying time points. B. Monitoring of perspiration using realtive humidity (%RH) sensor for three healthy subjects measured at various time points.....34

Figure 3.7. On-body continuous monitoring of cytokines. (A, B, C) SWEATSENSE	.....	36
Figure 3.8. Serum to sweat IL-8 levels in healthy and Sick cohort. (A) Schematic of subjects recruited for serum to sweat correlation. (B) Details of vitals and illness of each individual in sick cohort. (C) SWEATSENSE device worn on hand by a subject recruited for the study. (D) Comparison of IL-8 levels between healthy(n=10) and sick cohort (n=5). The levels between serum to sweat are also compared for each subject. Statistical significance p<0.05 was achieved between healthy and sick cohort using ANOVA ( $\alpha=0.05$ ) in both serum and sweat. ....	.....	39
Figure 4.1. Pathophysiology of IP-10 and TRAIL due to an infection. (A) Schematic representation of IP-10 production due to an infection trigger from bacterial/viral pathogen. (B) Schematic representation of TRAIL production and apoptosis mechanism in cell line due to an infection trigger from bacterial/viral pathogen. ....	.....	44
Figure 4.2. (A-C) Electrophoretic mobility demonstrating stability of specific capture antibody and binding of target protein to antibody of IP-10, TRAIL and CRP in sweat buffer. (D-F) Zeta potential characterization demonstrating stability of antibody and binding of specific target protein to antibody of IP-10, TRAIL and CRP. The increasing magnitude of Zeta potential from blank buffer confirms the stability and charge of the antibody and protein. ....	.....	49
Figure 4.3. Electrochemical characterization of SWEATSENSE. (A-C) Nyquist response of SWEATSENSE for study markers (A) IP-10, (B) TRAIL and (C) CRP using non-faradaic electrochemical impedance spectroscopy. (D-F) Chronoamperometric response of SWEATSENSE for (D) IP-10 (E) TRAIL and (F) CRP in sweat. ....	.....	50
Figure 4.4. SWEATSENSE device metrics. (A-C) Binding efficacy determined using $K_d$ value through saturation-binding study for (A) IP-10, (B) TRAIL, (C) CRP. (D-F) Spike & Recovery response of SWEATSENSE for (D) IP-10, (E) TRAIL and (F) CRP. The data is presented as Mean $\pm$ SEM for n $\geq$ 4 measurements. ....	.....	51
Figure 4.5. SWEATSENSE specificity response. A) Sensor functionalized with IP-10 antibody was dosed with non-specific TRAIL (256 pg/mL) and low response is observed while, a high reactivity for specific IP-10 was achieved. B) Sensor functionalized with TRAIL antibody was dosed with non-specific IP-10 (256 pg/mL) and low response is observed while, a high reactivity for TRAIL was achieved.....	.....	52

Figure 4.6. SWEATSENSE performance metrics. (A, B) SWEATSENSE repeatability for (A) IP-10; (B) TRAIL demonstrating ability to differentiate normal and elevated concentrations. (C, D) Stability of SWEATSENSE demonstrating the signal response is retained over 4 weeks (C) IP-10; (D) TRAIL for spiked concentrations from 2- 200 pg/mL.....	55
Figure 4.7. Pre-clinical utility of SWEATSENSE in healthy cohort. (A,C,E) Box plots demonstrating (A) IP-10, (C) TRAIL and (E) CRP levels reported by SWEATSENSE and reference method. (B,D,F) Bland-Altman analysis signifying good agreement between SWEATSENSE and reference method for (B) IP-10, (D) TRAIL and (F) CRP with low mean Bias and all the points within $\pm 1.96$ S.D.....	57
Figure 4.8. On-body monitoring and validation of relationship between serum and sweat of study markers using SWEATSENSE. (A) SWEATSENSE device worn on wrist by a subject. (B) On-body continuous monitoring using SWEATSENSE demonstrating stable response of SWEATSENSE for IP-10 and TRAIL measured in two-hour intervals for total of 6 hours in passive eccrine sweat. (C) Serum to sweat levels comparison of IP-10 in healthy cohort. (D) Serum to sweat levels comparison of TRAIL in healthy cohort of n=13 subjects.....	59
Figure 4.9. Comparison of serum to sweat levels of CRP in healthy cohort.....	60
Figure 5.1. Schematic illustration of the challenges with the current testing methods and role of SWEATSENSE device that can be utilized to bridge the technological gaps in offering better management to IBD patients.....	65
Figure 5.2. Demonstration using sensor for the detection and quantification of cytokine inflammatory biomarkers in sweat A. IL-1 $\beta$ , B. CRP .....	70
Figure 5.3. Assessment of sensor performance metrics. SWEATSENSE demonstrates repeatable response for the same concentration spiked 4 times on the sensor (A, B). 5 batches of functionalized SWEATSENSEs stored for 1 month confirm that the sensor response does not reduce over time, confirming the reproducibility of SWEATSENSE (C, D). .....	72
Figure 5.4. Evaluation of sensor performance in comparison to reference ELISA method using linear correlation with a Pearson's correlation coefficient $r \geq 0.95$ in a cohort of 26 healthy subjects A. IL-1 $\beta$ , C. CRP and Bland-Altman analysis demonstrating good agreement between SWEATSENSE and reference method with mean bias -02.5 pg/mL for (B) IL-1 $\beta$ , and -3.9 pg/mL for (D) CRP.....	76

Figure 5.5. On-body Human subject testing for IL-1 $\beta$  A. SWEATSENSE response over 4 days demonstrating reliable reporting of levels without any drift, B. Demonstration of ability of SWEATSENSE device for continuous monitoring over 30 hours, C. IL-1 $\beta$  levels in 20 human subject measurements measured with an average of 28 pg/mL. A statistical insignificance of  $p>0.05$  was reported in healthy cohort.....79

# **CHAPTER 1**

## **INTRODUCTION**

There has been a lot of emphasis on personalized health monitoring recently. Technology advancements and new at-home diagnostic tests have played an essential role in disease detection, evaluation, and management. "Point-of-care testing" (POCT) performed at or near the patient's location - was a phrase used in the early 1980s, however such a system was first established in 1972. The progress in wearable diagnostics has opened plethora of opportunities for real-time continuous monitoring of vitals and physiological parameters to get active feedback on health status.

### **1.1    Wearable Biosensors for point-of-care applications**

There is a paradigm-shift in the health monitoring with the emergence of wearable devices revolutionizing health care by enabling continuous monitoring[1]. Wearables offer the capability to be worn from head to toe to measure various parameters[2]. Wearable sensors have attracted a great deal of interest with the launch of smartphones and other mobile devices, owing to their possibility of giving helpful insights about people's performance and health[3]–[5]. Early versions of wearables mobility and vital indications including steps, calories expended, and heart rate. In recent years, scientists have shifted their research focus from tracking physical activity to applying wearable devices for solving more challenging healthcare applications such as diabetes treatment and remote monitoring of older population[6]. In line with the objectives, significant advancement in wearable biosensors (WB) were made in the recent years. WBs are sensing devices worn as a watch, tattoo, glove that include a biological recognition component (such as

enzyme, antibody) as a functional element to detect a target marker. These biosensors integrate with mobile or portable electronic devices for enabling in vivo sensing, collection of data, and computation. WBSs are recognized to foster two-way communication between clinicians and patients. These technologies also allow for the non-invasive and real-time measurement of biochemical markers in human bodily fluids such as saliva, perspiration, skin, and tears.

Wearable monitoring technologies, which enable continuous, real-time monitoring of indicators relevant to a wearer's health and performance, can provide insights into dynamic biochemical processes in these biofluids. Such real-time monitoring can offer information on wellbeing and health, improve chronic condition management, and notify the user or medical experts of aberrant or unexpected conditions [7]. Despite rapid progress in wearable biosensor technology over the past 5 years, we are only at the beginning of understanding how wearable biosensor technologies can improve health and performance [8].

## **1.2     Sweat as biofluid for wearable biosensing**

The development of efficient screening techniques for the early recognition of clinical biomarkers in bodily fluids is critical for detecting illness and physiological characteristics that are indicative of prospective disease states swiftly. While some publications have shown the use of saliva[9], urine[10], tears[11], [12] for wearable sensing, they have their own limitations. The biggest challenge with salivary monitoring is the interference with microbes that can cause contamination[13]. On the other hand, tear fluid has fewer analytes which makes limited for wearable biosensing[8]. While, urinalysis can be means to monitor health condition, it is still not viable for wearable biosensing as it requires the calibration of analyte levels which relies on the

individuals hydration levels[8]. Among various biofluids, sweat is ideal for wearable sensing as it is readily available and does not require complex sampling. The widespread acceptance of wearable biosensor devices for sweat necessitates a thorough understanding of the biochemical makeup as well as the relationship to blood chemistry[14].

### **1.3 Innovation and Novelty**

Considering the advantages of sweat-based biosensing and the significance of real-time monitoring for patient-centric healthcare management, we developed a wearable SWEATSENSE device for real-time tracking of infection and inflammatory biomarkers in sweat. The advent of wearable technology-enabled hardware and software platforms has allowed the feasibility of sensor technologies for continuous monitoring of biomarkers in sweat. A vast majority of them are focused on ions (sodium, potassium, chloride), metabolites and small molecules (glucose, cortisol) from stimulated sweat. However, passively expressed sweat (i.e., sweat expressed without any external stimulation methods such as iontophoresis, exercise, etc.) is critical for measuring and correlating cytokines to that in circulation (serum). A stimulation event may be viewed as being synonymous to an inflammation event and therefore, may not be an actual representation of the infection/inflammatory event driven cytokine levels in circulation. Further, other limitations such as limited duration of sampling and limited volume from stimulated sweat can impede monitoring of cytokines [15]. Therefore, this dissertation demonstrates of a wearable SWEATSENSE technology platform that measures cytokine biomarkers in passively expressed eccrine sweat in quadruplex manner to distinguish between healthy cohort and sick cohort and has been analytically correlated with blood serum cytokine

levels. The developed SWEATSENSE technology was evaluated for infection monitoring such as influenza and for chronic diseases such as Inflammatory bowel disease.

## CHAPTER 2

### DESCRIPTION AND CHARACTERIZATION SWEATSENSER DEVICE

#### 2.1 Prior Publication

Badrinath Jagannath (B.J.), Kai-Chun Lin (K.C.L), Shalini Prasad (S.P.), and Sriram Muthukumar (S.M.) conceptualized the study and designed the experiments. B.J., K.C.L, and Madhavi Pali (M.P.) performed the experiments and data analysis. Devangsingh Sankhala (D.S.) designed the wearable reader. B.J., M.P., S.M., S.P., and K.C.L., analyzed and interpreted results. B.J., S.M., and S.P. wrote the manuscript. This work was published in Bioengineering and Translational medicine (<https://doi.org/10.1002/btm2.10220>).

#### 2.2 Description of SWEATSENSER

The wearable SWEATSENSER device platform uses an electrochemical biosensor strip that is functionalized with capture probes specific to study biomarkers and a reader for electrochemical transduction for real-time, continuous reporting of cytokines in sweat. The schematic of the sensor strip stack is represented in Fig. 2.1.

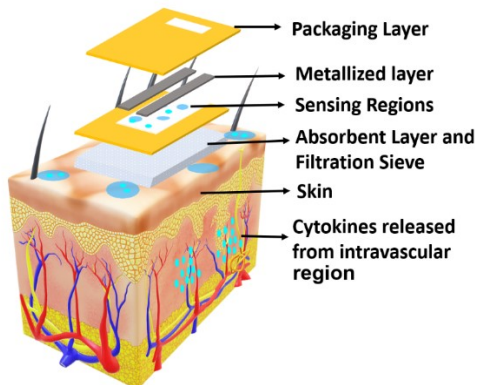


Figure 2.1. Schematic of sensing layers. Schematic was created in Biorender.

The sensor strip comprises of multiple fluid transport sites that have been carefully designed to ensure effective capture of sweat. An absorbent layer of an FDA approved PharmChek patch interfaces with the skin to capture the sweat, and the sweat diffuses through the porous sieve that allows the biomolecules to diffuse. The next layer comprises of sensing regions functionalized with specific capture probe antibodies via a cross-linker on semiconducting zinc oxide (ZnO) nanofilm (100-200 nm in thickness) that entraps the target biomarkers. Above this layer, four pairs of identical working and reference electrodes were deposited using screen-printing technique. Each pair of working and reference electrode was separated from the other to avoid any signal response interference. The printed electrode was then covered using a packaging layer to allow for moisture control i.e. prevent any external moisture from entering the strip while, allow the collected sweat to evaporate after measurement. On the fabricated SWEATSENSE strip, each monoclonal antibody was immobilized separately on the working electrode (i.e. only one antibody type per each working electrode) to enable transduction of affinity-based interaction between the target biomarker and capture probe antibody into a measurable electrochemical signal. The electrochemical binding interactions are transduced through the metallized layer. The sweat then diffuses into the next layer to be released out. The top-most layer is a packaging layer that allows for the used sweat to release out and prevent any external moisture to enter, thus, maintaining the fluid dynamics of the sensor strip in a controlled manner.

Fig. 2.2 illustrates a schematic of the skin-SWEATSENSE interface when the SWEATSENSE is in contact with skin. The device is designed to rapidly detect and track levels of biomarkers in a multiplexed manner in conjunction with the vitals of a person. The

wearable device also simultaneously measures skin temperature and perspiration for assessing vitals and the user sweating profiles respectively.

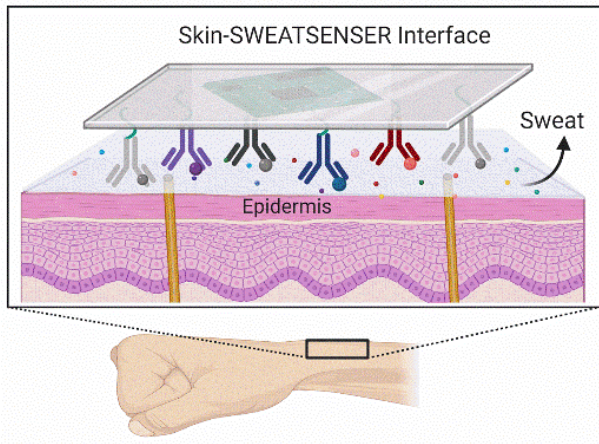


Figure 2.2. Skin-SWEATSENSOR device interface, where, SWEATSENSOR is functionalized with specific antibodies to capture the study biomarkers. Schematic was created in Biorender.

### 2.3 SWEATSENSOR electronic reader design

The architecture of the electronic reader used in this work is shown in Fig. 2.3. A component off-the-shelf (COTS) temperature and relative humidity (RH) sensor (Texas Instruments Inc., USA), a battery management system (Texas Instruments Inc., USA) and Bluetooth Low Energy (BLE) module (RayTac Corporation, Taiwan) were added to a central Acron Risc machine (ARM) core processor. The integrated temperature and RH sensor helps measure the temperature and RH conditions at the epidermal surface where the sensor is applied. The battery management system manages a regulated charge-discharge operation of the battery in the recommended safe operating region (SOA). The Bluetooth Low energy module helps establish wireless communication to a smartphone with the lowest power consumption and form factor. A 3.7 V LiPo battery with suitable charge capacity was used that has a lifetime of 168 hours on single charge.

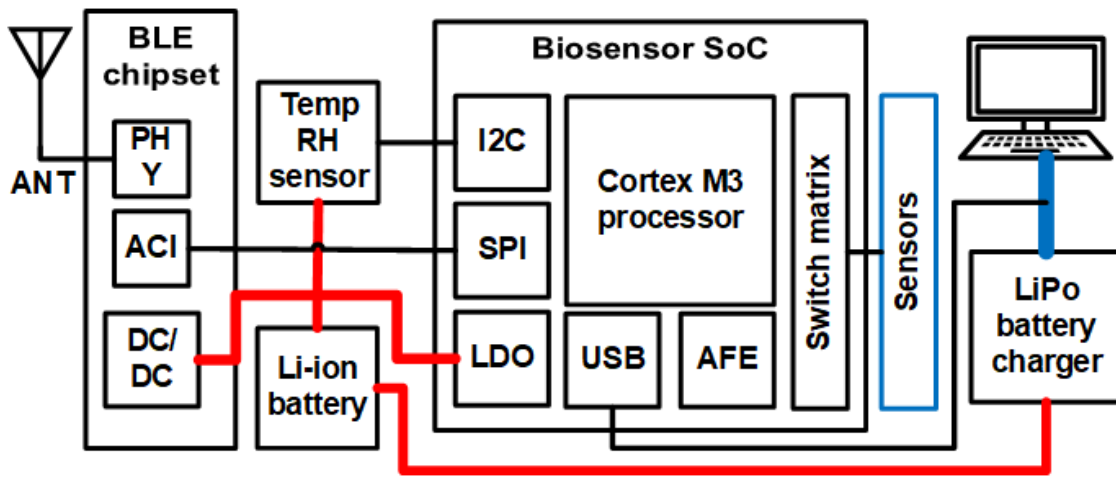


Figure 2.3. Architecture of the SWEATSENSE reader indicating various components used for transduction and processing of the biochemical interaction.

#### 2.4 Material Characterization of SWEATSENSE

We first performed material characterization of the SWEATSENSE using scanning electron microscopy (SEM) and Energy dispersive X-ray Analysis (EDX) to ensure the ZnO nanofilm was uniformly deposited on the patch membrane.

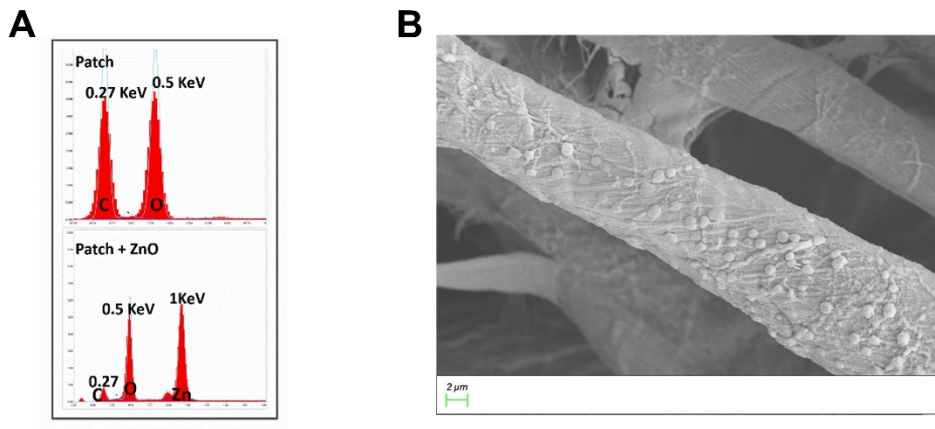


Figure 2.4. **A)** EDX spectra of patch membrane and ZnO deposited on patch membrane. Carbon and oxygen peaks at 0.27 and 0.5 KeV respectively are observed due to the polymeric structure of porous patch. Upon deposition of ZnO, a peak at 1 KeV corresponding to L-shell of Zinc with an increase in oxygen peak intensity and decrease of carbon peak is observed. **B)** SEM image of uniform deposition of ZnO on patch membrane.

Fig. 2.4A demonstrates the EDX spectrum of the patch membrane before and after ZnO deposition. The carbon and oxygen peaks at 0.27 and 0.5 KeV of only patch membrane (Fig. 2.4A (i)) correspond to the polymeric structure of the PharmChek patch. After deposition of ZnO on the patch membrane, a distinct peak observed at 1 KeV corresponds to the L-shell of zinc (Fig. 2.4A (ii)) with an increased peak-height of oxygen at 0.5 KeV. The corresponding SEM image of uniform deposition of ZnO is demonstrated in Fig. 2.4B.

Further, X-ray photoelectron spectroscopy (XPS) was performed to confirm the binding of thiol cross-linker linker on the ZnO thin film. A comparison of the XPS spectra measured pre- and post-functionalization of the cross-linker is demonstrated in Fig. 2.5. On the pre-functionalized bare ZnO surface, the Zn 2p<sub>3/2</sub> peak at 1022.4 eV and O 1s peaks at 532.2 eV respectively were observed in bare ZnO thin film. Post functionalization with the linker, a peak shift of Zn 2p<sub>3/2</sub> to 1023.9 eV was observed indicating a displacement at the surface due to Zn–S bonds. Further, the peak shift observed of O 1s to 534.2 eV was due to adsorbed –O-H species [16]–[18].

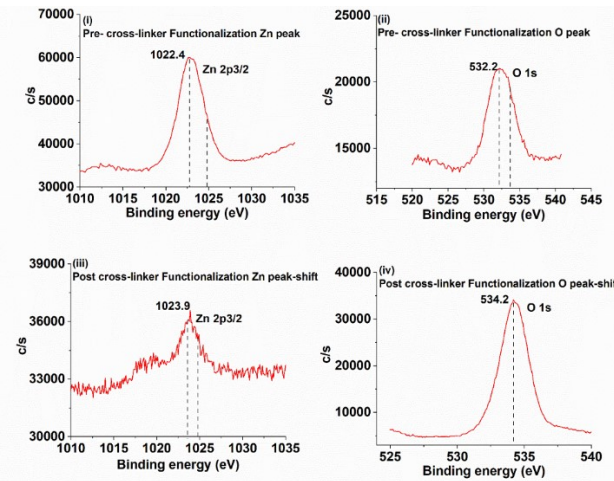


Figure 2.5. XPS characterization of ZnO sensor surface pre- and post-functionalization of cross-linker. Zn and O peak-shifts from 1022.4 eV to 1023.9 eV and 532.2 eV to 534.2 eV respectively are observed due to Zn–S bonds.

## 2.5 SWEATSENSE functional electrode characterization

Finite element analysis (FEA) through COMSOL simulations was performed to understand the electrical current density distribution of the semiconducting electrode system on the porous PharmChek patch which is critical for electrochemical sensing. The electrical density profile of the electrode was characterized by simulating the experimental conditions used for impedance spectroscopy. A sinusoidal input bias voltage of 10 mV with Neumann's boundary equations was applied between the working and reference electrode.

$$Q_1 = \nabla J_1, \quad J_1 = -\sigma_1 \nabla \phi_1 \quad (1)$$

$$Q_s = \nabla J_s, \quad J_s = -\sigma_s \nabla \phi_s \quad (2)$$

$$E_{eq} = \phi_s - \phi_1 \quad (3)$$

Where,

$J_1$  and  $J_s$  correspond to current density ( $A/m^2$ ) of electrode and electrolyte. The conductivities of electrode and electrolyte are represented as  $\sigma_1$  and  $\sigma_s$ . The equilibrium potential between the electrode and electrolyte is represented as  $E_{eq}$ . The corresponding current distribution across the electrode surface was determined with saline buffer (as electrolyte) covering the working and reference electrode. Fig. 2.6 confirms that the electrode potential is focused across the working electrode uniformly and no parasitic voltage gets distributed at the reference electrode due to the buffer solution, thus, confirming that the developed electrode system has a stable potential distribution and is not influenced by the ionic gradient of the saline buffer solution. The current density distribution extracted as line graphs (Fig. 2.6) demonstrate that the current density is maximum at the working electrode and is zero at the reference electrode. The current distribution

plot also confirms negligible parasitic current between the working and reference electrode indicating good stability of the developed electrode system.

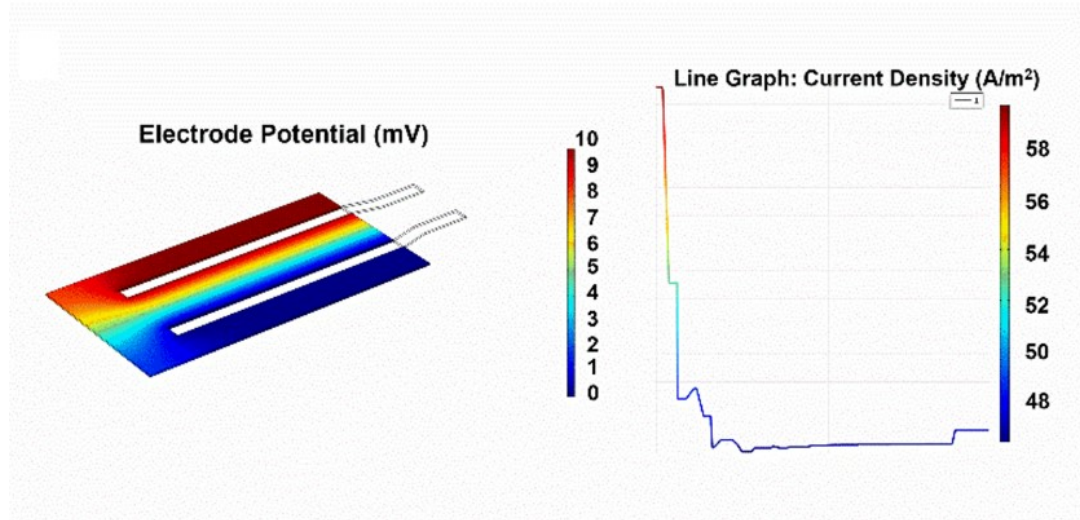


Figure 2.6. Finite element analysis characterization of sensor. Electrode potential distribution between working and reference electrode signifying the uniform distribution of voltage across working electrode. Electrical current density distribution between working and reference electrode showing peaks at working electrode.

## 2.6 Electrochemical Characterization of SWEATSENSER

The stability of the electrode system demonstrated by FEA simulations was also experimentally confirmed through equilibrium potential study. Typically, an electrochemically stable electrode system will have an equilibrium potential  $\sim 0$  V. The equilibrium potential of the electrode system was measured over five minutes as demonstrated in Fig. 2.7. It can be observed from the plot that the SWEATSENSER has very low equilibrium potential. These results confirm that the developed SWEATSENSER device is electrochemically stable and suitable for biosensing.

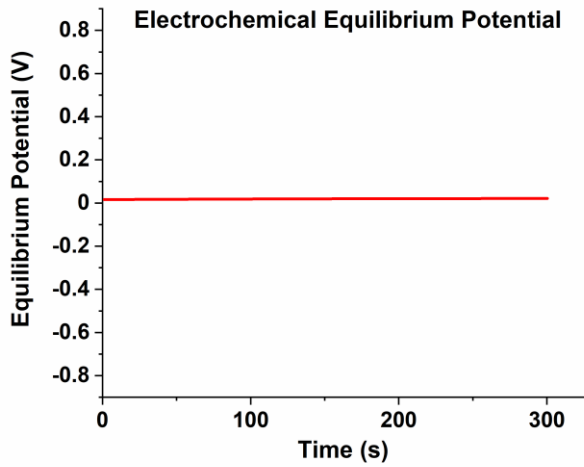


Figure 2.7. Stable electrochemical equilibrium potential between working and reference electrode.

## 2.7 Detection modality of SWEATSENSE

Non-faradaic electrochemical impedance spectroscopy (EIS) is a powerful technique that can measure subtle changes in the electrical double layer due to binding interactions between capture probe-target analyte without the need for redox labels by application of a small input AC voltage [19]. The measured impedance is directly associated with target biomolecule binding to the capture probe antibody. The results of an impedance measurement can be illustrated using a bode plot, (which plots absolute impedance ( $|Z_{mod}|$ ) and phase ( $\phi$ ) as a function of frequency) [20]. The resulting response was calibrated to a fixed frequency for reporting the concentration values of the target in the sample specimen. All this computation and analysis were performed using the handheld electronic reader onto which the sensors are mounted, and the output results of concentration over time can be interfaced via Bluetooth to report on a smartphone app. EIS can effectively differentiate the binding interactions from any surface and bulk effects such as pH and conductivity variations through frequency tuning and

thus, providing a molecular specific response. These bulk effects occur beyond the electrical double layer and are a characteristic at high frequency, whereas, the binding interactions occur in the low frequency region <1000 Hz [21]–[23].

## 2.8 Analytical algorithm for real-time detection of biomarker levels

Fig. 2.8 shows the training architecture of the proposed training system. This training system consists of four major parts: (1) Data collection and organization (2) Feature selection and extraction (3) Model training (4) Model optimization for low error. The training data was obtained from multiple replicates for varying dose concentrations of each target biomarker. This training data was generated by simulating a dose profile within physiological range. Once the impedance data was collected, it was split into multiple model inputs or features such as absolute impedance, phase response, real and imaginary impedance, temperature, and RH which are closely related with the operation of the sensor. Impedance response for each concentration of particular biomarker was used as an input as it helps confine the data to a normal distribution [24]. The running difference of impedance w.r.t previous concentration's impedance response was used to define the rate of change of sensor impedance. The percentage change of impedance defines the change of sensor impedance from the time of start of use for the sensor. These features account for the cumulative accumulation of doses on the sensor.



Figure 2.8. Schematic of the methodology implemented for training and prediction of levels of the biomarkers.

The training was performed on  $N = 20$  by splitting the collected data into groups of train series and test series in a 70:30 splits. Various commonly known training models such as linear regression, quadratic support vector machine (SVM), bagged ensemble regression and decision tree regression were studied for this application. Table 2.1 shows the highest  $R^2$  for the decision ensemble regression system.

Table 2.1. Training algorithm outcomes

Model type	$R^2$
Linear regression	.56
Tree	0.96
<b>Ensemble</b>	<b>.98</b>
Quad SVM	.47

Among the various training algorithm, Ensemble demonstrated a statistically higher  $R^2 = 0.98$  and was used for reporting the cytokine and chemokine biomarkers.

## CHAPTER 3

### DETECTION OF INFECTION FROM SWEAT USING SWEATSENSER DEVICE

#### 3.1 Prior Publication

Badrinath Jagannath (B.J.), Kai-Chun Lin (K.C.L), Shalini Prasad (S.P.), and Sriram Muthukumar (S.M.) conceptualized the study and designed the experiments. B.J., K.C.L, and Madhavi Pali (M.P.) performed the experiments and data analysis. Devangsingh Sankhala (D.S.) designed the wearable reader. B.J., M.P., S.M., S.P., and K.C.L., analyzed and interpreted results. B.J., S.M., and S.P. wrote the manuscript. This work was published in Bioengineering and Translational medicine (<https://doi.org/10.1002/btm2.10220>).

#### 3.2 Abstract

This work presents the viability of passive eccrine sweat as a functional biofluid towards tracking the human body's inflammatory response. Cytokines are biomarkers that orchestrate the manifestation and progression of an infection/inflammatory event. Hence, non-invasive, real-time monitoring of cytokines can be pivotal in assessing the progression of infection/inflammatory event which may be feasible through monitoring of host immune markers in eccrine sweat. This work is the first experimental proof demonstrating the ability to detect inflammation/infection such as fever and influenza directly from passively expressed sweat in human subjects using a wearable 'SWEATSENSER' device. The developed SWEATSENSER device demonstrates stable, real-time monitoring of inflammatory cytokines in passive sweat. An accuracy >90% and specificity >95% was achieved using SWEATSENSER for a panel of cytokines (interleukin-6, interleukin-8, interleukin-10, and tumor necrosis factor- $\alpha$ ) over an

analytical range of 0.2-200 pg mL<sup>-1</sup>. The SWEATSENSE demonstrated a correlation of Pearson's r>0.98 for the study biomarkers in a cohort of 26 subjects when correlated with standard reference method. Comparable IL-8 levels (2-15 pg mL<sup>-1</sup>) between systemic circulation (serum) and eccrine sweat through clinical studies in a cohort of 15 subjects, and the ability to distinguish healthy and sick (infection) cohort using inflammatory cytokines in sweat provides pioneering evidence of the SWEATSENSE technology for non-invasive tracking of host immune response biomarkers. Such a wearable device can offer significant strides in improving prognosis and provide personalized therapeutic treatment for several inflammatory/infectious diseases.

### **3.3 Introduction**

Cytokines are low molecular proteins produced by the immune system in response to external infectious agents or inflammatory event [25], [26]. They play an important role in protecting against viral and bacterial infections[27] and are actively involved in the pathogenesis of infection. Cytokines induce biological effects to act as powerful mediators of immune response to counteract infectious pathogen attack [28]. In the event of an infection due to acute respiratory diseases such as influenza or COVID-19, the complex interplay between the viral pathogen virulence and host resistance dictates the severity of progression of disease in the host [29]. The complications associated with such infections are often attributed to hyper-induction of pro-inflammatory cytokine production, and in severe cases leads to a phenomenon called as ‘cytokine storm’[29]–[32]. High levels of tumor necrosis factor (TNF), cytokines, and chemokines were determined in cytokine storm events pertinent to influenza and more recently with SARS-CoV-2 patients[33]–[35]. Fig. 3.1. illustrates a series of systemic events and

mediators resulting in the release of several pro-inflammatory and anti-inflammatory cytokines such as tumor necrosis factor- $\alpha$  (TNF- $\alpha$ ), interleukin-6 (IL-6), interleukin-8 (IL-8), and interleukin-10 (IL-10) due to a bacterial or viral pathogen attack [36]. Cytokine levels, therefore, orchestrate the time-course of progression of inflammation in a host[37]. Hence, tracking the cytokines associated with infections from the time of pathogen attack in the host can effectively be used for improved prognosis and better management of an infection. Real-time monitoring of critical inflammatory cytokine markers will not only aid in early disease risk stratification and mitigation but can also help guide clinicians in customizing treatments based on host immune response.

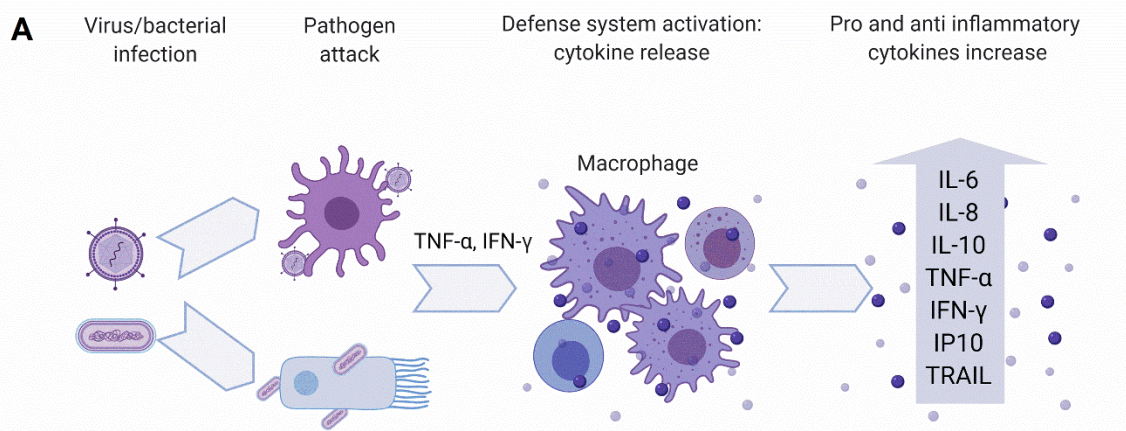


Figure 3.1. Schematic of immunological cascading effects of inflammatory response.

However, there are no continuous monitoring systems that can report the levels of cytokines in real-time as current methods rely on blood plasma/serum or saliva as the biofluid for detecting these markers which is not suitable for continuous monitoring. In contrast, eccrine sweat as a biofluid is an excellent alternative for real-time, non-invasive monitoring of cytokines. Passively expressed eccrine sweat has a plethora of biological information that comprises of ions, small

molecules, metabolites and proteins[38], [39]. Various chemical species (hormones, ions, metabolites, acids, small proteins and peptides) enter the sweat through the dermal duct and secretory coil[40]. During an inflammatory response, cytokines are released from the intravascular membrane. The adherent intercellular junctions get diminished, causing immunoglobulins, cytokines, and water to move into the dermal interstitium[41]. These cytokines and other protein molecules then diffuse into eccrine sweat gland and reach the skin surface by hydrostatic pressure. Cizza et al., [42] and Marques-Deak et al., [43] have quantified the levels of IL-6, IL-8, TNF- $\alpha$  in sweat. Furthermore, the levels of the cytokine markers between healthy cohort and major depressive disorder (MDD) patients were easily distinguishable. Additionally, Dai et al., validated the presence of IL-10 in sweat [44]. While all these studies are significant in validating the presence of cytokines in sweat, they were single-point measures that required cumbersome processing methods and then, measured using standard laboratory techniques. We analytically validated sweat cytokine levels with serum cytokine measurements. The developed SWEATSENSOR can differentiate healthy cohort from sick subjects with fever or viral infection such as influenza. This critical finding provides pioneering evidence that reporting sweat cytokine levels in a continuous manner as demonstrated with the SWEATSENSOR device platform can be used for designing non-invasive wearable diagnostics for infection monitoring. The SWEATSENSOR device can be useful in monitoring the host-immune states that is vital and is a characteristic of the ‘wellness’ to ‘illness’ and back to ‘wellness’ state in the patient. Such a technology platform can welcome a radical change in point-of-care (PoC) diagnostics for monitoring infections during seasonal epidemics and pandemic diseases.

### **3.4 Materials & Methods**

**Reagents and Instrumentation:** DTSSP (3,3'-dithiobis (sulfosuccinimidyl propionate)) cross-linker and phosphate buffered saline (PBS) were purchased from Thermo Fisher (USA). The capture probe monoclonal antibodies (mAb) and recombinant proteins for IL-6, IL-8, TNF- $\alpha$  were purchased from Abcam (MA, USA) while IL-10 antibody was purchased from Thermo Fisher. IL-6 ELISA kit was procured from Abcam, TNF- $\alpha$  from Thermo Fisher, IL-8 and IL-10 kits were purchased from Raybiotech. The reagents for ELISA measurements were stored and reconstituted according to the protocol from the manufacturer.

**Sensor Immunoassay Functionalization:** 10 mM DTSSP cross-linker mixed with 10  $\mu\text{g mL}^{-1}$  of monoclonal capture antibody of each marker immobilized on the sensing electrode surface via thiol-binding mechanism. Each working electrode specific to a biomarker was independently functionalized to achieve specific detection of target biomarkers. For sensor performance metric studies such as repeatability, reproducibility and stability, the functionalized sensors were lyophilized and immediately vacuum sealed until further use.

**SWEATSENSE Device:** The SWEATSENSE device comprises of a replaceable sweat sensing strip and an electronic reader. The sensing strip is functionalized with specific target capture probes i.e., IL-6, IL-8, IL-10 and TNF- $\alpha$  monoclonal antibodies as described previously. This sensor strip is mounted onto a wearable electronic reader that transduces the impedance response from the sensor and reports the measured biomarker levels in sweat. The sensor fabrication process has been adapted from Munje et al. and has been described in detail previously [45]. Briefly, a sensing-electrode system is fabricated on the SWEATSENSE strip

for enabling transduction of affinity-based interaction between the target biomarker and capture probe antibody into a measurable electrochemical signal. The sensor has been designed to handle low volumes of sweat and the design has been optimized by considering the sweat gland density, sweating rate, surface area of contact. Non-faradaic EIS was used as the detection modality to determine the sensing response of the binding interactions between the specific capture probe and target molecule. A very low input 10 mV sinusoidal voltage was applied to the sensing electrodes and the change in impedance due to the binding interaction between target molecule and capture probe antibody resulting in charge modulation was recorded at 180 Hz. Calibration curve for each study marker was developed by measuring the impedance response for varying concentrations of the target analyte over the physiological range of 0.2- 200 pg mL<sup>-1</sup>.

**SWEATSENSER Characterization:** Fourier transform infrared spectroscopy (FTIR) spectroscopy was performed using Nicolet iS-50 (Thermo Scientific Inc.). The samples were prepared as previously described in SWEATSENSER design section and the measurement was done in attenuated total reflectance mode. 256 Spectral scans at a resolution of 4 cm<sup>-1</sup> were collected using Germanium crystal for a wavelength range between 4000 cm<sup>-1</sup> to 600 cm<sup>-1</sup>. Electrochemical characterization of antibody functionalization was performed using Gamry Instruments potentiostat. A small input voltage of 10 mV AC was applied, and the impedance response was measured over a frequency range of 1 Hz - 1 MHz.

**Human subjects sweat sample collection, handling, and processing:** Sweat samples were collected, processed, and evaluated in compliance with the protocol approved by the Institutional Review Board (IRB) at the university (IRB# 19-42). 26 human subjects were recruited with their informed written consent for participation in this study. The protocol for sweat sample collection

was adapted from Hladek et al [38] where, two FDA approved PharmChek® patches were placed (one on each arm of the volunteer) at the same time. One patch was removed at 24 hour and the other at 72 hours from the time the patch was put on the volunteer. The samples were de-identified and stored in freezer immediately upon collection in 5 mL tube until used for analysis. Samples were removed and thawed prior to analysis. 2 mL of elution buffer prepared as per the protocol described in Hladek et al.[46] was added to the tube containing the sample. The sample with the elution buffer in the 5 mL tube was placed in a secondary container with ice and operated on a shaker plate for 45 minutes. Next, the sample tube was centrifuged at 20x g for three min operated at 4°C. Any remaining sample was extracted by placing the patch in a syringe and the residual sample fluid was extracted by squeezing out that was entrapped in the patch.

**ELISA analysis:** The extracted patch samples were evaluated using ELISA as the reference method to establish correlations with SWEATSENSOR. The individual kit's protocol was followed as per manufacturer instructions. Absorbance at 450 nm was used to read the optical density (O.D) response and determine the levels of biomarkers in samples.

**In-vitro sweat sensor analysis for patch samples:** The extracted and aliquoted samples were evaluated and compared with the ELISA results to better understand the accuracy of the SWEATSENSOR device in reporting the levels of biomarkers in human subjects. As the collected samples were from a healthy cohort, elevated concentrations were spiked into the buffer to demonstrate the performance of device in capturing the concentration levels of sick cohort. These concentrations were identically evaluated with ELISA as well. The measured levels using the SWEATSENSOR device was compared with the obtained ELISA results using

statistical methods such as Pearson's correlation and Bland-Altman analysis to determine the efficacy of the sweat sensor when compared to the reference ELISA method.

### **On-body SWEATSENSE measurements on human subjects for comparing cytokine**

**levels in healthy and sick cohort:** All enrolled subjects with written informed consent wore the SWEATSENSE devices during testing and measurements were recorded in compliance with the protocol approved by the IRB# 19-136. Serum and sweat samples were collected from 10 healthy and 5 sick subjects to perform serum to sweat correlation in healthy and sick cohort. Prior to the sample collection, temperature was checked for all the subjects and a questionnaire was recorded on the patient symptoms. This was followed by collection of ~5 mL blood sample by a physician which was converted to serum and stored at -20° C until further use. Then, SWEATSENSE was immediately placed on the lower forearm of the subject for ~1 hour to allow for sufficient sweat collection. SWEATSENSE device was covered with full-sleeve or a sweat-band to keep the device enclosed and prevent interactions with the ambient environment. The inclusion criterion for sick cohort were that subjects must have been experiencing inflammatory/infection symptoms such as fever, flu, or diagnosed with some type of bacterial or viral infection. Subjects were asked if they were taking any medication related to illness in the last 48 hours. No dietary information was collected from the subjects. The collected serum levels were analyzed using a standard laboratory reference method. Analysis of on-body sweat measurements using the SWEATSENSE were performed using the developed analytical algorithm. Complete details of the analytics for determining sweat levels through continuous monitoring has been described in Chapter 2.

**Statistical Analyses:** Several statistical tests were performed using Origin Pro. Statistical t-test and ANOVA were carried out with a C.I. of 95% for reproducibility and temporal monitoring studies. Pearson's correlation and Bland-Altman analysis were performed to determine the extent of agreement of sweat sensor with the reference method.

### 3.5 Results and Discussion

#### 3.5.1 Characterization of SWEATSENSER

The functionalization of the immunoassay owing to the binding of the capture probe via a thiol cross-linker on the sensor surface was confirmed using FTIR (Fig. 3.2).

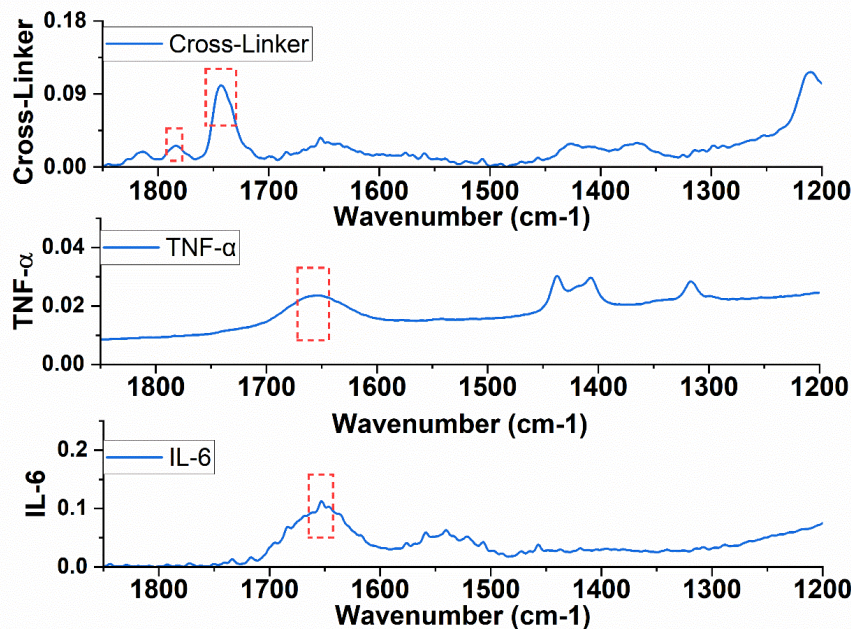
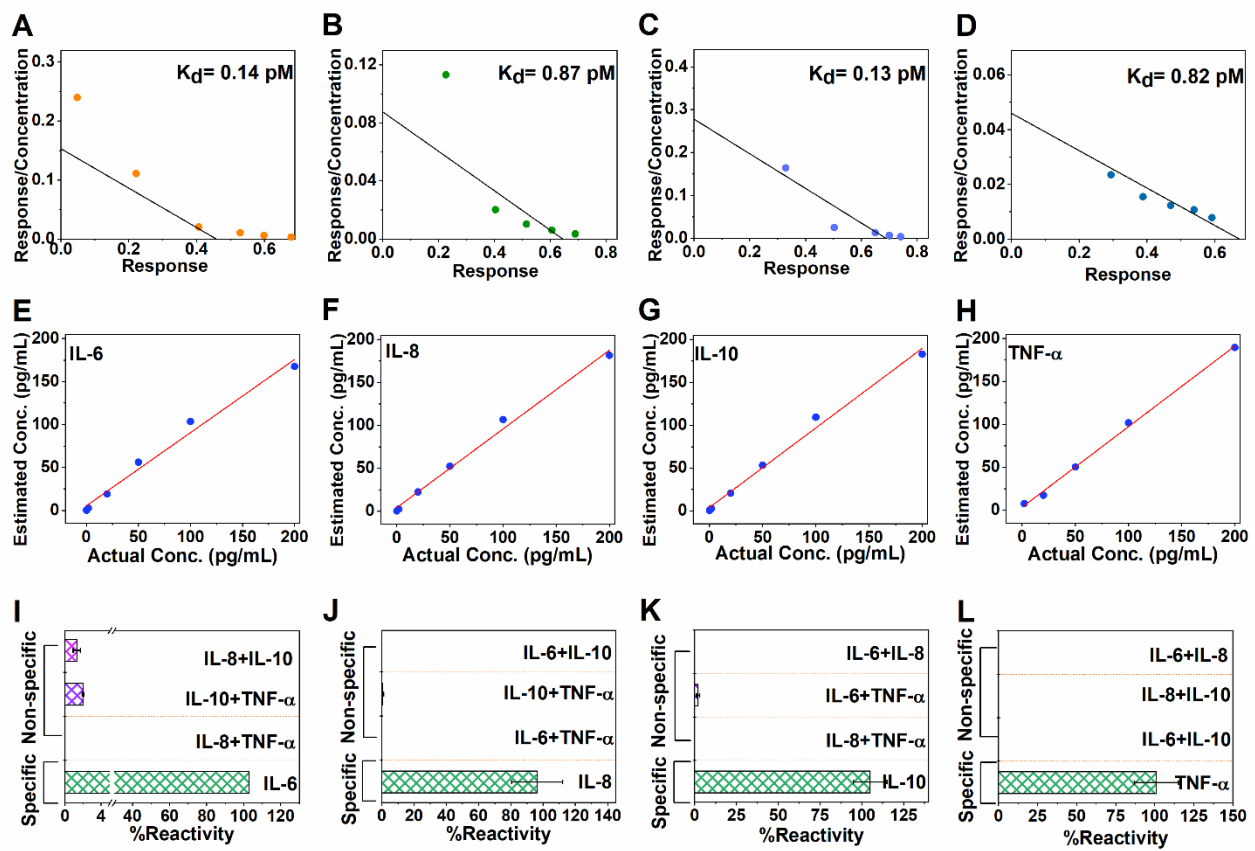


Figure 3.2. FTIR spectra confirming conjugation of the antibodies on the sensor surface. The top spectrum indicates the binding of the cross-linker on the sensor surface with NHS ester bond (peak at 1780 cm<sup>-1</sup>) and free carboxylic acid peak (1740 cm<sup>-1</sup>). The conjugation of both antibodies shows cleaving of C-O bond of NHS ester and the peak at 1780 cm<sup>-1</sup> disappears,

while, enhanced aminolysis peak (at  $1652\text{ cm}^{-1}$ ) is observed confirming the binding of the antibody.

After validating the successful immobilization of the capture probe antibody on the sensor surface, immune-sensing performance of the SWEATSENSE was evaluated to understand the binding affinity between the capture probe and target molecule as the developed sensing system works on an affinity-based mechanism. Firstly, the affinity of the capture probe antibodies to the target analyte were determined using the saturation binding curve studies by measuring the equilibrium constant ( $K_d$ ). Typically,  $K_d$  is used as a key parameter in determining the ability of the antibody to quickly dissociate and capture the antigen molecule. Concentrations of the analyte were varied and the impedimetric response was measured to determine the  $K_d$  for each capture probe using saturation binding curve fitting equations in Graphpad Prism. Affinity of an antibody is inversely proportional to the  $K_d$ . Ideally, an excellent affinity-based system will have a  $K_d$  value in the lower pico-molar range for a cytokine affinity capture probe[47]. The SWEATSENSE satisfies this criterion with a very low  $K_d$  of 0.14, 0.83, 0.13, and 0.82 pM for IL-6, IL-8, IL-10, and TNF- $\alpha$ , respectively (Fig. 3.3 (A-D)) for n=3 measures, thus, indicating high affinity of the capture probe antibody used for target marker detection. Such low equilibrium constant also reflects high sensitivity for detecting ultra-low analyte concentrations which is important specifically for sweat-based systems, wherein, one can anticipate diluted biomarker levels in sweat compared to the systemic blood circulation levels. After establishing high affinity of the capture probes to the target markers in sweat, we evaluated whether the SWEATSENSE can report the levels of the study markers reliably.



**Figure 3.3. Characterization of SWEATSENSE.** (A-D) Binding efficiency determined through Kd values for cytokines (A: IL-6, B: IL-8, C: IL-10, D: TNF-a). (E-H) Spike and Recovery plots demonstrating ability to report concentrations reliably for cytokines in sweat (E: IL-6, F: IL-8, G: IL-10, H: TNF-a); Linear regression analysis was performed between ‘Actual’ and ‘Reported’ concentration and  $R^2 > 0.95$  was achieved for  $n \geq 3$  measures. (I-L) Selectivity and Specificity of SWEATSENSE for target cytokine marker in sweat (I: IL-6, J: IL-8, K: IL-10, L: TNF-a); SWEATSENSE demonstrates minimal (<2%) or no response to non-specific molecules, while is highly specific (>97%) to target biomarker. Data is represented as mean  $\pm$  SEM

In order to determine this, SWEATSENSE was functionalized with specific capture probe antibody individually to measure the response devoid of crosstalk. A series of six concentrations ranging from 0.2 to 200  $\text{pg mL}^{-1}$  (in the physiological range) for each study marker were prepared independently in neat sweat (without non-specific molecules) and dispensed on the corresponding sensor. EIS, the core sensing technology (described in the methods section) of the

SWEATSENSE was used to record the signal response, and the corresponding concentrations were estimated. EIS can effectively differentiate the binding interactions from any surface and bulk effects such pH and conductivity variations through frequency tuning and thus, providing a molecular specific response. These bulk effects occur beyond the electrical double layer and are a characteristic at high frequency, whereas, the binding interactions occur in the low frequency region <1000 Hz [21]–[23]. Therefore, the response to the specific interaction was captured at 180 Hz. It is observed from Fig. 3.3(E-H) that the SWEATSENSE reliably determined the levels of the study biomarkers. Further, SWEATSENSE demonstrates a linear response with  $R^2>0.98$  over a 3 log-order dynamic range of 0.2-200 pg mL<sup>-1</sup> for all the study markers of interest for at least n=3 measures. This dynamic range conveniently covers the range for determining infection levels including acute infections such as influenza, SARS-CoV-2 and sepsis [48]. SWEATSENSE was further evaluated for its selectivity and specificity to the study biomarkers. The sensors were prepared in a similar manner as the previous experimental design reported for linearity. Three combinations of cocktail solutions were prepared by mixing two non-specific analytes in sweat analog at a high concentration of 200 pg mL<sup>-1</sup> (final concentration after mixing) to determine the cross-reactivity of each capture probe with the non-specific molecules. This solution was devoid of the specific target biomolecule. The prepared cocktail of non-specific markers was dispensed on the sensor and the response was recorded. The reactivity was determined as a percentage ratio of measured concentration to the actual concentration of the biomarkers. The SWEATSENSE demonstrates excellent selectivity with negligible (<2%) or no reactivity to the non-specific molecules while, a high signal response (~>98%) was reported for the specific marker as demonstrated in Fig. 3.3(I-L).

### **3.5.2 Evaluation of SWEATSENSE analytical performance metrics**

The temporal profile of cytokines orchestrates the time-course of an infection event and recovery from infection [49]. Dynamic profiling of host immune markers using infection monitoring wearable devices can significantly mitigate the effects of a pathogen attack by aiding in pre-symptomatic alarm and early therapeutic intervention. Therefore, the study presented in this section evaluated the potential of the SWEATSENSE to be synergistically used as a wellness dashboard for reporting the temporal dynamic changes in levels of the study biomarkers. We evaluated the functionality and the response of the SWEATSENSE by mimicking the temporal profile of the host immune cytokine markers in response to the infectious pathogen attack as represented in Fig. 3.4(A-E). The band (in orange with double-headed arrow) in the cytokine profile graphs indicate the time snapshot window of the body's immune host biomarker response due to an infection trigger. This snapshot reveals the relative biomarker levels at a specific time interval during various stages of an infection/inflammatory event. To assess the ability of the SWEATSENSE to report the levels reliably in a multiplexed manner, the temporal infection profile was classified into five stages right from onset to recovery. In this context, Fig. 3.4(A-C) describes the cytokine profile of the wellness to illness phase i.e. from infection onset to illness while, Fig. 3.4D and 3.4E represent the temporal snapshot of illness to recovery phase. Based on the relative profile of the biomarkers, the sensor was dispensed with concentrations pertinent to that specific time-interval and the reported levels were calculated for n=4 measures per biomarker at each inflammatory response phases. In an infectious event, the pro-inflammatory response of TNF- $\alpha$  rises rapidly which triggers other pro-inflammatory markers such as IL-6 and IL-8 [50]. As the levels of IL-6 and IL-8 elevate and peak, the anti-inflammatory markers such as

IL-10 begin to elevate to help the body in immuno-suppression [51]. As seen from Fig. 3.4(A-E), the SWEATSENER can reliably report the relative temporal levels of cytokine markers during various stages of inflammatory response, thus being suitable for dynamic profiling in the event of an infection.

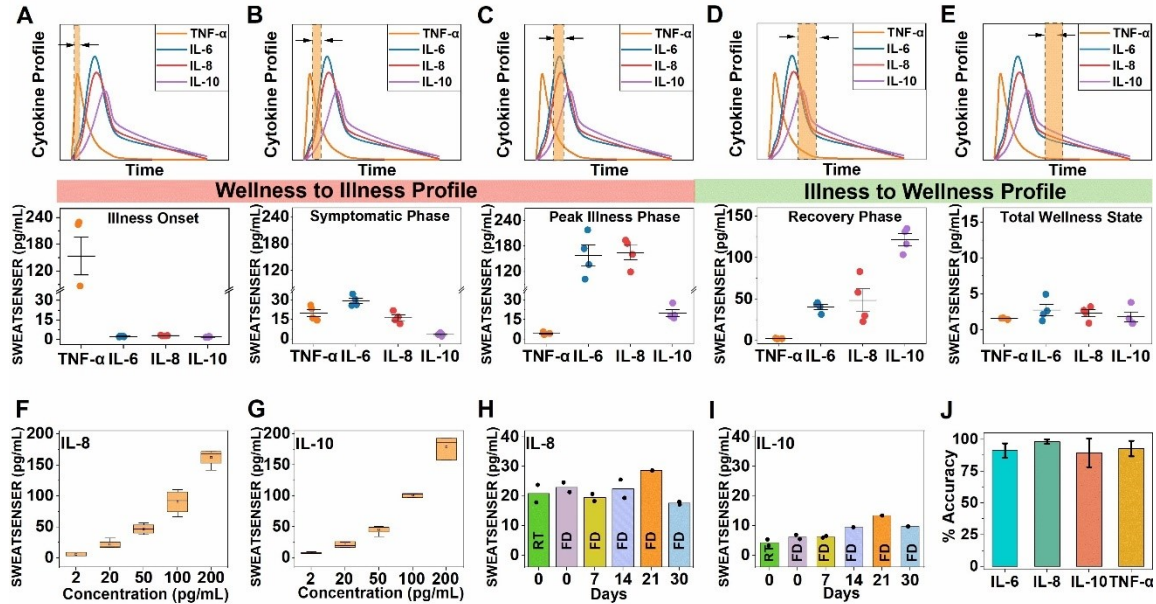


**Figure 3.4. Analytical metrics of SWEATSENER.** (A-E) Ability of SWEATSENER to reliably track biomarker levels during various stages of infection from early-stage pathogen attack to recovery. Temporal profiles of biomarkers during various stages of infection (Top part) and the corresponding levels reported by SWEATSENER is represented as whisker plot. The band with double-sided arrow (indicated in the top half of the graph) indicates time snapshot of cytokine profile during various stages of infection. Specifically, (A-C) demonstrates the SWEATSENER response tracking of cytokine markers during wellness to illness phase and (D, E) demonstrate the recovery phase which is illness to wellness. (F,G) Reproducibility of SWEATSENER demonstrated with Pro-inflammatory (F: IL-8) and Anti-inflammatory (G: IL-10) cytokines for  $n \geq 4$  sensors. (H, I) Time stability of SWEATSENER for (H: IL-8) and (I: IL-10) cytokines. RT refers to sensor incubated in room temperature without lyophilization and FD refers to freeze-dry (i.e. lyophilized sensor) for  $n=2$  measures. (J) Accuracy of SWEATSENER in reporting cytokine markers in sweat. Data is represented as mean  $\pm$  SEM Note: Lyophilized SWEATSENERS were used for reproducibility and stability studies.

As the temporal profile of the study markers change dynamically during an infection, it is critical for a continuous monitoring system to be stable, long-lasting, and reliable without being prone to

drifts due to external and environmental factors. Hence, we investigated the SWEATSENSE through critical evaluation of performance metrics such as reproducibility, precision, accuracy, and stability. The performance of biosensors that function based on immunoassay mechanism is primarily dependent on the stability and specificity of the capture probe. The sensor strips were functionalized with specific antibodies and then lyophilized to enhance the shelf-stability. Lyophilization removes water and prevents the antibody from denaturing [52]. The samples were then vacuum sealed and opened just prior to testing the sensors. Firstly, the ability to demonstrate consistent response with different sensors was validated using reproducibility studies. Reproducibility determines the degree of closeness in response between different sensors comprehending the analytical range of the study biomarker. Here, five different sensors for each of pro-inflammatory (IL-8) and anti-inflammatory (IL-10) were measured. The sensors were dosed with concentrations from 2-200 pg mL<sup>-1</sup> and the corresponding reported concentration was calculated from the calibration curve to determine if the response is identical from five sensors. Fig. 3.4 F,G represent the box plots for reproducibility response of pro and anti-inflammatory cytokines. It is observed that the SWEATSENSE demonstrates a reproducible response between multiple sensors over the entire range of 2-200 pg mL<sup>-1</sup>. Additionally, the non-overlapping interquartile ranges of the box plots confirm the ability of the sensor to reliably distinguish concentration levels of the cytokines. Stability of the wearable sensors is also critical for practical use on human subjects. Therefore, we evaluated if the stability of the SWEATSENSE is retained at least for a month without loss in sensitivity. Five batches of sensors were functionalized each with pro-inflammatory (IL-8) and anti-inflammatory (IL-10) capture probe antibodies. The functionalized sensors were then lyophilized and immediately

vacuum sealed for storage. The response of the lyophilized sensors were evaluated by dosing ~20 pg mL<sup>-1</sup> IL-8 and ~5 pg mL<sup>-1</sup> IL-10 on the corresponding specific antibody functionalized sensors. The stability of the SWEATSENSE platform was assessed by measuring the response of the sensors on Day 0, 7, 14, 21 and 30 from the day of the antibody functionalization and lyophilization. Fig. 3.4H,I demonstrate that the stability of the sensor is retained over a month without a loss in signal response for n=2 measures on each day of measurement. The SWEATSENSE reported a concentration ~18-24 pg mL<sup>-1</sup> for IL-8 concentration of 20 pg mL<sup>-1</sup> and ~5-10 pg mL<sup>-1</sup> for the IL-10 dosed concentration of 5 pg mL<sup>-1</sup>, indicating that the sensitivity is retained for one month even in the low concentration range. Furthermore, the lyophilized sensors (indicated as FD in bar plots) demonstrate similar response to that of the sensors measured directly after functionalization without lyophilization (indicated as RT in bar plots), thus, confirming reliability of SWEATSENSE for over month. The SWEATSENSE reported an accuracy > 90% for all the study biomarkers (Fig. 3.4J). Thus, these detailed and rigorous characterization results elucidate the robustness and signify operability of the SWEATSENSE for real use-case scenarios.

### **3.5.3 Pre-Clinical utility of SWEATSENSE on healthy subjects**

In order to use the developed SWEATSENSE for clinical use-cases, it is imperative for the device to demonstrate a good agreement with the current standard reference methods. Therefore, we compared whether the SWEATSENSE performance is congruent to standard commercial ELISA. Sweat was passively collected using an FDA approved sweat collection PharmChek® patch from 26 healthy volunteers who had no reported signs or symptoms of infection in compliance with the protocol approved by IRB. PharmChek® patches have been widely used for

the analysis of several molecules including proteins and cytokines in sweat [46], [53]–[55]. The protocol for sample collection, processing and handling was adapted from Hladek et al., [46]. Fig. 3.5A represents passive eccrine sweat collection from the arm of volunteers which is a high sweat gland density region ~110-120 glands/cm<sup>2</sup> [56]. After collecting and processing the sample as illustrated in the schematic in Fig. 3.5B, the samples were tested on both the SWEATSENSE and ELISA. Pearson's correlation and Bland-Altman analysis were implemented to determine the degree of agreement between SWEATSENSE and standard reference method. The two methods show excellent linear correlation with Pearson's coefficient  $r=0.99$  for all the study markers (Fig. 3.5(C-F)). Additionally, Bland-Altman analyses confirm agreement between the results using two methods of detecting the biomarkers. A very low mean bias of -1.99, -9.43, -0.5 and 0.55 pg mL<sup>-1</sup> was achieved for IL-6, IL-8, IL-10 and TNF- $\alpha$  respectively (Fig. 3.5(G-J)). Although the mean bias is higher for IL-8, it is well within the limits to clearly differentiate healthy and sick levels. All the sample points are scattered around the mean bias line indicating that neither of the methods over-predict or under-predict. The tight 95% C.I bands ( $\pm 1.96$  S.D) further confirm there is no significant deviation between SWEATSENSE and reference method. A continuous monitoring sweat analytics platform involves a dynamic accumulation of sweat on the patch, therefore, we wanted to understand if this phenomenon would alter or cause any variation in the marker levels over time. Two patches, one on each arm were put on some of the healthy subjects for this investigation. One patch was removed at 24 hours while the other was removed at 72 hours. We found that the levels do not vary significantly between 24 and 72 hours with a statistical insignificance with  $p>0.05$  (95% C.I), indicating that sweat biomarker levels do not alter with time in healthy cohort. These results affirm that the temporal levels in

healthy cohort do not significantly vary over time and dynamic change in the levels may imply an infection/inflammatory trigger.

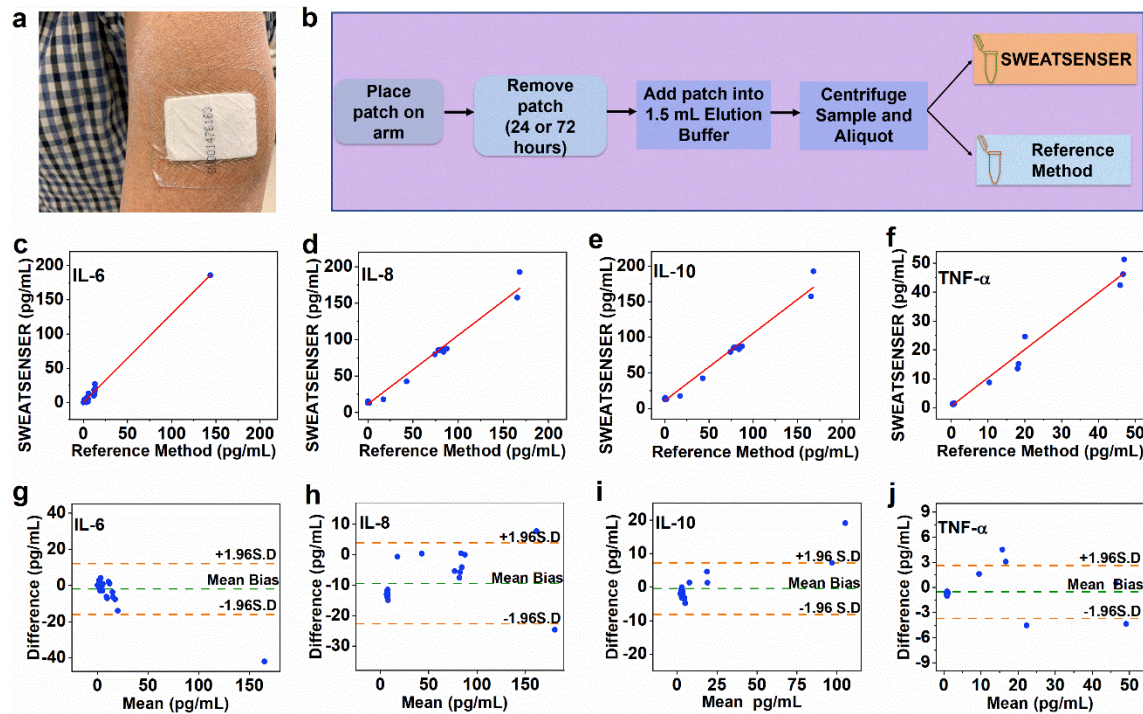


Figure 3.5. Validation of SWEATSENSOR with standard reference method for human subject samples. (A) PharmChek sweat patch worn by subject on arm. (B) Schematic of sweat sample collection using patch for correlation of SWEATSENSOR with ELISA. (C-F) Pearson's Correlation between SWEATSENSOR and reference ELISA method with Pearson's correlation coefficient  $r= 0.99$  for all biomarkers from  $n= 26$  healthy human subject measures. (G-J) Bland-Altman analysis between SWEATSENSOR and ELISA from  $n=26$  healthy human subject measures with a mean bias  $-1.99 \text{ pg mL}^{-1}$  IL-6 (G),  $-9.43 \text{ pg mL}^{-1}$  IL-8 (H),  $-0.5 \text{ pg mL}^{-1}$  IL-10 (I),  $0.55 \text{ pg mL}^{-1}$  TNF- $\alpha$  (J).

### 3.5.4 On-body testing of cytokines in passive eccrine sweat

While there has been significant amount of work on continuous monitoring in sweat, most of it has been on the detection of ions, metabolites and small molecules such as  $\text{Na}^+$ ,  $\text{K}^+$ , lactate, glucose, cortisol[57]–[59] through external stimulation of sweat. Only recently, Alexander et

al.,[60] and Jagannath et al.,[61] have demonstrated detection of cytokines such as IL-1 $\alpha$ , IL-1Ra, IL-1 $\beta$  collected in a patch for wearable applications from passive sweat. However, these were performed only on healthy cohort and did not involve any serum to sweat assessment. We believe that passive sweat collection for real-time detection would offer significant strides in sweat-sensing wearable technologies. The two most common practices for continuous monitoring of sweat biomarkers are exercise and stimulation by iontophoresis. While sweat analytics through exercise may be useful for certain activity-based applications, it is not a viable option for monitoring and tracking biomarkers in infectious patients. The other method, iontophoresis, involves stimulation of sweat glands. This method can cause inflammation and discomfort [62], which may lead to inaccurate cytokine levels influenced by localized inflammation of stimulated site rather than actual inflammatory response of infection. Moreover, sweat can be induced only for a limited time [63] and requires periodic stimulation which may not be suitable for implementing on infectious patients. Other limitations with iontophoresis include limited sweat volume and suppression of markers in induced sweat [64]. Further, we identified biomarkers such as IL-6 and TNF- $\alpha$  were not readily expressed in induced sweat, whereas, passive sweat collection showed the presence of all the study biomarkers. Considering these, it is imperative to have a sweat sensing system that relies on passive collection of the biofluid for monitoring infection markers [62]. Thus, the SWEATSENSE was evaluated for on-body monitoring of biomarkers from passively perspired sweat. First, three healthy subjects were recruited to understand the cytokine profile over time. Participants were refrained from any rigorous activity such as exercise throughout the duration of test to ensure the sweat was collected in a passive manner. The SWEATSENSE device was placed on the lower arm that

has high sweat gland density of 130-134 glands/cm<sup>2</sup> [56]. SWEATSENSER has an effective area of 1.34 cm<sup>2</sup> and has been designed such that it can report levels reliably even with low sweating rates. Typically, the sweating rate can be ~1-3 nL gland<sup>-1</sup> min<sup>-1</sup> [38]. The effective sweating volume would amount to ~0.2- 0.6 µL min<sup>-1</sup>. The device also houses a temperature and perspiration (reported in % relative humidity (%RH)) sensor. The purpose of the temperature sensor is two-fold; one to measure the skin temperature to ensure that device was in-contact with the skin and the other to confirm body vital temperature to assess whether the person has fever. The RH sensor was used to gauge the relative sweating profile of the subject (Fig. 3.6.).

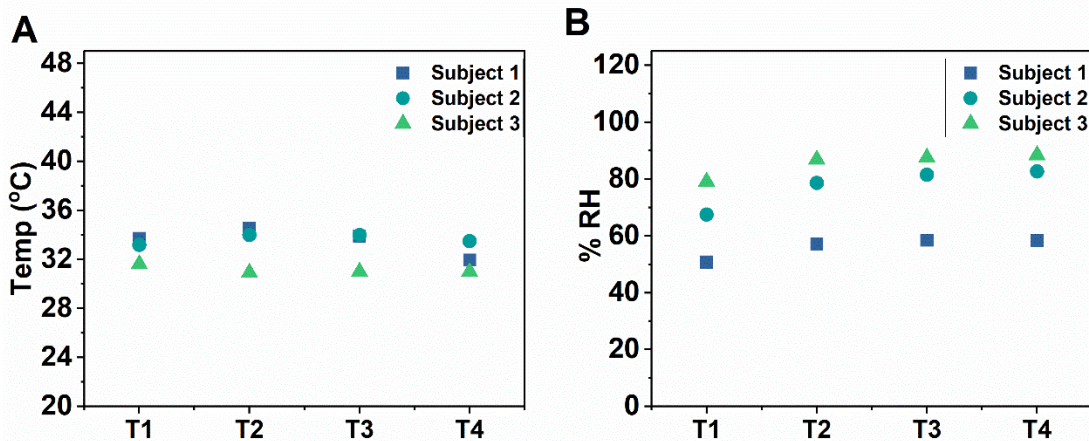


Figure 3.6. **A.** Temperature measured in three healthy subjects across varying time points. **B.** Monitoring of perspiration using realtive humidity (%RH) sensor for three healthy subjects measured at various time points measured every 2 hours.

As the developed sensor is based on an affinity capture assay method, the number of binding sites may decrease over time during continuous detection. Therefore, the sensor surface was sufficiently functionalized with the capture probe to ensure that sensor does not saturate for the measured time duration as previously demonstrated [45]. Further, we devised a unique data

analytics strategy through implementation of an analytical framework to report concentrations in real-time. The developed analytical algorithm considers absolute impedance, change in impedance, and running difference in impedance to assess the levels (as mentioned in chapter 2). Impedance measurements were recorded for every one-hour of target analyte binding on the sensor surface. Changes in cytokine levels may dynamically change over a few hours, therefore, we hypothesize that such a sampling rate will provide a temporal snapshot of cytokine profile. Initial baseline measurement was performed. The previously measured impedance parameters such as running difference and normalized change in impedance were calculated. This was to account for the binding sites occupied on the sensing surface until the previous measurement step and recalibrate the sensor with respect to the previous step. All the above-mentioned signal responses were used as features to train the Ensemble model to achieve high accuracy with  $R^2=0.98$  and low root mean square error (RMSE)= 7.8. Using this developed analytical framework, the levels of the biomarkers were determined for continuous on-body measurements.

Fig. 3.7(A-C) demonstrate the cytokine concentrations in three healthy subjects measured every one-hour for a total of four hours. It is observed that the levels are <12 pg/mL for IL-6, IL-8 and IL-10. Although, a slight increase was observed in subject 2 and subject 1 for IL-6 and IL-8 respectively at T2 and T3 hours of measurement, the levels do not change significantly over time. Subject 3 demonstrated higher cytokine levels as compared to subjects 1 and 2. While the exact reason for this is unknown, there may be several factors including dietary intake that may have influenced the levels and will require further investigation. Next, we wanted to understand if the levels of cytokines change over days. Cytokine levels for IL-8 and IL-10 were measured over 4 successive days (Fig. 3.7D). The results demonstrate that cytokine levels remained <12

pg/mL and did not change significantly over the measured time period ( $p>0.05$ ). While this work demonstrates the proof-of-feasibility of wearable sweat sensing platform for continuous monitoring through affinity-based mechanism, future efforts can be emphasized in implementing methods to regenerate the sensor surface of affinity-based assays for enhancing the performance for continuous monitoring[65]. However, we believe that these results provide a basis for future exploration on continuous monitoring of cytokines for various inflammatory/infectious diseases.

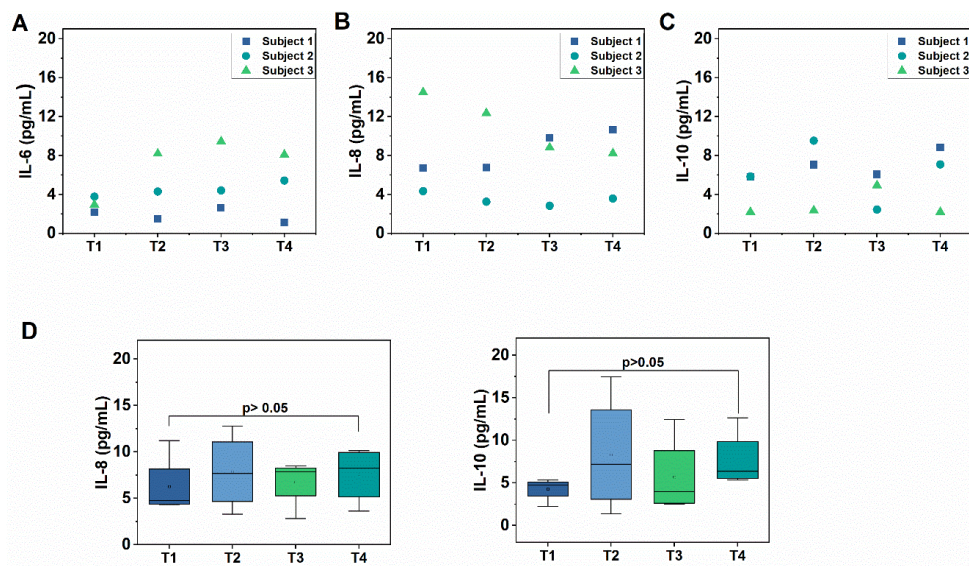


**Figure 3.7. On-body continuous monitoring of cytokines.** (A, B, C) SWEATSENSE demonstrates levels of biomarkers in 3 subjects measured every 1 hour. (D) Box-plot of IL-8 and IL-10 in multiple healthy volunteers measured across various time-points in a day demonstrating there is no significant change in cytokine levels over time in healthy cohort.

### 3.5.5 Clinical utility of SWEATSENSE for infection detection from eccrine sweat

The SWEATSENSE was then used to identify the levels in the sick cohort and compare to the serum levels to demonstrate the technology's feasibility for non-invasive monitoring of inflammatory response (Fig. 3.8A). Ten healthy subjects and five sick subjects were recruited in

compliance with the approved IRB protocol. Among the five patients, three were male and two were female. All the subjects were taking medications. The description of sickness type of each patient has been described in Fig. 3.8B. A comparison of IL-8 levels between healthy and sick cohort in passively expressed sweat was performed. Fig. 3.8C shows the SWEATSENSE worn by a subject. While real-time monitoring of infection-related cytokine markers using SWEATSENSE can offer significant strides in tracking infection, it is also important to understand how sweat cytokine levels compare to its systemic circulation. Fig. 3.8D shows a comparison of IL-8 serum levels to SWEATSENSE measured IL-8 levels from passively expressed sweat in healthy and sick cohort. Sweat IL-8 levels are in the similar range as the serum IL-8 levels of 2-15 pg/mL. The slopes of serum to sweat levels follow a similar pattern among most healthy subjects with sweat levels lower than that of serum, thus showing a definitive relationship between serum to passively expressed sweat cytokines. An average sweat to serum ratio of IL-8 ~1.01 from nine volunteers (one data point excluded as an outlier) was obtained. Further, a similar relationship was observed in a patient cohort of five subjects. These results confirm that the levels of IL-8 in sweat can be correlated to that in circulation. IL-8 levels in patient cohort are relatively higher in serum and sweat compared to the healthy cohort. A statistical significance  $p<0.05$  using ANOVA ( $\alpha=0.05$ ) for IL-8 was determined between healthy and sick cohort for both serum and sweat, thus, demonstrating that eccrine sweat may be used for determining infections. In the sick cohort, levels were comparable between female and male subjects. Four subjects were mildly sick with symptoms such as fever, cough and chills, while one subject tested flu positive (Fig. 3.8B). These results present some interesting perspectives and signify the role of non-invasive sweat-based monitoring for diagnosis and prognosis of

diseases. Subjects 2 and 5 demonstrated similar kind of symptoms. Three subjects had fever at the time of measurement while two subjects did not have fever at the time of sample collection, but experienced other inflammatory or viral infection symptoms as described in the Fig. 3.8B. However, these two subjects also had fever on the previous days prior to sample collection. All the subjects had taken fever reducing medication. It should be noted that subject 4 was sicker compared to other patients as this patient tested flu positive while, others had minimal fever. This is also reflected in higher IL-8 levels in serum and sweat, of subject 4 than other subjects in the sick cohort. Interestingly, the levels in patient cohort were not extremely elevated and closer to the healthy cohort, although the levels of sick cohort are statistically significant from the healthy cohort. We hypothesize the relatively lower levels were probably because the samples (serum and sweat) were collected at least 2-3 days after the occurrence of illness. It could also be that these patients were taking medication and were in their recovery phase. However, the key takeaway from this study is that such nuanced changes in levels can be effectively captured by the SWEATSENSE to identify illness. Further, the finding that the levels of sweat in healthy subjects is lower compared to the sick cohort demonstrates the significance of continuous monitoring of illness in real-time. These preliminary results present an understanding on the relationship between systemic circulation levels of cytokines to that of circulation in passive eccrine sweat. Thus, setting the path for future studies to explore and validate serum to sweat relationship for enabling sweat analytics as a clinical diagnostic platform for non-invasive, robust and pre-symptomatic tracking of infection. As a proof-of-feasibility, we first evaluated with IL-8. Future studies will focus on evaluation of other cytokine biomarkers.

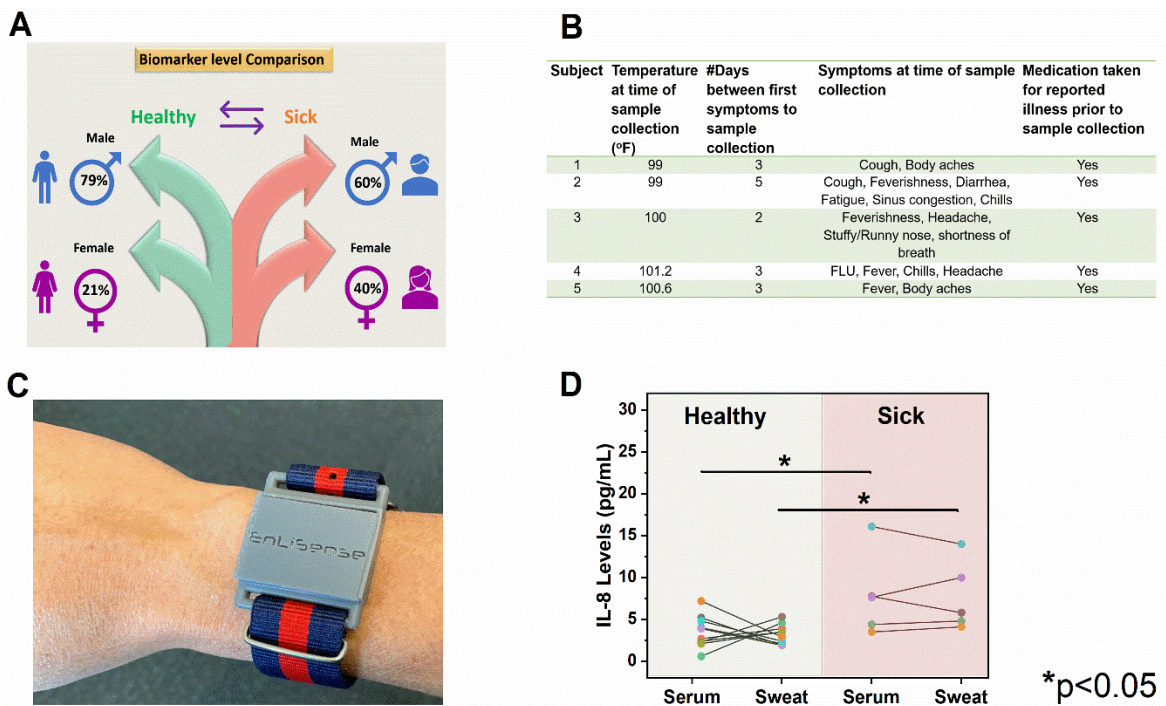


**Figure 3.8. Serum to sweat IL-8 levels in healthy and Sick cohort.** (A) Schematic of subjects recruited for serum to sweat correlation. (B) Details of vitals and illness of each individual in sick cohort. (C) SWEATSENSER device worn on hand by a subject recruited for the study. (D) Comparison of IL-8 levels between healthy(n=10) and sick cohort (n=5). The levels between serum to sweat are also compared for each subject. Statistical significance  $p<0.05$  was achieved between healthy and sick cohort using ANOVA ( $\alpha=0.05$ ) in both serum and sweat.

### 3.6 Conclusion

This work establishes a wearable technological platform that can detect infection/inflammation non-invasively from eccrine sweat. Such a technological platform can empower users with actionable data for necessary precautions even prior to experiencing infection symptoms. The ability demonstrated by the SWEATSENSER in differentiating biomarker levels between healthy and sick cohort in passively expressed eccrine sweat will offer new insights to clinicians for better management and prognosis of inflammatory/infectious diseases. The agreement between the developed device and state-of-art reference method through pre-clinical healthy

cohort studies establishes the usability of SWEATSENSEr device for on-field testing. the correlations established between serum to sweat IL-8 levels and the ability of identifying illness using SWEATSENSEr will be of significant interest to researchers, clinicians to look at sweat as an alternative biofluid for improving therapeutic diagnosis and prognosis of several inflammatory/infectious diseases.

### **3.7 Acknowledgments**

We thank Paul Rice for fabrication of SWEATSENSErS, Sayali Upasham for SEM/EDX characterization and Ambalika Tanak for helping with the schematics. We would like to thank Dr. Sita Boppana at Boppana Primary Care Clinic, Richardson for helping with blood sample collection. This project has been funded in whole or in part with Federal funds from the Department of Health and Human Services; Office of the Assistant Secretary for Preparedness and Response; Biomedical Advanced Research and Development Authority, DRIVe, under the contract HHSO100201800026C awarded to EnLiSense LLC.

## **CHAPTER 4**

### **NOVEL APPROACH TO TRACK THE LIFECYCLE OF INFLAMMATION FROM CHEMOKINE EXPRESSION TO INFLAMMATORY PROTEINS IN SWEAT**

#### **4.1 Abstract**

Inflammatory biomarkers are modulated during the course of any infectious disease, and currently, there is no wearable technology that enables patient management through non-invasive monitoring of these markers. This work is the first demonstration of the discovery and quantification of interferon-inducible protein (IP-10) and tumor necrosis factor-related apoptosis-inducing ligand (TRAIL), two key prognostic markers of infection in human sweat. The levels of IP-10 and TRAIL in sweat were quantified, validated and confirmed using a standard reference method through pre-clinical human subject studies. Additionally, we demonstrate simultaneous and continuous detection of IP-10, TRAIL and C-reactive protein (CRP), for infection monitoring in sweat using a wearable SWEATSENSE device. The SWEATSENSE is ultra-sensitive with a limit of detection of 1 pg/mL (IP-10 and TRAIL) and 0.2 ng/mL (CRP) with a wide dynamic range. Bland-Altman analysis demonstrated good agreement between SWEATSENSE and standard reference methods through human subject studies. Serum to sweat relationship demonstrated the potential of the SWEATSENSE to track infection etiology.

#### **4.2 Introduction**

Infectious diseases cause over 17 million deaths every year worldwide [66]. When a pathogen enters the host, cytokines and chemokines act as mediators for information exchange between the host tissue cells and the immune system[67]. Several studies have reported elevation of pro-inflammatory chemokines in blood in the early stages of an infection[26], [68] including the

current ongoing COVID-19 pandemic[32], [69]. The temporal profile of cytokine and chemokine accumulation in response to the infection event determines the time course and severity of infection within the host. Hence, monitoring temporal profiles of cytokines and chemokines can aid in pre-symptomatic detection and patient stratification towards evidence-based clinical management. Interferon-inducible protein (IP-10) and tumor necrosis factor-related apoptosis-inducing ligand (TRAIL) in combination with C-reactive protein (CRP) are considered highly relevant biomarkers in patients suffering from viral or bacterial infections[70], [71]. The levels of these biomarkers in blood have been reported to be elevated during bacterial and viral infections that can lead to serious conditions including sepsis and acute respiratory distress syndrome. Oved et al., described the combination IP-10, TRAIL, and CRP as a triage for determining and classifying bacterial or viral infection[70]. Elevated levels of IP-10 were also reported in COVID-19 positive patients [72], [73]. Further, elevated IP-10 levels were observed in severe acute respiratory syndromes (SARS) caused by SARS CoV, SARS CoV2, and Middle East Respiroatory Syndrome (MERS) coronaviruses [32], [74]–[76]. IP-10 is considered to be a definitive marker of respiratory infections as lung epithelial airways cells are the prime generators of IP-10 [75], [76]. Several studies including our group have previously reported the levels of cytokines in human sweat (primarily TNF- $\alpha$ , IL-6, IL-8) mimicking that of serum[42], [43]. We have previously demonstrated the presence of CRP in sweat [61]. However, there have been no reports on the detection of IP-10 and TRAIL in human sweat. This work highlights for the first time the quantification of IP-10 and TRAIL in healthy human sweat and its correlation to serum through an enabling wearable SWEATSENSE device. The discovery of the presence of these biomarkers in sweat was also cross-validated using commercial reference methods such

as ELISA and Luminex. The SWEATSENSE device we have developed employs a sweat sensing strip mounted onto a wearable electronic reader for simultaneous detection of IP-10, TRAIL, and CRP from passive eccrine sweat in a real-time continuous manner toward enabling patient-centric monitoring for infectious diseases. The concentration measurement of the study markers was cross-validated with standard immunochemistry reference methods. Further, we demonstrate real-time continuous monitoring of the study markers from passive eccrine sweat in healthy human subjects over 6 hours. Serum to sweat correlations in healthy cohort for these markers demonstrate that the levels in sweat are in a comparable range to the circulation levels providing promising evidence to further explore sweat as a biofluid for non-invasive monitoring of infection. The SWEATSENSE device can help act as an early warning system from infectious diseases and prevent severe effects such as cytokine storm through continuous monitoring of infection markers.

#### **4.3 Pathway of IP-10 and TRAIL**

Fig. 4.1A outlines the signaling pathway involving IP-10 production in epithelial cells which leads to activation of cellular defenses. In the infected host, pattern recognition systems lead to stimulation of IFN- $\gamma$  and TNF- $\alpha$  which, in turn cause the release of IP-10 through the JAK/STAT1 mechanism [77]. This mechanism activates innate immunity by T<sub>h1</sub> cells in response to pathogen attack[78], [79]. TRAIL plays a key role in immunotherapy and is critical in inducing apoptosis[80], [81]. Fig. 4.1B provides a detailed description of TRAIL production, reaction mechanism to an inflammatory response, and phenomenon of apoptosis. In response to an infection, TRAIL binds to its receptors (TRI and TRII) leading to activation of cysteine dependent aspartate directed proteases (caspase-3,8,9) [82] which, in turn initiate apoptosis and

pathogen clearance. Rapid increases in TRAIL are indicative of host cell inflammation caused by a number of bacterial pathogens[83]. Evaluating the levels of IP-10, TRAIL and CRP can help determine bacterial or viral infection. In the case of a viral infection, IP-10, TRAIL and CRP are up-regulated while, for a bacterial infection IP-10 and CRP are upregulated but TRAIL is down-regulated[70]. In the case of severe infections, over-expression of these pro-inflammatory markers can result in a phenomenon called ‘cytokine storm’ leading to deleterious effects even in diseases such as COVID-19 and influenza. Therefore, monitoring the temporal dynamics of IP-10, TRAIL and CRP levels can be pivotal for patient stratification in infectious disease management and serve as an early warning system perhaps from an impending cytokine storm.

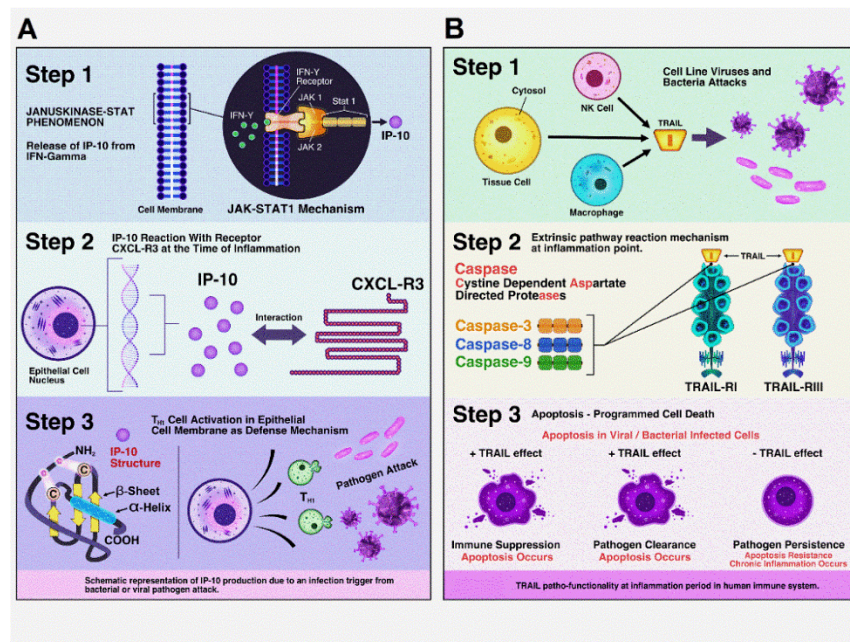


**Figure 4.1. Pathophysiology of IP-10 and TRAIL due to an infection. (A)** Schematic representation of IP-10 production due to an infection trigger from bacterial/viral pathogen. **(B)** Schematic representation of TRAIL production and apoptosis mechanism in cell line due to an infection trigger from bacterial/viral pathogen.

#### **4.4 Materials and Methods**

**Reagents and Instrumentation:** The cross-linker DTSSP and PBS were purchased from Thermo Fisher (MA, USA). Capture probe monoclonal antibodies (mAb) and recombinant proteins for IP-10, TRAIL and CRP were purchased from Abcam (MA, USA). ELISA kits were purchased from Invitrogen (CA, USA) for IP-10 analysis and R&D systems (MN, USA) for TRAIL.

**Sensor Immunoassay Functionalization:** 10 mM DTSSP thiol cross-linker was mixed in a 1:1 volumetric ratio with 10 µg/mL of each monoclonal IP-10, TRAIL, or CRP capture antibody individually. The DTSSP/Antibody solution was immobilized separately on the sensing electrode surface i.e. only one type of capture probe antibody was immobilized on each sensing electrode. The incubation period was for about 1 hour to allow thiol cross-linker to bind on the electrode surface. The cross-linker couples to the ZnO electrode surface via a strong covalent thiol chemistry while, the antibody end is used to capture the target molecule. We have demonstrated the thiol-based mechanism for functionalization previously[84]. The sensors were used immediately after functionalization for calibration and human subject studies. For the repeatability and stability studies, the sensors were lyophilized after immobilization with capture probe antibody and stored in 4°C until use.

**Electrochemical Characterization:** Gamry potentiostat was used for electrochemical characterization techniques such as Equilibrium potential, chronoamperometry and Nyquist response using EIS. Equilibrium potential was measured for 300 seconds. For chronoamperometry measurements, a potential bias of -0.25 V was applied and the response was

measured for 12 sec. Non-faradaic EIS was implemented to determine the sensor response for varying concentrations of target biomarker over a frequency range of 1 Hz- 1 MHz with a sinusoidal input voltage of 10 mV [85]. The resulting impedance owing to the binding of the target molecule to the capture probe antibody was recorded. A calibration curve was developed by measuring the impedance response at optimized frequency of 180 Hz for varying concentrations of the target marker.

**Human subject enrollment sweat sample collection, and handling:** 18 human subjects for sweat sample collection in compliance with the protocol approved by Institutional Review Board (IRB) at the University of Texas at Dallas (IRB# 19-136) were enrolled. Consent was taken from all participants prior to sample collection. After enrolling the subject for the study, an FDA approved Macrproduct sweat inducer and collector was used to collect the sweat samples for validation using reference method. The collected sweat was then immediately aliquoted and stored in -80°C until further use. In order to perform serum to sweat correlations, a blood draw was performed by a physician. Within 5 minutes of blood sample collection, the SWEATSENSOR device was placed on the wrist region and measured for one to two hours. The obtained sweat concentration was correlated to serum level.

**Reference method analysis:** Reference methods such as ELISA and Luminex were used to establish correlations with SWEATSENSOR for both the markers, IP-10 and TRAIL. The IP-10 assay kit had a dynamic range of 0- 500 pg/mL with a LOD of < 2pg/mL, while the TRAIL assay kit had a dynamic range of 7- 5600 pg/mL with a LOQ of 7.4 pg/mL. The dynamic range for CRP was 0.4- 30 ng/mL with a LOQ of 0.43 ng/mL. Absorbance at 450nm was used to read the O.D response and determine the levels of biomarkers in samples.

**On-body SWEATSENSE measurements on human subjects:** All enrolled subjects wore the SWEATSENSE device during testing. Continuous measurements were recorded in compliance with the protocol approved by the IRB committee. The wearable sweat sensor device was placed on the lower forearm of the subject and sampled every minute for the duration of testing. The SWEATSENSE also houses a temperature and RH sensor to measure skin temperature and the sweating profile respectively.

## 4.5 Results and Discussion

### 4.5.1 Characterization of Capture probe antibodies

The charge stability of the capture probe antibodies in sweat biofluid was characterized using Zeta potential (ZP). Electrophoretic mobility of the capture probe antibodies was measured and the corresponding ZP was determined using the equation:

$$\mu = \frac{\epsilon \zeta}{\eta} \quad (4)$$

Where,  $\mu$ - Electrophoretic mobility,  $\epsilon$ - dielectric constant,  $\eta$ - dynamic viscosity of buffer solution and  $\zeta$ - Zeta potential

ZP also indicates the over-all charge-complex of the molecule. The measured electrophoretic mobility is represented in Fig. 4.2 (A-C) for all 3 antibodies and the conjugation of the specific antibody to the protein. Fig. 4.2 (D-F) represents the zeta potential of capture probe antibody for 3 study marker and the charge modulation due to the binding of specific target marker to the antibody. Here in, first the zeta potential of blank PBS buffer was measured in which the antibody is diluted. It can be observed that blank buffer consisting of ions has a very low zeta

potential of -4 mV. The magnitude of zeta potential of antibody is higher as compared to the blank buffer due to the charge moieties of the antibody. Further, it can be observed that the high charge-complex of the antibody confirms it is stable and does not aggregate as the zeta potential is beyond the isoelectric point (point of zero charge). Further, upon binding of specific target protein in sweat to the corresponding antibody, the over-all charge-complex gets modulated and the magnitude of zeta potential increases. This is due to the modulation of the electrical double layer formed around the antibody-antigen complex. These results demonstrate that the antibody is stable upon interaction with sweat buffer and confirm the binding of target marker to the specific antibody.

#### **4.5.2 SWEATSENSEr device metrics for IP-10, TRAIL, CRP measurements**

We demonstrate here, a multiplexed SWEATSENSEr that can detect simultaneously and continuously the three biomarkers under study. Firstly, a calibration curve was developed for n=4 measurements by dosing varying concentrations of the biomarkers in human sweat on the sensors individually functionalized with specific IP-10, TRAIL and CRP monoclonal antibodies. The SWEATSENSEr leverages electrochemical impedance spectroscopy for a highly sensitive response.

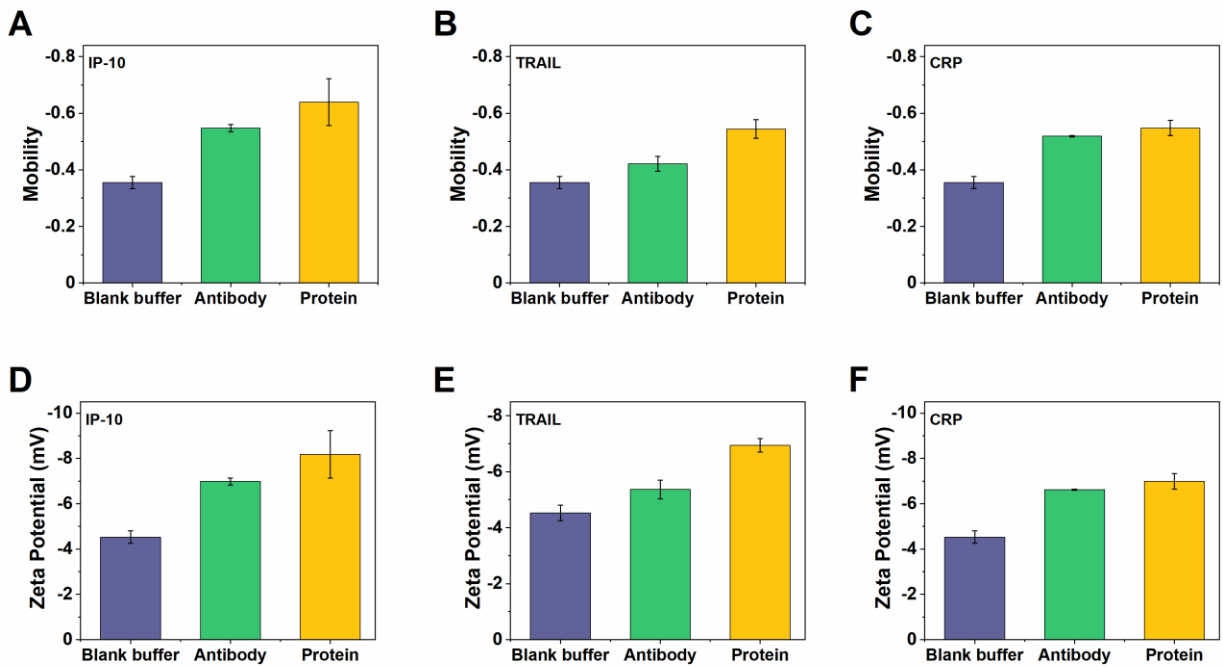


Figure 4.2. (A-C) Electrophoretic mobility demonstrating stability of specific capture antibody and binding of target protein to antibody of IP-10, TRAIL, and CRP in sweat buffer. (D-F) Zeta potential characterization demonstrating stability of antibody and binding of specific target protein to antibody of IP-10, TRAIL and CRP. The increasing magnitude of Zeta potential from blank buffer confirms the stability and charge of the antibody and protein.

Non-faradaic impedance spectroscopy measures subtle changes of the affinity-based interaction between the specific primary antibodies to the target analyte, resulting in an amplified impedance signal response [19]. Fig. 4.3(A -C) demonstrates the Nyquist response of the sensor for varying concentrations of the study biomarkers. As this is a non-faradaic method of detection (i.e. without the use of Redox probes), the binding interactions can be captured as modulation of double layer capacitance ( $C_{dl}$ ) which can be observed as Zimagine changes (Fig. 4.3A-C). Further, the SWEATSENSE was also evaluated using chronoamperometry to confirm the binding of the target marker to the specific capture probe (Fig. 4.3D-F). Chronoamperometry measures the current response owing to the binding interactions with respect to time when a

constant direct current (DC) potential is applied. Typically, the chronoamperometric response is characterized as (i) quick charging of the electrical double layer (EDL) followed by (ii) discharge of the EDL with time due to the binding between the capture probe antibody and target biomarker when operated in non-faradaic mode. The magnitude of the current response due to binding events can be represented as

$$|I| \propto e^{\frac{-t}{RC}} \quad (5)$$

Where, I- Current response, R-solution resistance, C- double layer capacitance

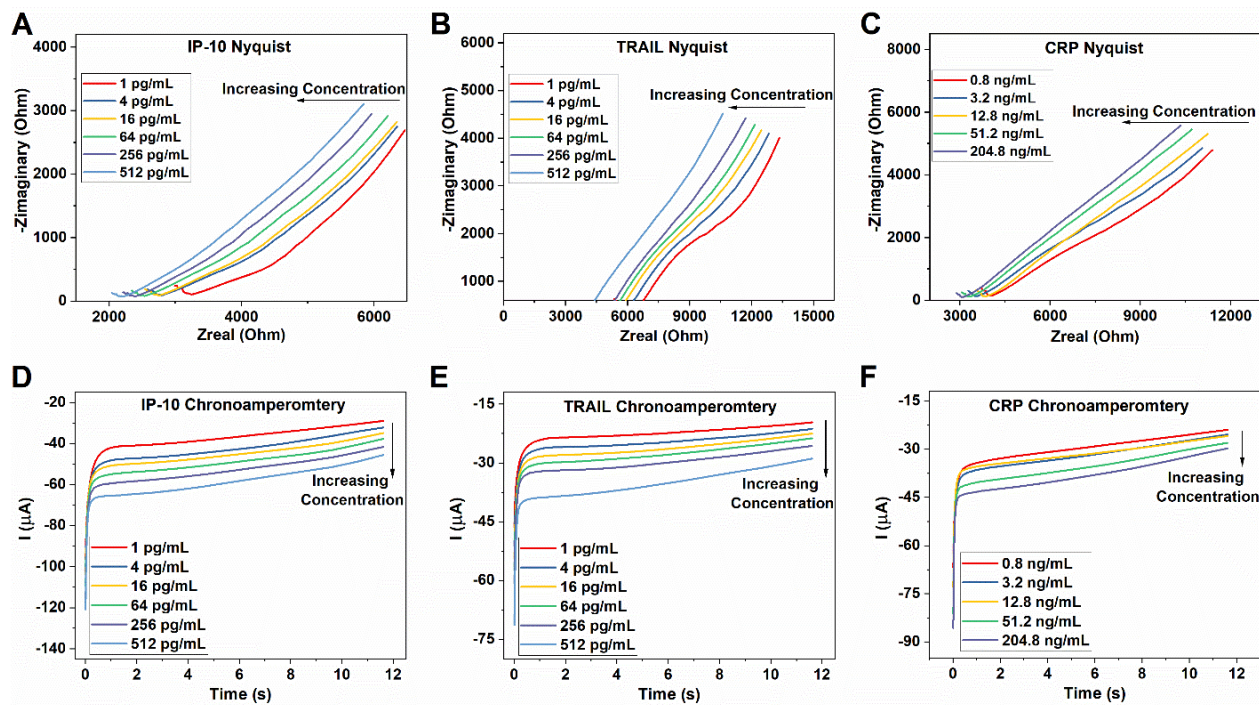


**Figure 4.3. Electrochemical characterization of SWEATSENSOR.** (A-C) Nyquist response of SWEATSENSOR for study markers (A) IP-10, (B) TRAIL and (C) CRP using non-faradaic electrochemical impedance spectroscopy. (D-F) Chronoamperometric response of SWEATSENSOR for (D) IP-10 (E) TRAIL and (F) CRP in sweat.

As observed from the plots in Fig. 4.3D-F, the magnitude of the current response increases with increasing concentration. These results confirm a higher double layer capacitance with increasing concentration of target marker. These results corroborate with impedance spectroscopy response and cross-validate the binding interactions on the sensor surface using two electrochemical methods. High affinity of the capture probe to the target biomarker was determined with  $K_d$  values in the lower pM range (Fig. 4.4A,B) for IP-10 and TRAIL respectively and in lower nM range (Fig. 4.4C). The SWEATSENSOR demonstrated a dynamic range of 1-512 pg/mL for both IP-10 and TRAIL and 0.2- 204 ng/mL for CRP in sweat. Limit of detection of 1 pg/mL for IP-10 and TRAIL, and 0.2 ng/mL for CRP was achieved which was calculated as 3 times the standard deviation of blank. We then validated the sensor performance metrics through spike & recovery, specificity, repeatability, and stability studies.

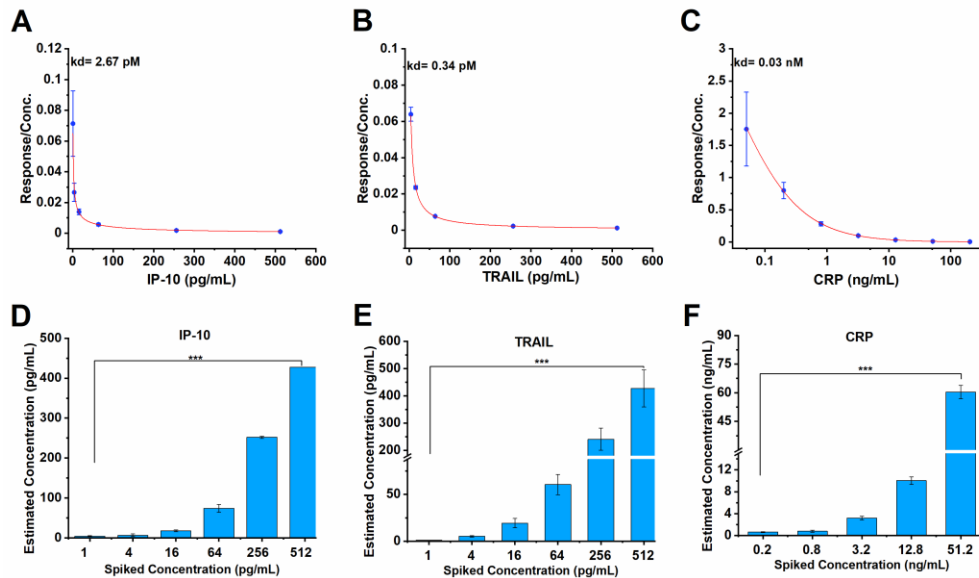


**Figure 4.4. SWEATSENSOR device metrics.** (A-C) Binding efficacy determined using  $K_d$  value through saturation-binding study for (A) IP-10, (B) TRAIL, (C) CRP. (D-F) Spike & Recovery response of SWEATSENSOR for (D) IP-10, (E) TRAIL and (F) CRP. The data is presented as Mean $\pm$  SEM for  $n\geq 4$  measurements.

We evaluated whether the sensor could accurately detect spiked concentrations of the biomarkers from 1-512 pg/mL for IP-10 and TRAIL (Fig. 4.4D,E) for  $n \geq 3$  individual measurements. CRP was measured at an elevated range from 0.2- 50 ng/mL as demonstrated in Fig. 4.4F. Additionally, analysis of variance (ANOVA) was performed to determine the statistical significance of the sensor in differentiating the spiked dose concentrations. A significance  $p < 0.001$  with a 95% C.I. between the measured dose concentrations confirmed the ability of the SWEATSENSOR to reliably detect the study markers in sweat. Further, the SWEATSENSOR demonstrated excellent selectivity, with negligible to no signal response for non-specific molecules. Each specific capture probe functionalized sensor was evaluated by spiking high concentration (512 pg/mL) of non-specific molecule as demonstrated in Fig. 4.5 i.e. on IP-10 antibody functionalized sensor, non-specific TRAIL antigen (512 pg/mL) was spiked and vice versa. It can be observed that the response to non-specific molecule is negligible compared to the specific response. Here, as a proof-of-feasibility we demonstrated for IP-10 and TRAIL. However, similar response can be anticipated for CRP as it is a larger molecule.

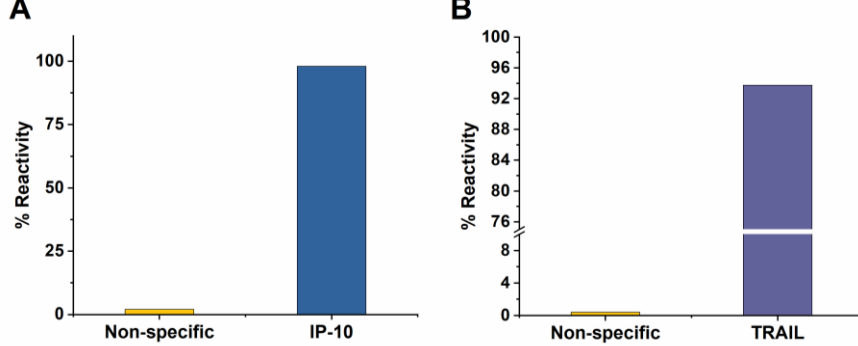


Figure 4.5. SWEATSENSOR specificity response. **A)** Sensor functionalized with IP-10 antibody was dosed with non-specific TRAIL (256 pg/mL) and low response is observed while, a high reactivity for specific IP-10 was achieved. **B)** Sensor functionalized with TRAIL antibody was

dosed with non-specific IP-10 (256 pg/mL) and low response is observed while, a high reactivity for TRAIL was achieved.

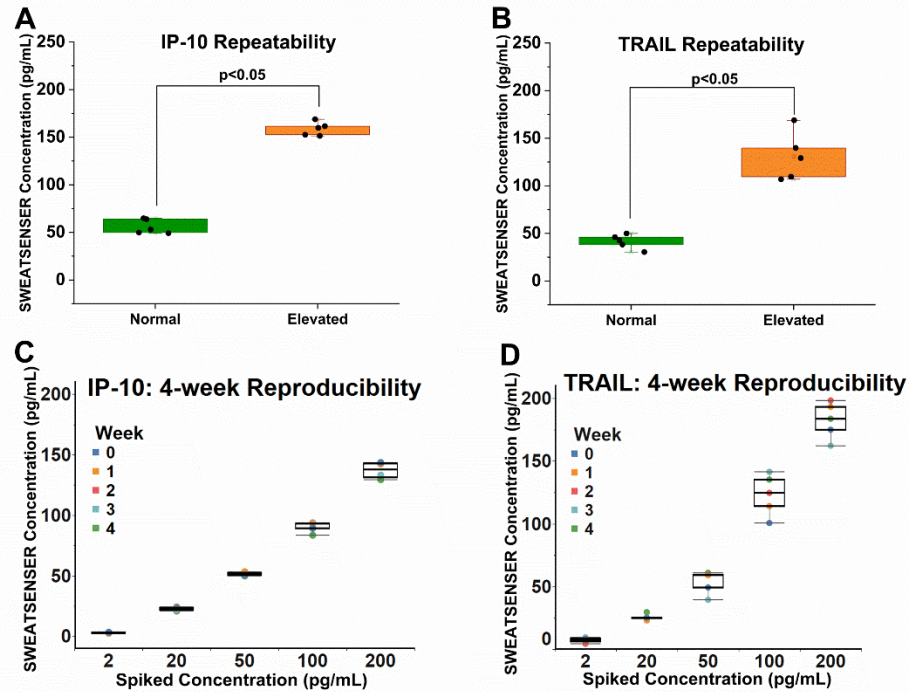
Next, the sensor was tested for its repeatability and stability which are key metrics for real-world use applications. The repeatability study provided an insight on the sensor's ability to accurately determine the levels on repeated basis i.e. a reliable sensor must demonstrate similar response for the same concentration level when repeated multiple times. In order to validate this, n=4 measurements for each concentration of IP-10 and TRAIL were measured. The sensors were dispensed with 50 pg/mL and 150 pg/mL concentrations of the specific target and the corresponding response was measured. Fig. 4.6A,B demonstrate that the sensor accurately measured the concentrations over multiple measurements. The sensors measured a concentration of  $56.2 \pm 3.3$  pg/mL and  $158.8 \pm 3.1$  pg/mL for the dosed concentrations levels on IP-10 antibody functionalized sensors (Fig. 4.6A). Similarly, the sensor reported  $41.5 \pm 3.3$  pg/mL and  $130.8 \pm 11.3$  pg/mL for the spiked 50 pg/mL and 150 pg/mL concentrations for TRAIL functionalized sensors as demonstrated in Fig. 4.6B. Furthermore, a statistical t-test confirms that the sensor can reliably distinguish the two levels with a statistical significance of  $p < 0.001$ (95% C.I). These results confirm that the sensor demonstrates a repeatable response. Next, the response of the SWEATSENSE was measured over time and assessed if a stable response will be obtained over a period of 4 weeks. The results over the measured 4 weeks for spiked concentrations of 2, 20, 50, 100 and 200 pg/mL respectively are represented as box plots (Fig. 4.6C,D). The non-overlapping inter-quartile ranges (IQRs) of the box plots confirm that the developed sensor system demonstrates excellent reproducibility and stability. The sensor showed similar response to the spiked concentrations with coefficient of variation ( $CV < 10\%$ ) over the 4 weeks, further validating the reproducibility of the developed sensor for both IP-10 and TRAIL.

Furthermore, a statistical ANOVA for the obtained response was performed which confirmed that the measured concentrations can be reliably distinguished with  $p<0.001$ . These results confirm that the SWEATSENSE shows reliable performance metrics.

#### **4.5.3 Validation of IP-10, TRAIL, and CRP in eccrine sweat of healthy cohort**

The SWEATSENSE's pre-clinical utility was validated after establishing the performance metrics. We first evaluated if these markers can be detected and quantified in sweat. In order to determine this, levels of study markers in healthy human subjects were measured using both the SWEATSENSE and the standard reference method. Next, the SWEATSENSE reported levels were compared with the reference method to determine the degree of agreement between the two methods. Unlike the SWEATSENSE device that measures biomarkers levels directly from passively expressed sweat, the reference method requires an external sweat collect system to collect sample from the human subject. For this analysis method and to preserve the sweat sample source integrity, FDA approved Macrodust sweat inducer and collection device was used to get sweat from 18 healthy subjects. Table 4.1 provides details on the enrolled subjects. The macrodust sweat collection involves stimulation of the sweat glands in the brachioradialis muscle region of the arm for 5 minutes using the provided pilocarpine discs. After stimulation, a sweat collector was placed in the stimulated region and sweat was collected for ~45 minutes. The adopted method of sweat collection is widely used for cystic fibrosis diagnosis and other sweat biomarkers [86]. The collected sweat samples were then used for measuring the concentration levels using reference method and SWEATSENSE. Although there have been several studies that have reported the detection of various biomolecules in sweat such as glucose, cortisol,

interleukins [84] this work is the first investigation to determine the presence of IP-10 and TRAIL in human sweat. Similar response is expected for CRP as it is larger and stable molecule.



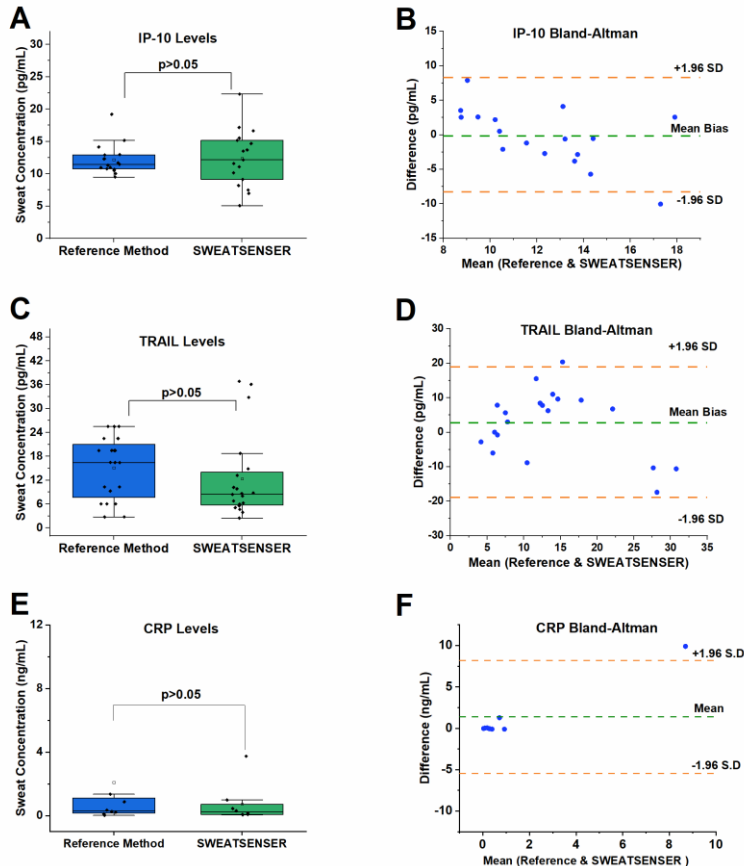
**Figure 4.6. SWEATSENER performance metrics.** (A, B) SWEATSENER repeatability for (A) IP-10; (B) TRAIL demonstrating ability to differentiate normal and elevated concentrations. (C, D) Stability of SWEATSENER demonstrating the signal response is retained over 4 weeks (C) IP-10; (D) TRAIL for spiked concentrations from 2- 200 pg/mL.

Table 4.1. Description of the human subject volunteers for IP-10, TRAIL, CRP sweat sample analysis between reference method and SWEATSENER

Human Subject Testing	
# of Subjects	18
Age Range	18-65 years
Gender	Male: 14; Female: 4
Medication Consumption	None
Health Condition	Healthy Individuals; No reported condition of illness, fever or infection

Fig. 4.7A demonstrates the sweat levels of IP-10 in the healthy cohort from both the SWEATSENSE and the reference method. It is observed that IP-10 levels in sweat range from 10-20 pg/mL in healthy human subjects for the macrourine induced sweat. A statistical t-test was performed which confirms there is no significant difference in the levels reported between reference method and SWEATSENSE with  $p>0.05$  (95% C.I.). Additionally, Bland-Altman (BA) analysis was performed to validate the degree of agreement of SWEATSENSE with the reference method (Fig. 4.7B). Typically, in a BA plot the mean bias should be very close to zero indicating there is no difference between the 2 methods. The BA result in Fig. 4.7B shows a mean bias of 0.2 pg/mL with all the measured points lying within the  $\pm 1.96$  S.D (95% C.I. line) confirming that the SWEATSENSE demonstrates good agreement with reference method. Furthermore, the measured data points were scattered in a random order in and around the mean bias indicating that no method over predicts or under predicts as compared to the other. Similarly, Fig. 4.7C demonstrates similar sweat levels of TRAIL for both the SWEATSENSE and reference method ranging between 5- 20 pg/mL. A statistical insignificance  $p>0.05$  (95% C.I.) was determined between the 2 methods. The BA result in Fig. 4.7D for TRAIL shows a mean bias of 2.5 pg/mL with all the measured points lying within the  $\pm 1.96$  S.D (95% C.I. line) confirming that the SWEATSENSE demonstrates an agreement with the reference method. On the other hand, CRP levels were in the range 0.05- 3 ng/mL in healthy as demonstrated in Fig. 4.7E. The BA plot for CRP shows a mean bias of 1.34 ng/mL and all data points except one lie within  $\pm 1.96$  S.D (Fig. 4.7F). It should be noted that only 8 samples were analyzed for CRP as the volume obtained from stimulated sweat from some subjects was insufficient to measure all 3 biomarkers using the reference method. This is a major constraint of the reference methods that

require high sample volume for a single measurement. In contrast, the SWEATSENSE device requires ultra-low volumes of passive sweat to measure levels of biomarkers in real-time. The obtained results thus, validate the pre-clinical utility of SWEATSENSE device to quantitatively detect IP-10, TRAIL and CRP levels in human sweat.



**Figure 4.7. Pre-clinical utility of SWEATSENSE in healthy cohort.** (A,C,E) Box plots demonstrating (A) IP-10, (C) TRAIL and (E) CRP levels reported by SWEATSENSE and reference method. (B,D,F) Bland-Altman analysis signifying good agreement between SWEATSENSE and reference method for (B) IP-10, (D) TRAIL and (F) CRP with low mean Bias and all the points within  $\pm 1.96$  S.D.

#### 4.5.4 On-body measurements in healthy human subjects using SWEATSENSE

Continuous on-body monitoring was performed to better demonstrate the applicability of the wearable SWEATSENSE for real-time applications. The SWEATSENSE device was

mounted on the wrist of the subject (Fig. 4.8A). In compliance with the IRB, subjects were only allowed to wear the SWEATSENSE in the laboratory and office space where the testing was conducted to ensure all the data was from passively expressed sweat with no external stimulation. Fig. 4.8B shows a stable measurement of IP-10 and TRAIL recorded from one of the subjects over 3 time points in a day. Each time point represents the concentration levels recorded over two hours. As shown in the figure, a mean concentration of 30 pg/mL and 35 pg/mL was obtained for IP-10 and TRAIL respectively. It can be observed that the levels of these markers do not vary within the day. It should be noted that the measured levels are from 100% passively expressed eccrine sweat from the volunteer and that there was no iontophoresis or any external stimulation performed prior to testing. This study provides a proof-of-feasibility that a wearable SWEATSENSE device sampling passively expressed human sweat in real-time can enable the detection and quantification of biomarkers such as IP-10 and TRAIL that have been associated with classification of bacterial or viral infections. Next, we compared the levels of these biomarkers in sweat to that in circulation (serum) from healthy subjects as per the protocol approved by the IRB. The comparison of serum to sweat levels of each subject is represented in Fig. 4.8C,D. It can be observed that the levels of sweat are in a similar range to that of serum for IP-10 while, TRAIL showed lower values for all the samples. However, the levels of CRP were lower by a factor >100 in sweat compared to serum levels as demonstrated in Fig. 4.9. These results demonstrate that the sweat biomarker levels are in a range comparable to that in serum for IP-10 and TRAIL or can be compared to serum by a weighted factor such as for CRP. These promising results lay the foundation to further explore sweat as biofluid for non-invasive monitoring of inflammatory biomarkers to stratify for infectious diseases.

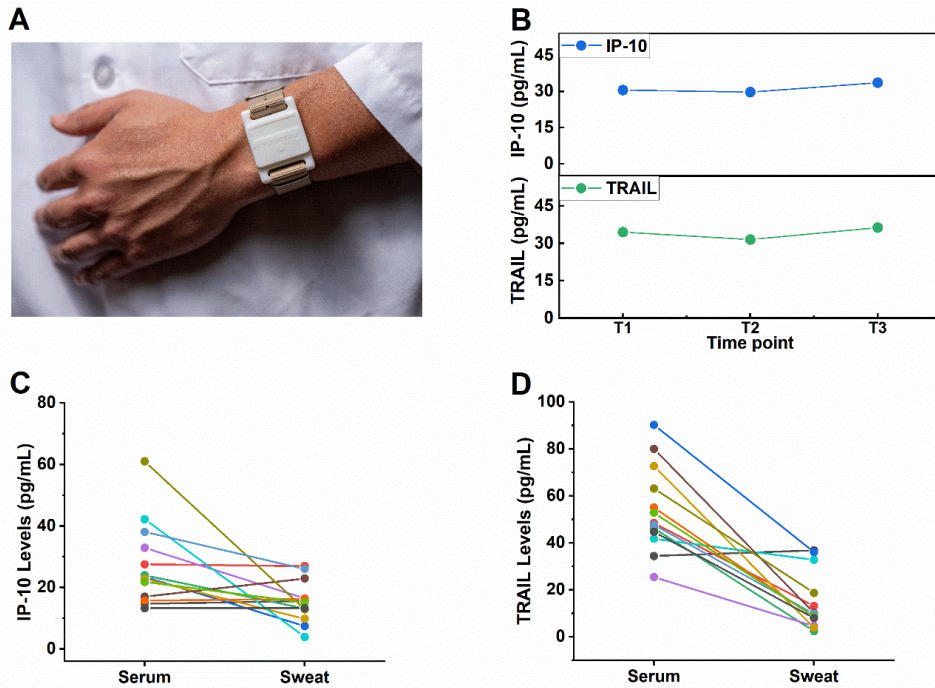


**Figure 4.8. On-body monitoring and validation of relationship between serum and sweat of study markers using SWEATSENSER.** (A) SWEATSENSER device worn on wrist by a subject. (B) On-body continuous monitoring using SWEATSENSER demonstrating stable response of SWEATSENSER for IP-10 and TRAIL measured in two-hour intervals for total of 6 hours in passive eccrine sweat. (C) Serum to sweat levels comparison of IP-10 in healthy cohort. (D) Serum to sweat levels comparison of TRAIL in healthy cohort of n=13 subjects.

#### 4.6 Conclusion

In conclusion, we report here for the first time the detection and quantification of IP-10 and TRAIL in sweat and continuous, direct on-body monitoring from passive eccrine sweat in human subjects. The identification of these biomarkers in sweat from healthy cohort through the pilot study is of significant value as it demonstrates the technology enablement of real-time, continuous monitoring for early pre-symptomatic reporting of an infection event.

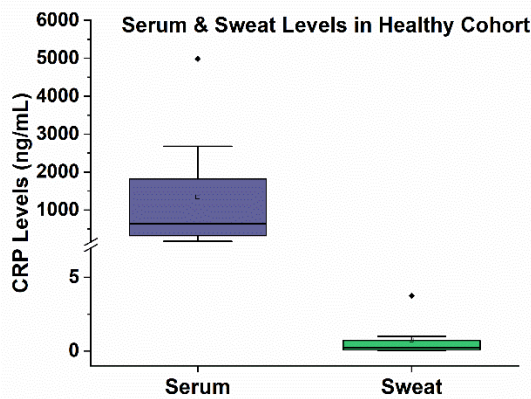


Figure 4.9. Comparison of serum to sweat levels of CRP in healthy cohort.

#### 4.7 Acknowledgements

We thank Paul Rice and MohanRaj Ramasamy for the support with sensor characterization. This project has been funded in whole or in part with Federal funds from the Department of Health and Human Services; Office of the Assistant Secretary for Preparedness and Response; Biomedical Advanced Research and Development Authority, DRIvE, [grant # HHSO100201800026C] awarded to EnLiSense LLC.

## **CHAPTER 5**

### **SWEAT-BASED WEARABLE ENABLING TECHNOLOGY FOR REAL-TIME MONITORING OF IL-1B AND CRP AS POTENTIAL MARKERS FOR IBD**

#### **5.1 Prior Publication**

Badrinath Jagannath (B.J.), Kai-Chun Lin (K.C.L), Shalini Prasad (S.P.), and Sriram Muthukumar (S.M.) conceptualized the study and designed the experiments. B.J., K.C.L, and Madhavi Pali (M.P.) performed the experiments and data analysis. Devangsingh Sankhala (D.S.) designed the wearable reader. B.J., M.P., S.M., S.P., and K.C.L., analyzed and interpreted results. B.J., S.M., and S.P. wrote the manuscript. This work was published in Inflammatory Bowel diseases (<https://doi.org/10.1093/ibd/izaa191>)

#### **5.2 Abstract**

More than 1.2 million people in the United States are affected by inflammatory bowel disease (IBD). IBD has a natural course characterized by alternating periods of remission and relapse. Currently, disease flares are unpredictable as they occur in a random way. Further, current testing methods and practices lack the ability for real-time tracking of flares. There exists no technology that can be utilized for continuous monitoring of biomarkers, as most of these rely on samples such as blood, feces and testing methods by which continuous monitoring is not feasible. Cytokines play a key role in IBD using which the development, recurrence and exacerbation of the inflammatory process is orchestrated by their levels in time and space. Cytokines are also present in sweat. We hypothesize that demonstrating real-time continuous monitoring of IL-1 $\beta$  and CRP may embark an enabling technology to track inflammation in IBD patients and identify flare ups and assess efficacy of therapy. The sensor device can detect

interleukin-1 $\beta$  (IL-1 $\beta$ ) and CRP in sweat over a dynamic range of 3 log orders. Pearson correlation of  $r= 0.99$  and  $r= 0.95$  was achieved for IL-1 $\beta$  and CRP respectively for the sweat sensor with ELISA. This work demonstrates the first proof-of-feasibility of multiplexed cytokine and inflammatory marker detection in passively expressed eccrine sweat in a wearable form-factor that can be utilized towards better management of IBD.

### 5.3 Introduction

IBD is characterized by chronic or recurring immune response where in the intestinal cells are attacked when the body mistakes food, bacteria, and other materials as foreign substances thus, causing inflammation<sup>1</sup>. More than 1.2 million people in the United States are affected by the two common conditions of IBD (ulcerative colitis (UC) and Crohn's disease (CD))[87]–[91]. It is hypothesized that a genetic susceptibility coupled with environmental factors, such as smoking, antibiotics, oral contraceptives, appendectomy, or diet, may influence the development of IBD[92]–[95]. IBD has a natural course characterized by alternating periods of remission and relapse. Currently, disease flares are unpredictable as they occur in a random way for the most part[96]. In order to adequately facilitate treatment decisions and avoid overtreatment, it is necessary to identify benign or unfavorable clinical course[96]. A combination of inflammatory biomarkers may be a viable option for effective IBD management as a single marker is not reliable in predicting an exacerbation or flare[88]–[90], [96]–[98].

Cytokines play a key role in IBD using which the development, recurrence and exacerbation of the inflammatory process is orchestrated by their levels in time and space[99]. They provide key signals in the intestinal immune system. Cytokines may also cause disruption of the normal state of controlled inflammation (physiological inflammation of the gut)[90], [97],

[98], [100]. The inflammation in IBD is orchestrated by lymphocytes and antigen presenting cells, mainly TNF- $\alpha$  which is produced by innate immune cells such as macrophages and differentiated T cells. The pro-inflammatory effects of TNF- $\alpha$  causes increased production of IL-1 $\beta$ , proliferation of fibroblasts and procoagulant factors, and initiation of cytotoxic, apoptotic, acute-phase responses[99]. It is reported that levels of IL-1 $\beta$  increase in CD and UC patients[101]. Vounotripidis et al., demonstrated that the levels of IL-1 $\beta$  are elevated during flares in IBD patients[102]. Furthermore, a significant variation in the genotype frequency of IL-1 $\beta$  promoter was found between control and IBD patients[101]. Additionally, CRP is another inflammatory marker that is usually elevated in the event of an IBD flare[103]. Based on this knowledge set, we hypothesize that demonstrating real-time continuous monitoring of IL-1 $\beta$  and CRP may embark an enabling technology to track inflammation in IBD patients and identify flare ups and assess efficacy of therapy[88]–[90], [97], [98], [104], [105].

However, current testing methods and practices lack the ability for real-time tracking of flares. There exists no technology that can be utilized for continuous monitoring of biomarkers, as most of these rely on samples such as blood, feces and testing methods by which continuous monitoring is not feasible. Sweat is an attractive biofluid for real-time monitoring that can provide plethora of health of information but is less explored, thus far. Sweat contains a range of analytes from ions, metabolites, small molecules to a variety of proteins. In this work, we have demonstrated with the study biomarkers IL-1 $\beta$  and CRP, the technology enablement in detecting and real-time monitoring of host response inflammatory biomarkers from human sweat. It is to be noted that whether the biomarkers are definitively associated with IBD flares have not yet been fully validated, however the cytokine candidates are up regulated during an IBD flare. The

key aspect is that they are also expressed in eccrine human sweat and their temporal dynamics mimics their expression in human serum[42], [43]. For instance, Cizza et al.[42], demonstrated the levels of IL-1 $\beta$ , IL-6, TNF-a in sweat are similar to that of blood in healthy human cohort and patients with major depressive disorder (MDD). Although, it has not been evaluated if the above-mentioned markers are elevated in eccrine sweat during a flare, we hypothesize that the levels of these markers may be elevated in sweat in IBD patients as the sweat dynamics mimics the expression in human serum. Considering the short-comings of the current methods and their inability to support near-patient measurements, we have designed and tested a novel non-invasive sweat sensing device that opens new avenues towards offering effective solutions for management of IBD.

The novelty of this work lies in the enabling of EnLiSense's SWEATSENSE platform for non-invasive, continuous monitoring of inflammatory biomarkers, which may have implications in IBD patient care. Fig. 5.1 illustrates on how the sweat sensor technology can be envisioned in providing better aid for IBD patients. Currently, a patient would experience the symptoms and the flare with a certain delay from the triggering events. This causes a lot of discomfort and trauma to the patient. The key reason being lack of technology that can alarm the patient prior to the occurrence of a flare-up as no continuous monitoring is done. However, we aim to address these technological deficiencies through continuous monitoring of biomarkers using a wearable SWEATSENSE platform that can be utilized as an alarm by monitoring IBD markers to report the occurrence of a flare-up. Hence, the developed sweat sensor can be extremely useful in prognosis and monitoring the efficacy of a treatment therapy.

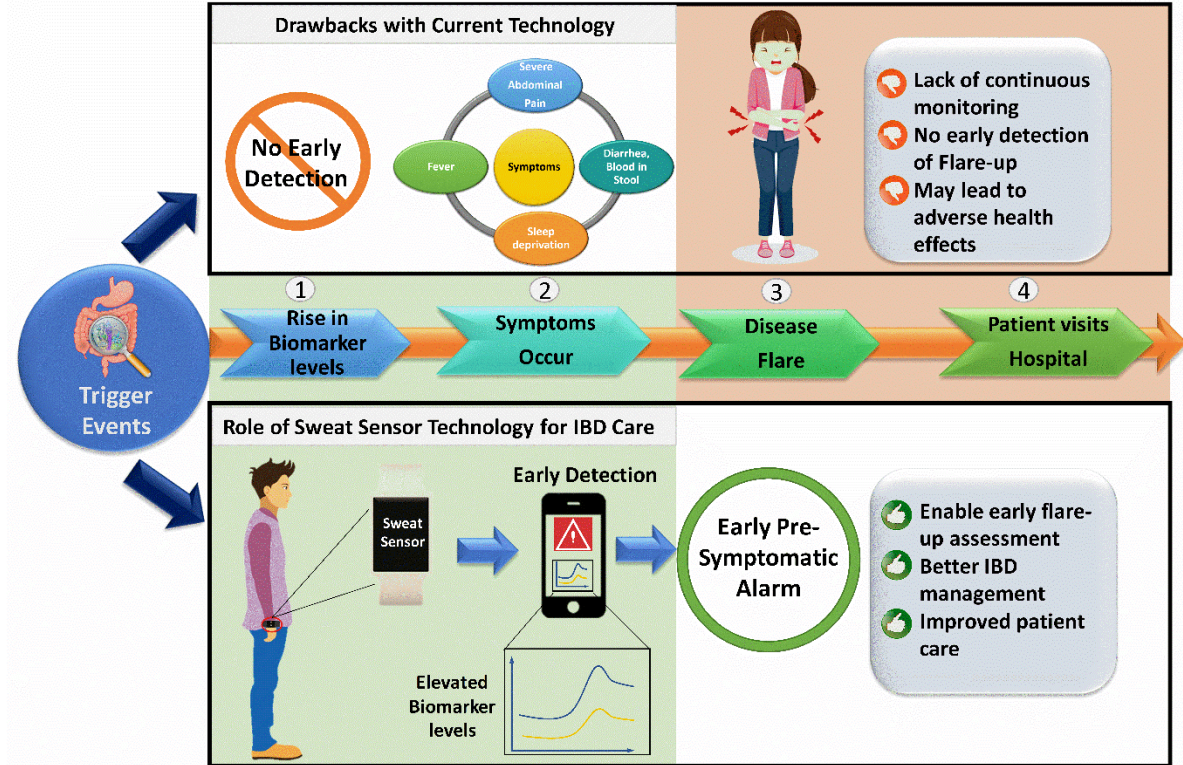


Figure 5.1. Schematic illustration of the challenges with the current testing methods and role of SWEATSENSE device that can be utilized to bridge the technological gaps in offering better management to IBD patients.

#### 5.4 Materials and Methods

**Reagents and Instrumentation:** The cross-linker DTSSP along with PBS were purchased from Thermo Fisher (MA, USA). The capture probe antibodies, IL-1 $\beta$  antibody and CRP antibody were procured from Abcam (MA, USA). IL-1 $\beta$  ELISA kit was purchased from Thermo Fisher while CRP ELISA kit from Creative diagnostics (NY, USA). FDA approved sweat patches were purchased from PharmChek® (TX, USA). All reagents were used as provided and without any purification.

**Sensor Immunoassay Functionalization:** A thiol cross-linker of 10mM was immobilized onto the sensing electrode. The other end of the cross-linker was functionalized with 10 µg/mL of monoclonal IL-1 $\beta$  or CRP capture antibody through aminolysis to achieve specific detection of target biomarker. Monoclonal antibody was selected for achieving highly specific interaction.

**Evaluation of SWEATSENSE performance:** The performance of the SWEATSENSE device was evaluated for the detection of IL-1 $\beta$  and CRP. A calibration curve for each of the target biomarker was established using in-vitro benchtop experiments with the SWEATSENSE device. Concentrations of each biomarker specific to the functionalized sensor were varied from low to high and the corresponding impedance response for each dosed concentration was recorded. A 4-parameter fit was used to build the calibration curve using the obtained impedance response for each target marker. After developing the calibration curve, the performance of the sensor was evaluated using spike and recovery experiments. Various concentrations from low to high levels for each target biomarker was spiked on the sensor and the impedance response was recorded. The corresponding recovered concentration was computed from the developed calibration equation using the obtained impedance response. This methodology was implemented for both the biomarkers.

**Human subjects sweat sample collection, handling and processing:** Sweat samples were collected, processed and evaluated in compliance with the protocol approved by the IRB at the University of Texas at Dallas, TX (IRB# 19-42). 26 human subjects were recruited with their informed written consent for participation in this study. The protocol for sweat sample collection was adapted from Hladek et al.,[46]. Here in, 2 FDA approved PharmChek® patches were placed (one on each arm of the volunteer) at the same time. One patch was removed at 24h and

the other at 72h from the time the patch was put on the volunteer. The samples were de-identified and stored in -80°C immediately upon collection in 5 mL tube until used for analysis. At the time of analysis, the samples were removed and thawed. 2 mL of elution buffer comprising of PBS, 0.2% bovine serum albumin (BSA) and, 0.1%Tween was added to the tube containing the sample. The sample with the elution buffer in the 5 mL tube was placed in a secondary container with ice. This setup was placed on a shaker plate operating at its maximum speed for 45 min. The settings of the shaker plate were adjusted for a uniform movement to extract the sample from the patch. After placing on the shaker for 45min, the tube containing the sample was centrifuged at 20x g for 3 min operated at 4°C. The patch sample was then placed in a syringe and any remaining sample fluid was extracted by squeezing out the residual liquid entrapped in the patch.

**ELISA analysis:** The extracted patch samples were evaluated to determine the sweat levels of the biomarkers using ELISA as the reference method. IL-1 $\beta$  ELISA kit was purchased from ThermoFisher while CRP kit was purchased from Creative Diagnostics. The protocol described with the individual kits were followed as per manufacturer instructions. Absorbance at 450 nm was used to read the O.D response and determine the levels of biomarkers in samples.

**In-vitro sweat sensor analysis for patch samples:** The extracted and aliquoted samples were evaluated and compared with the ELISA results to better understand the accuracy of the SWEATSENSE device in reporting the levels of biomarkers in human subjects. As the collected samples were from a healthy cohort, elevated concentrations were spiked into the buffer to demonstrate the performance of device in capturing the concentration levels of sick cohort. The sensor strips were prepared in a similar manner as described previously in the

Immunoassay functionalization section. The functionalized sensor strips were then connected to the reader. Each sample was dispensed on separate sensors and the impedance response was measured. The measured impedance response was used to determine the concentration levels. The measured levels using the SWEATSENSE device was compared with the obtained ELISA results. Statistical methods such as Pearson's correlation and Bland-Altman analysis were implemented to determine the efficacy of the sweat sensor when compared to the reference ELISA method.

**On-body measurement on human subjects:** In order to demonstrate the ability of the SWEATSENSE platform for real-time monitoring of IBD biomarkers aimed at better management, continuous measurements were recorded in compliance with the protocol approved by the IRB committee. 20 subjects with their written consent were recruited for this study. The wearable SWEATSENSE device for IL-1 $\beta$  measurement was placed on the anterbrachial region (lower forearm) of the subject. The use of the SWEATSENSE device is very simple similar to wearing a watch. The on-body measurements were obtained for up to 30 hours from an individual subject, with continuous measurements recorded every one minute for a duration of at least 1 hour depending on the availability of the subject. The concentration profile of the biomarker was reported over the entire time period of recording.

**Statistical Analyses:** Several statistical tests were performed using Origin Pro. ANOVA was carried out with a C.I. of 95% for spike and recovery experiments to determine the ability of sweat sensor to differentiate varying concentrations. Pearson's correlation and Bland-Altman analysis were performed to determine the extent of agreement of sweat sensor with the reference method.

## **5.5 Results and Discussions**

### **5.5.1 Demonstration of SWEATSENSE device for detection of IL-1 $\beta$ and CRP in passive sweat**

Individual calibration curves were developed for both IL-1 $\beta$  and CRP with a dynamic range encompassing the normal and elevated levels over 3 log orders. The efficacy of sweat sensor for measuring the biomarker levels was validated by spiking varying concentrations of the biomarkers on the sensor and determining the concentration levels from the calibration curve as represented in Fig. 5.2 for n=6 measurements. It can be observed from the bar plots that the SWEATSENSE device can reliably distinguish each of the spiked concentration. The non-overlapping error bars (S.D) confirm the distinguishability between concentrations. Furthermore, statistical ANOVA of p<0.05 with a confidence interval of 95% validates the ability of the SWEATSENSE device to distinguish concentrations. The sensor demonstrates a sensitive response with a LOD of 0.2 pg/mL (calculated as smallest detectable concentration that is 3 times S.D of blank) and has a dynamic range spanning over at least 3 log orders (0.2- 200 pg/mL) for IL-1 $\beta$  while the LOD for CRP is 1 pg/mL with a dynamic range up to 10 ng/mL. Such a wide dynamic range and sensitive response are due to the novel sensor design comprising of a porous substrate functionalized with selective monoclonal antibody coupled to a semiconducting electrode.

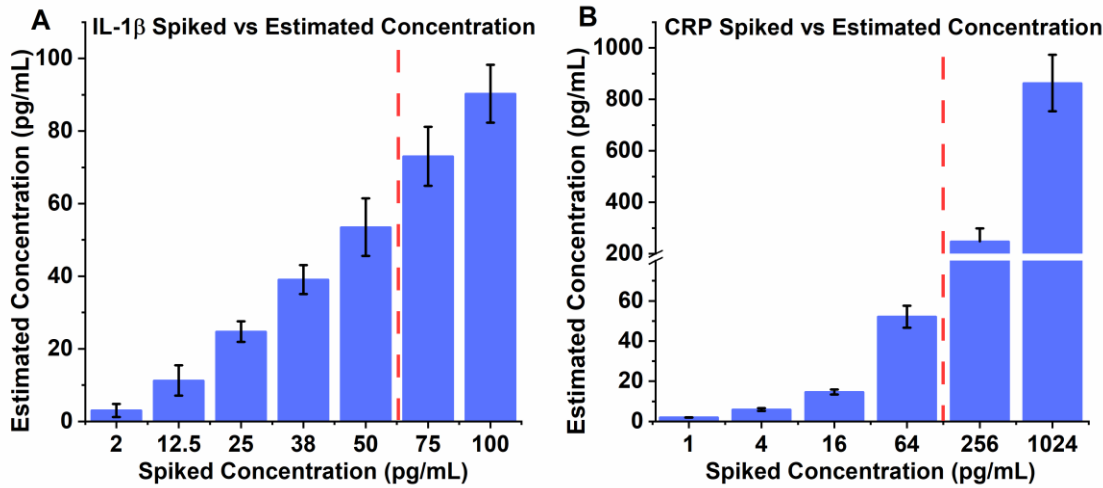


Figure 5.2. Demonstration using sensor for the detection and quantification of cytokine inflammatory biomarkers in sweat A. IL-1 $\beta$ , B. CRP.

Additionally, the detection modality leveraged here enhances the sensing response by amplifying the electrochemical signal response owing to subtle changes at the sensing interface due to the target molecule interaction with the antibody. The device is an affinity-based impedimetric measurement tool that has an ability to measure the biomarker concentration levels in real-time. Typically, in an impedimetric system, the binding of the target biomarker with the capture probe antibody results in a change in impedance response corresponding to the analyte's concentration level. The design and functioning of the SWEATSENSE device to measure impedance response has been described in detail previously from our group [39], [85], [106].

### 5.5.2 Evaluation of sensor performance: repeatability and reproducibility studies

Rigorous testing through repeatability and reproducibility studies was performed on IL-1 $\beta$  functionalized sensors to demonstrate the efficacy of the sensor for wearable use applications. As the concentrations of the biomarkers may not significantly change within a few minutes or hours, especially if the person is healthy or there is no flare-up, it becomes imperative to test the ability

of the device to report repeatable concentrations over time. Here in, 2 sensors were functionalized with IL-1 $\beta$  antibody to evaluate the repeatability of the device platform. The repeatability of the sensor was tested for 3 days in room temperature. Two physiologically relevant dose concentrations 50 and 200 pg/mL were selected. The normal dose concentration (50 pg/mL) was added on one sensor while an elevated dose concentration (200 pg/mL), ~4 times of normal level was dispensed on the other sensor each day during the 72h period. The concentration reported to the added dosing concentration was then evaluated. It can be observed from Fig. 5.3A that the sensor demonstrates a repeatable performance for each of the added dose concentrations over 72h. A mean concentration  $\sim 40 \pm 5$  pg/mL was reported for the normal and  $\sim 160 \pm 10$  pg/mL for the elevated concentration. A statistical  $p < 0.05$  confirms that the normal and elevated levels are reliably distinguished. Fig. 5.3B shows the coefficient of variation (%CV) over 3 days for the same dose concentration which is well within the limit of CLSI standards [107]. It is observed that the sensor reports  $<10\%$  variation when same dose is repeated on the sensor, thus, confirming the repeatability of the sensor platform even after 72h. Reproducibility study was performed to understand the stability and storage of the sensor. It is expected that wearable or POC sensors are stable over time. The goal of the reproducibility study was to demonstrate that the sensitivity of the developed sensor does not reduce over time from the time of immobilization of the antibody. This would demonstrate a proof-of-feasibility for translation of the device for daily use application, where a person can store and use the sensors after multiple days. Sensors were incubated with IL-1 $\beta$  at the same time and stored in 4°C until used. A new sensor strip was taken from the batch of functionalized sensors each week to measure the response of normal (50 pg/mL) and elevated concentrations (200 pg/mL). Fig. 5.3C shows the

response of functionalized sensors over ~30 days with the normal level reported at  $48.2 \pm 3.67$  pg/mL and elevated concentration of  $167.42 \pm 8.36$  pg/mL. The sensors demonstrate a CV <10% (Fig. 5.3D) over a 4-week period, indicating the developed sensor is highly stable and reproducible post 30 day after functionalization. Similar response may be anticipated for CRP as the concentration levels are much higher as compared to IL-1 $\beta$ .

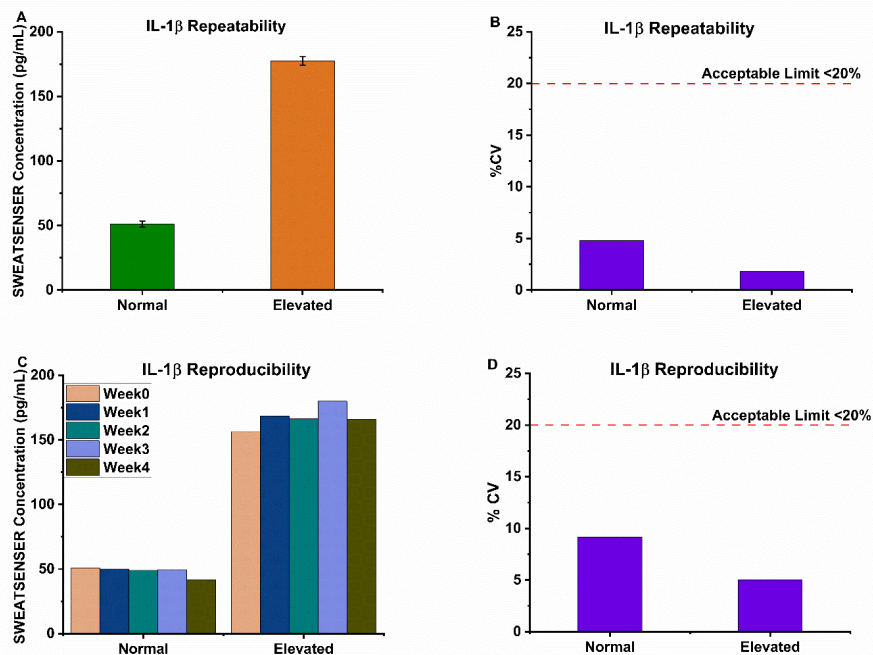


**Figure 5.3. Assessment of sensor performance metrics.** SWEATSENSOR demonstrates repeatable response for the same concentration spiked 4 times on the sensor (A, B). 5 batches of functionalized SWEATSENERS stored for 1 month confirm that the sensor response does not reduce over time, confirming the reproducibility of SWEATSENSOR (C, D).

### **5.5.3 Comparison of performance of SWEATSENSE device with reference methods to report biomarker levels in sweat**

After confirming the ability of the sensor to determine and distinguish concentrations of IBD markers, performance of sweat sensor was validated for measuring sweat IBD biomarkers in healthy human subjects. In order to demonstrate the efficacy of sweat sensor, the developed sensing platform was compared with standard reference method in reporting sweat levels in healthy human subjects. The sweat levels of IL-1 $\beta$  and CRP, were evaluated in the sweat sample, which were collected using an FDA approved PharmChek™ patch. The protocol was adapted from Hladek et al. [46]. A total of 26 healthy adult human subjects were recruited in the study with an informed consent for participation as per the approved IRB at UT Dallas (IRB# 19-42). An appropriate sample size of  $\geq 19$  through power analysis study was determined for obtaining a Pearson's correlation coefficient of  $r > 0.9$  [108]. The individuals showed no symptoms of illness. Two patches (one on each arm) were put on the participant, wherein, one was removed at 24h while the other removed at 72 h. Arm is a region with high sweat gland density  $\sim 221$ - 226 glands/cm<sup>2</sup> [56][42], [43]. All the participants wore the patch for 72 h and no signs of discomfort was reported. After removing the patch and eluting in buffer, samples from the subjects was then analyzed using reference ELISA method and sweat sensor. A mean concentration of 2 pg/mL with a median of 1.8 pg/mL was obtained for IL-1 $\beta$  using sweat sensor that is similar to the reference method. Interestingly, both the reference method and sweat sensor demonstrated the presence of CRP in sweat albeit CRP being a large molecule. A mean concentration of CRP was reported to be 11.6 pg/mL with a median of 9.33 pg/mL using SWEATSENSE device. While the results demonstrating the presence of CRP in sweat is very encouraging, the physiological

pathway for the presence of CRP in sweat is unknown, and not within the scope of the study.

Future work may be carried out to investigate on how CRP diffuses into sweat and the associated pathway with further validation testing. These results may be of significant interest to other researchers that use CRP as a biomarker for diagnosing various diseases conditions. There have been several studies that have reported the levels of cytokines, although, several inconsistencies emerge. Furthermore, these studies were single time-point measurement measured using standard reference methods and lack real-time monitoring [42]–[44]. After determining the levels of the biomarkers using both the methods individually, Pearson's correlation analysis was performed between SWEATSENSE device and ELISA as reference method to better understand the efficacy of the SWEATSENSE device for human subject testing (Fig. 5.4). Sweat sensor demonstrated very good correlation with the reference method Pearson's  $r= 0.99$  for IL-1 $\beta$  as demonstrated in Fig. 5.4A. Additionally, Bland-Altman (BA) analysis was performed to further evaluate the goodness of agreement between sweat sensor and reference method. Bland-Altman provides an insight on any bias or offsets in measurements between both methods and the difference in measurements between 2 methods. It can be observed that sweat sensor shows a good agreement with the reference method (Fig. 5.4B). The x-axis is the mean concentration reported between 2 methods and the y-axis is the difference between the 2 methods for each measured sample. A very small mean bias of -0.25 pg/mL closer to 0 indicates no significant difference in measurement between both techniques. Furthermore, most of the samples lie within  $\pm 2$  S.D., confirming good agreement between both methods. The points are distributed above and below the mean bias line in random order implying there is no treatment-based bias i.e. one method does not over-predict or under-predict concentrations compared to the other.

Similarly, CRP levels correlated well with the Pearson's  $r= 0.95$  (Fig. 5.4C) between both methods validating the reliable performance of sweat sensor in reporting CRP levels in sweat. Furthermore, BA analysis also confirmed a good agreement between both methods with a mean bias of -3.9 pg/mL and all the points lying within  $\pm 2$  S.D. interval (Fig. 5.4D). The measured points spread above and below the mean bias line in a random fashion, similar to the IL-1 $\beta$  response, confirming no treatment bias of either sweat sensor or the reference method. Interestingly, it may be seen that the sweat CRP levels is very low (~1- 30 pg/mL) as compared to the normally reported blood/serum/plasma levels (~100- 1000 ng/mL) in healthy human subjects[109]. One may anticipate such difference between blood and sweat levels, owing to the diffusion dynamics of CRP from blood to sweat due to its bulky size. Further, it may also be noted that the sweat samples were collected using a patch and mixed in an elution buffer which would've resulted in dilution of the sample. Hence, it is imperative to conduct several tests and validate further on the pathway of CRP expression in sweat, which is currently beyond the scope of this study. However, the confirmation of presence of CRP in sweat serves as a good starting point for further exploration. Furthermore, the established correlation of developed sensor platform with reference method through validation studies demonstrates robustness of the SWEATSENSE platform in measuring and quantifying the study biomarkers from passively expressed sweat.

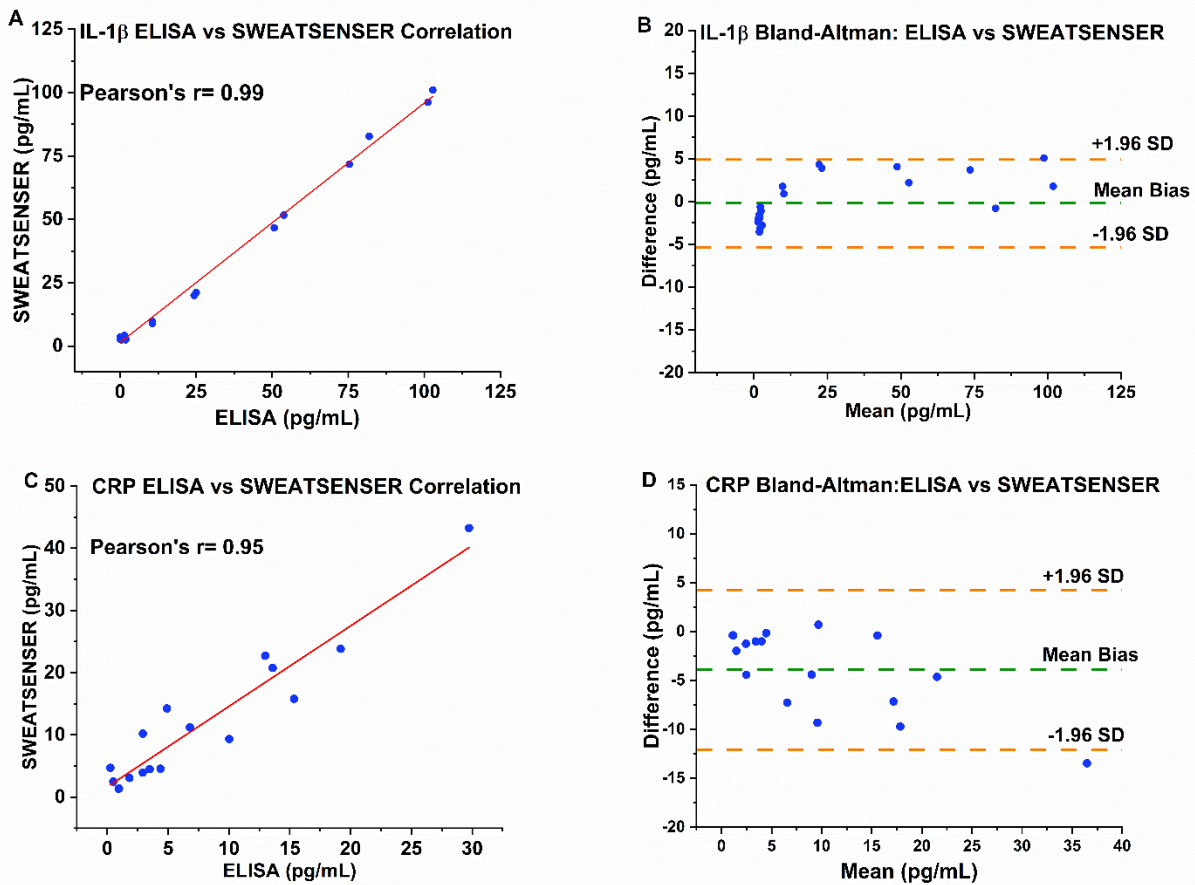


Figure 5.4. Evaluation of sensor performance in comparison to reference ELISA method using linear correlation with a Pearson's correlation coefficient  $r \geq 0.95$  in a cohort of 26 healthy subjects. A. IL-1 $\beta$ , C. CRP and Bland-Altman analysis demonstrating good agreement between SWEATSENSOR and reference method with mean bias -0.2 pg/mL for (B) IL-1 $\beta$ , and -3.9 pg/mL for (D) CRP.

#### 5.5.4 Pre-clinical utility and continuous on-body measurements of IBD biomarkers in healthy human subjects

In order to better demonstrate the applicability of the SWEATSENSOR device for real-time continuous monitoring, on-body measurements were carried out on 20 healthy human subjects determined through power study analysis with  $\alpha=0.05$  and power  $(1-\beta) = 0.8$  for determining IL-1 $\beta$  levels. Table 2. provides a summary of the information of human subjects. A total of 16 male

and 4 female subjects were enrolled for the study. All the enrolled subjects reported no signs or symptoms of illness.

Table 5.1. Summary of Human subjects for on-body continuous testing of IL-1 $\beta$

<b>Human Subject On-body Testing</b>	
# of Volunteers Measurements	20
Age range	18- 65 years
Gender	Male: 16; Female: 4
Medication consumption	None
Health Condition	Healthy Individuals; No reported condition

The SWEATSENSE is a watch-like device attached with the sensor strip specific to IL-1 $\beta$  placed on the hand of each subject. The device also has a skin temperature sensor incorporated within it. All the participants had a body temperature to be between 35- 37°C throughout the testing duration. Real-time measurements were recorded continuously for a minimum of 1h and up to 30h depending on the availability of the volunteer. The measurements were sampled at 1 min. Firstly, the device was evaluated for reporting stable response. While using devices for continuous monitoring as a wearable, it is important to ensure that the device reports the levels reliably over time, as the overarching goal of the device is to capture IBD flares. In order to evaluate the efficacy of the device in reporting accurate levels, a control test was performed. Here, a healthy subject volunteered to wear the device for 4 consecutive days for ~6 hours each day. The device reports similar levels over 4 days (Fig. 5.5A). As it is hypothesized that the levels in healthy subjects do not vary significantly with time, the demonstrated stable response confirm the device does not drift over multiple days. After confirming the ability of the device to

report stable response over multiple days, the sensor was tested for ~30 hours continuously. Fig. 5.5B represents the continuous measurement recorded from one subject for over 30 hrs. As observed from the plot, a stable measurement is recorded over the 30-hour duration, indicating that IL-1 $\beta$  levels did not vary much over the day. However, there is a sharp peak in the initial measurement which may be attributed to the initial equilibration dynamics of sweat diffusion. A mean concentration of ~43 pg/mL was obtained over the 30h measurement for this subject. The data recorded from 20 subjects was further analyzed (Fig. 5.5C). The descriptive statistics was calculated for a period of 1hour which is the least common measured time for the subjects. As shown in the figure, a mean concentration of 28 pg/mL was obtained for 20 subjects. The levels varied from 6- 58 pg/mL among the subjects. The overlap of the error bars indicates that IL-1 $\beta$  levels are in a similar range in healthy subjects. These results further validate the efficacy of the SWEATSENSE device for real-time continuous monitoring of IBD markers. This study provides a proof-of-feasibility of a wearable sweat based technology that can enable real-time tracking and may be used for detection of IBD flare through the continuous on-body monitoring capability. Our next step is to test the device on IBD patients to further evaluate if the levels of the markers can be differentiated between healthy and IBD patient cohort. The device is envisioned to serve IBD patients for reporting a flare-up in real-time for better IBD management.

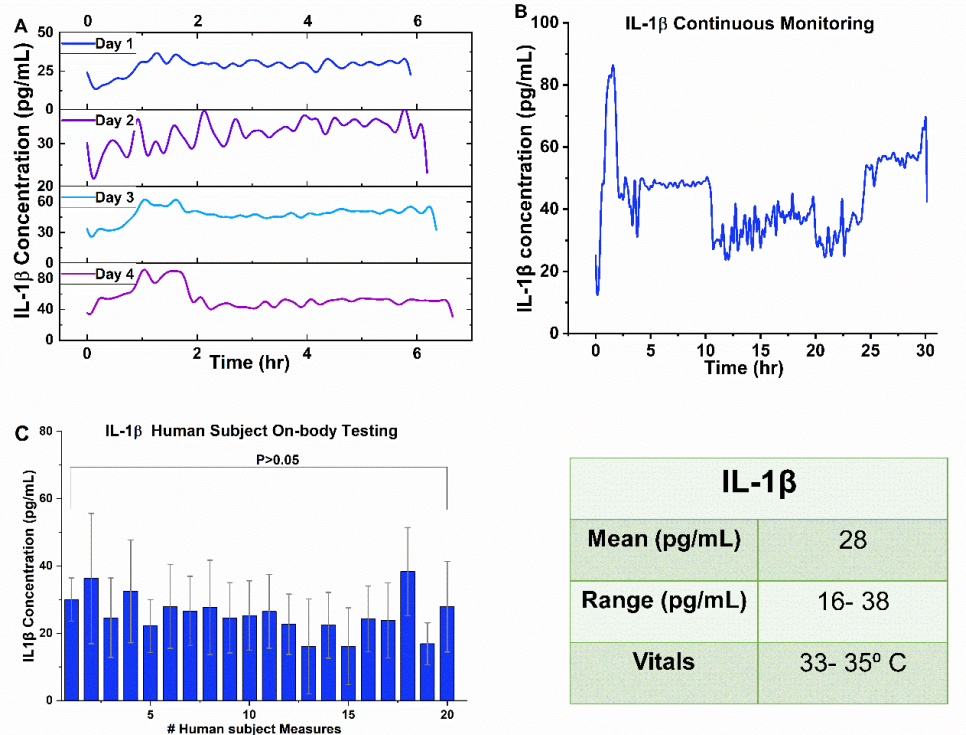


Figure 5.5. On-body Human subject testing for IL-1 $\beta$ . A. SWEATSENSE response over 4 days demonstrating reliable reporting of levels without any drift, B. Demonstration of ability of SWEATSENSE device for continuous monitoring over 30 hours, C. IL-1 $\beta$  levels in 20 human subject measurements measured with an average of 28 pg/mL. A statistical insignificance of p>0.05 was reported in healthy cohort.

### 5.5.5 Comparison of CRP levels between healthy and IBD subjects

In order to evaluate whether basal sweat levels between healthy and IBD subjects can be differentiated, we determined the levels continuously using SWEATSENSE in 10 healthy and one IBD subject. The basal level comparison between healthy and IBD cohort is shown in Fig. 5.6. Each data point on the box plot is a measure of levels reported over 2 hours and collected over multiple days. As seen from the box plots, CRP levels in healthy cohort is lower than the IBD subject and a statistically significance of p<0.05 was determined. Interestingly, the IBD subject demonstrated a bimodal distribution of the CRP levels. We hypothesize such a

distribution could be due to the dynamic change in CRP levels over multiple days. However, this will need further investigation.

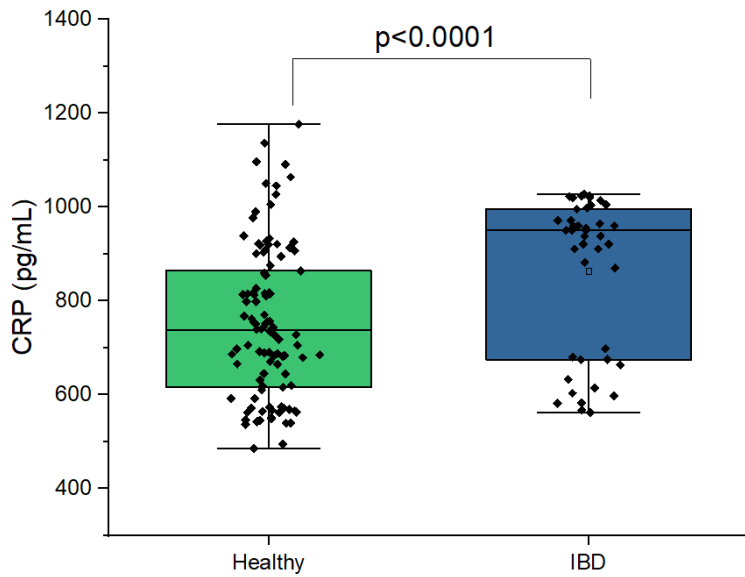


Figure 5.6. Comparison of CRP levels between healthy and IBD subjects demonstrating statistical significance indicating that the inherent levels can be differentiated between healthy and IBD subjects.

### **5.5.6 Quantification and comparison of Calprotectin levels in sweat**

A critical finding in this work is the identification of Calprotectin in sweat. Calprotectin is a key biomarker to identify flare in IBD patients. Typically, the levels of calprotectin are assessed from fecal samples and there is no prior literature that reported the presence of Calprotectin in sweat. Quantification of Calprotectin in sweat and correlation to disease flare can enable better prognosis and provide an opportunity to non-invasively track flares in IBD patients. Therefore, we evaluated if Calprotectin exists in sweat. To determine this, first 10 healthy subjects were recruited and sweat samples were collected. The levels of Calprotectin were determined using reference ELISA and the SWEATSENSE to confirm that the Calprotectin is truly present in

sweat. As seen in Fig. 5.7, both the reference method and the SWEATSENSE reported Calprotectin with a mean of ~350 ng/mL. Then, we recruited an IBD subject and the basal levels were reported to be 513 ng/mL which was higher compared to the healthy control. The same IBD subject experienced a flare a few weeks later and returned to provide sample. This collected sweat sample was assessed. The levels of Calprotectin increased 3-fold due to flare compared to the basal levels. This demonstrates the feasibility that elevated Calprotectin levels can be determined from sweat. However, further validation is required to confirm that sweat can be a viable biofluid to reliably determine flares in IBD subjects.

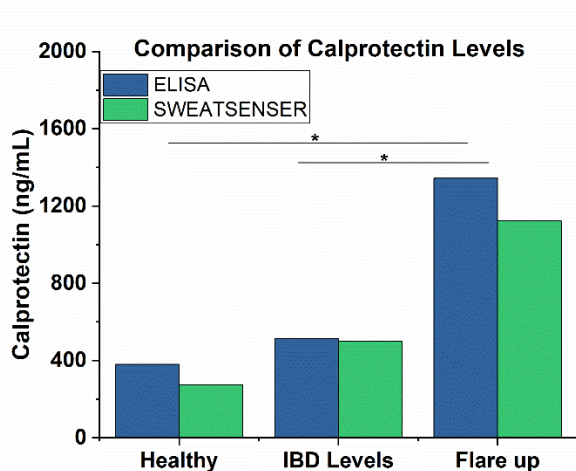


Figure 5.7. Comparison of Calprotectin levels in sweat between healthy and IBD cohort, and IBD basal levels to Flare up state. The bar plots demonstrate that IBD patient has higher basal levels compared to healthy cohort. The levels increase 3-fold during a flare up as compared to baseline IBD levels.

## 5.6 Conclusion

In summary, we demonstrate a wearable, non-invasive, multiplexed sweat sensor that can detect the study inflammatory biomarkers in a continuous manner. The developed sensing system was thoroughly validated for use on human subjects through comparison with the standard reference method. Strong correlations through Pearson's correlation and Bland-Altman illustrate the

efficacy of the device for human subject testing. Pre-clinical utility of the system was established through real-time, continuous on-body measurements on healthy human cohort. The stable measurements for over 30 hours signify the ability and efficiency of the device for reliable continuous monitoring. This work signifies of a promising non-invasive technology that allows for continuous monitoring of inflammatory markers that may be implicated in the IBD etiology. Hence, there is now a hitherto unexplored opportunity of non-invasively monitoring IBD markers in IBD patients to track and assess flare.

### **5.7 Acknowledgement**

This work has been supported by the Crohn's and Colitis Foundation (Grant# 611587) and by EnLiSense LLC.

## **CHAPTER 6**

### **CONCLUSION AND FUTURE WORK**

This work demonstrates a wearable SWEATSENSE technology for real-time monitoring of infection/inflammation non-invasively from eccrine sweat. The holy grail of the developed SWEATSENSE technology is to directly measure host immune cytokine markers in passive eccrine sweat for pre-symptomatic infection tracking and early detection of flare-ups in chronic inflammatory diseases such as IBD. This type of a real-time monitoring system can offer a fundamental change in the approach of the way infections are being diagnosed, assessed, and treated. This was achieved through designing the SWEATSENSE that can be worn on the hand in a watch-form that can simultaneously and continuously detect multiple immune biomarkers. This work has made fundamental contributions in the field of wearable biosensing. Further, the identification and quantification of certain inflammatory markers such as IP-10, TRAIL, CRP will be of significance toward non-invasively monitoring bacterial/viral infections.

The reliable and robust detection was achieved through a novel sensing platform that facilitates simultaneous multiplexed detection of biomarkers using monoclonal antibodies and impedimetric detection modality. The analytical performance metrics of the sensor was evaluated using spike and recovery, selectivity, accuracy, reproducibility and stability experiments which confirmed the reliability of the SWEATSENSE to accurately report the levels of cytokines and chemokines in sweat. The correlations achieved between the SWEATSENSE and standard reference method signifies the ability of the device for on-field measurements. Additionally, the correlations between serum and sweat cytokines demonstrate the viability of sweat as a biofluid for monitoring systemic circulation levels.

The developed wearable SWEATSENSE can be visualized not only for early detection but for monitoring therapeutic treatment regimens through real-time monitoring of cytokines that can mitigate severe consequences of pathogen attack.

Future work will be focused on further optimization, improvisation and strengthening the clinical validation of SWEATSENSE for acute respiratory infections, flu, and other viral/bacterial infections. Studies can be conducted to sample serum and sweat at multiple time points within a day and between days to better understand diurnal and circadian variations of cytokine biomarkers in sweat and their physiological role. One aspect of the SWEATSENSE device that can optimized further is to look at increase the longevity of the sensor strip to enhance the use of single sensor strip for longer duration of time. This can be achieved through use of novel materials called room temperature ionic liquids or deep eutectic solvents that enhance the stability of proteins. We have performed a few preliminary studies which extend the longevity of single sensor strip for about one week. However, further studies need to be conducted to validate their efficacy and compatibility for conforming on the skin surface.

There are various applications for which the SWEATSENSE technology will be useful for patient-centric health management. The feasibility for pre-symptomatic reporting in COVID-19 patients and the ability to guide clinicians to alter the administered therapeutic regimen in real-time for severe conditions such as sepsis. Longitudinal studies in IBD patients during the remission to relapse phase for reporting flare-ups can truly determine the ability of SWEATSENSE device as wearable for IBD monitoring. Another area of the SWEATSENSE technology is to explore the ability as a lifestyle monitoring device. The combination of inflammatory markers with stress biomarkers and glucose can provide valuable insights on the

health status of person. Therefore, SWEATSENSE technology can aid in providing active feedback and decision support on the health state for better patient healthcare management

## REFERENCES

- [1] J. Kim, A. S. Campbell, B. E.-F. de Ávila, and J. Wang, “Wearable biosensors for healthcare monitoring,” *Nat. Biotechnol.*, vol. 37, no. 4, pp. 389–406, 2019.
- [2] K. P. L. Chong and B. K. P. Woo, “Emerging wearable technology applications in gastroenterology: A review of the literature,” *World J. Gastroenterol.*, vol. 27, no. 12, p. 1149, 2021.
- [3] Y. Liu, M. Pharr, and G. A. Salvatore, “Lab-on-Skin: A Review of Flexible and Stretchable Electronics for Wearable Health Monitoring,” *ACS Nano*. 2017, doi: 10.1021/acsnano.7b04898.
- [4] M. Amjadi, K. U. Kyung, I. Park, and M. Sitti, “Stretchable, Skin-Mountable, and Wearable Strain Sensors and Their Potential Applications: A Review,” *Advanced Functional Materials*. 2016, doi: 10.1002/adfm.201504755.
- [5] J. Heikenfeld *et al.*, “Wearable sensors: Modalities, challenges, and prospects,” *Lab on a Chip*. 2018, doi: 10.1039/c7lc00914c.
- [6] K. Guk *et al.*, “Evolution of wearable devices with real-time disease monitoring for personalized healthcare,” *Nanomaterials*. 2019, doi: 10.3390/nano9060813.
- [7] T. H. Tulchinsky and E. A. Varavikova, “Measuring, Monitoring, and Evaluating the Health of a Population,” in *The New Public Health*, 2014.
- [8] S. Ye, S. Feng, L. Huang, and S. Bian, “Recent progress in wearable biosensors: From healthcare monitoring to sports analytics,” *Biosensors*, vol. 10, no. 12, p. 205, 2020.
- [9] J. Kim *et al.*, “Non-invasive mouthguard biosensor for continuous salivary monitoring of metabolites,” *Analyst*, vol. 139, no. 7, pp. 1632–1636, 2014.
- [10] E. Magiorkinis and A. Diamantis, “The fascinating story of urine examination: From uroscopy to the era of microscopy and beyond,” *Diagn. Cytopathol.*, vol. 43, no. 12, pp. 1020–1036, 2015.
- [11] N. M. Farandos, A. K. Yetisen, M. J. Monteiro, C. R. Lowe, and S. H. Yun, “Contact lens sensors in ocular diagnostics,” *Adv. Healthc. Mater.*, vol. 4, no. 6, pp. 792–810, 2015.
- [12] J. Kim *et al.*, “Wearable smart sensor systems integrated on soft contact lenses for wireless ocular diagnostics,” *Nat. Commun.*, vol. 8, no. 1, pp. 1–8, 2017.
- [13] L. Gao, T. Xu, G. Huang, S. Jiang, Y. Gu, and F. Chen, “Oral microbiomes: more and more importance in oral cavity and whole body,” *Protein Cell*, vol. 9, no. 5, pp. 488–500, 2018.

- [14] A. Sharma, M. Badea, S. Tiwari, and J. L. Marty, “Wearable biosensors: An alternative and practical approach in healthcare and disease monitoring,” *Molecules*. 2021, doi: 10.3390/molecules26030748.
- [15] L. B. Baker, “Physiology of sweat gland function: The roles of sweating and sweat composition in human health,” *Temperature*, vol. 6, no. 3, pp. 211–259, 2019.
- [16] D. Barreca, A. Gasparotto, C. Maragno, E. Tondello, and T. R. Spalding, “Analysis of nanocrystalline ZnS thin films by XPS,” *Surf. Sci. Spectra*, vol. 9, no. 1, pp. 54–61, 2002.
- [17] P. W. Sadik, S. J. Pearton, D. P. Norton, E. Lambers, and F. Ren, “Functionalizing Zn-and O-terminated ZnO with thiols,” *J. Appl. Phys.*, vol. 101, no. 10, p. 104514, 2007.
- [18] C. Y. Lim *et al.*, “Succinimidyl ester surface chemistry: implications of the competition between aminolysis and hydrolysis on covalent protein immobilization,” *Langmuir*, vol. 30, no. 43, pp. 12868–12878, 2014.
- [19] V. Kamakoti, N. R. Shanmugam, A. S. Tanak, B. Jagannath, and S. Prasad, “Investigation of molybdenum-crosslinker interfaces for affinity based electrochemical biosensing applications,” *Appl. Surf. Sci.*, vol. 436, 2018, doi: 10.1016/j.apsusc.2017.12.026.
- [20] K.-C. Lin, B. Jagannath, S. Muthukumar, and S. Prasad, “Sub-picomolar label-free detection of thrombin using electrochemical impedance spectroscopy of aptamer-functionalized MoS<sub>2</sub>,” *Analyst*, vol. 142, no. 15, 2017, doi: 10.1039/c7an00548b.
- [21] J. S. Daniels and N. Pourmand, “Label-free impedance biosensors: Opportunities and challenges,” *Electroanal. An Int. J. Devoted to Fundam. Pract. Asp. Electroanal.*, vol. 19, no. 12, pp. 1239–1257, 2007.
- [22] B.-Y. Chang and S.-M. Park, “Electrochemical impedance spectroscopy,” *Annu. Rev. Anal. Chem.*, vol. 3, pp. 207–229, 2010.
- [23] A. S. Tanak, B. Jagannath, Y. Tamrakar, S. Muthukumar, and S. Prasad, “Non-faradaic electrochemical impedimetric profiling of procalcitonin and C-reactive protein as a dual marker biosensor for early sepsis detection,” *Anal. Chim. Acta X*, vol. 3, p. 100029, Nov. 2019, doi: 10.1016/j.acax.2019.100029.
- [24] M. Shanker, M. Y. Hu, and M. S. Hung, “Effect of data standardization on neural network training,” *Omega*, vol. 24, no. 4, pp. 385–397, 1996.
- [25] G. R. Guy, N. S. Bee, and C. S. Peng, “Lymphokine signal transduction,” *Prog. Growth Factor Res.*, 1990, doi: 10.1016/0955-2235(90)90009-9.
- [26] Y. Vázquez *et al.*, “Cytokines in the respiratory airway as biomarkers of severity and prognosis for Respiratory Syncytial Virus infection: an update,” *Front. Immunol.*, vol. 10, 2019.

- [27] J. Imanishi, “Expression of cytokines in bacterial and viral infections and their biochemical aspects,” *J. Biochem.*, vol. 127, no. 4, pp. 525–530, 2000.
- [28] J. A. D. Bienvenu, G. Monneret, M. C. Gutowski, and N. Fabien, “Cytokine assays in human sera and tissues,” in *Toxicology*, 1998, doi: 10.1016/S0300-483X(98)00063-8.
- [29] Q. Liu, Y. Zhou, and Z. Yang, “The cytokine storm of severe influenza and development of immunomodulatory therapy,” *Cell. Mol. Immunol.*, vol. 13, no. 1, pp. 3–10, 2016.
- [30] N. V Frey and D. L. Porter, “Cytokine release syndrome with novel therapeutics for acute lymphoblastic leukemia,” *Hematology*, 2016, doi: 10.1182/asheducation-2016.1.567.
- [31] S. F. Pedersen and Y. C. Ho, “SARS-CoV-2: A Storm is Raging,” *J. Clin. Invest.*, 2020, doi: 10.1172/JCI137647.
- [32] P. Mehta, D. F. McAuley, M. Brown, E. Sanchez, R. S. Tattersall, and J. J. Manson, “COVID-19: consider cytokine storm syndromes and immunosuppression,” *Lancet*, 2020.
- [33] W. C. of the W. H. O. (WHO) C. on H. I. A/H5, “Avian influenza A (H5N1) infection in humans,” *N. Engl. J. Med.*, vol. 353, no. 13, pp. 1374–1385, 2005.
- [34] D. M. Del Valle *et al.*, “An inflammatory cytokine signature helps predict COVID-19 severity and death,” *medRxiv*, 2020.
- [35] F. Coperchini, L. Chiovato, L. Croce, F. Magri, and M. Rotondi, “The Cytokine storm in COVID-19: An overview of the involvement of the chemokine/chemokine-receptor system,” *Cytokine Growth Factor Rev.*, 2020.
- [36] J. M. Zhang and J. An, “Cytokines, inflammation, and pain,” *International Anesthesiology Clinics*. 2007, doi: 10.1097/AIA.0b013e318034194e.
- [37] B. Diao *et al.*, “Reduction and Functional Exhaustion of T Cells in Patients with Coronavirus Disease 2019 (COVID-19),” *medRxiv*, p. 2020.02.18.20024364, Jan. 2020, doi: 10.1101/2020.02.18.20024364.
- [38] Z. Sonner *et al.*, “The microfluidics of the eccrine sweat gland, including biomarker partitioning, transport, and biosensing implications,” *Biomicrofluidics*, 2015, doi: 10.1063/1.4921039.
- [39] B. Jagannath, S. Muthukumar, and S. Prasad, “Electrical double layer modulation of hybrid room temperature ionic liquid/aqueous buffer interface for enhanced sweat based biosensing,” *Anal. Chim. Acta*, 2018, doi: 10.1016/j.aca.2018.02.013.
- [40] C. Legner, U. Kalwa, V. Patel, A. Chesmore, and S. Pandey, “Sweat sensing in the smart wearables era: Towards integrative, multifunctional and body-compliant perspiration analysis,” *Sensors and Actuators, A: Physical*. 2019, doi: 10.1016/j.sna.2019.07.020.
- [41] K. Kabashima, T. Honda, F. Ginhoux, and G. Egawa, “The immunological anatomy of the skin,” *Nature Reviews Immunology*. 2019, doi: 10.1038/s41577-018-0084-5.

- [42] G. Cizza *et al.*, “Elevated neuroimmune biomarkers in sweat patches and plasma of premenopausal women with major depressive disorder in remission: the POWER study,” *Biol. Psychiatry*, vol. 64, no. 10, pp. 907–911, 2008.
- [43] A. Marques-Deak *et al.*, “Measurement of cytokines in sweat patches and plasma in healthy women: Validation in a controlled study,” *J. Immunol. Methods*, 2006, doi: 10.1016/j.jim.2006.07.011.
- [44] X. Dai *et al.*, “Eccrine sweat contains IL-1 $\alpha$ , IL-1 $\beta$  and IL-31 and activates epidermal keratinocytes as a danger signal,” *PLoS One*, vol. 8, no. 7, 2013.
- [45] R. D. Munje, S. Muthukumar, B. Jagannath, and S. Prasad, “A new paradigm in sweat based wearable diagnostics biosensors using Room Temperature Ionic Liquids (RTILs),” *Sci. Rep.*, vol. 7, no. 1, 2017, doi: 10.1038/s41598-017-02133-0.
- [46] M. D. Hladek *et al.*, “Using sweat to measure cytokines in older adults compared to younger adults: A pilot study,” *J. Immunol. Methods*, 2018, doi: 10.1016/j.jim.2017.11.003.
- [47] T. Rispens, H. Te Velthuis, P. Hemker, H. Speijer, W. Hermens, and L. Aarden, “Label-free assessment of high-affinity antibody–antigen binding constants. Comparison of bioassay, SPR, and PEIA-ellipsometry,” *J. Immunol. Methods*, vol. 365, no. 1–2, pp. 50–57, 2011.
- [48] X. Chen *et al.*, “Detectable serum SARS-CoV-2 viral load (RNAemia) is closely correlated with drastically elevated interleukin 6 (IL-6) level in critically ill COVID-19 patients,” *Clin. Infect. Dis.*, 2020.
- [49] M. Kotb and T. Calandra, *Cytokines and chemokines in infectious diseases handbook*. Springer Science & Business Media, 2003.
- [50] N. Fazal, “T Cell Suppression in Burn and Septic Injuries,” in *Immunosuppression - Role in Health and Diseases*, 2012.
- [51] S. Steeland, C. Libert, and R. E. Vandebroucke, “A new venue of TNF targeting,” *Int. J. Mol. Sci.*, vol. 19, no. 5, p. 1442, 2018.
- [52] F. Emami, A. Vatanara, E. J. Park, and D. H. Na, “Drying technologies for the stability and bioavailability of biopharmaceuticals,” *Pharmaceutics*, vol. 10, no. 3, p. 131, 2018.
- [53] B. A. Katchman, M. Zhu, J. Blain Christen, and K. S. Anderson, “Eccrine Sweat as a Biofluid for Profiling Immune Biomarkers,” *Proteomics - Clin. Appl.*, 2018, doi: 10.1002/prca.201800010.
- [54] L. Tavares, F. Monedeiro, D. M. Bordin, and B. S. De Martinis, “Investigation of Ayahuasca  $\beta$ -Carboline Alkaloids and Tryptamine in Sweat Samples from Religious Community Participants by GC-MS,” *J. Anal. Toxicol.*, 2020.

- [55] C. Schummer, B. M. R. Appenzeller, and R. Wennig, “Quantitative determination of ethyl glucuronide in sweat,” *Ther. Drug Monit.*, vol. 30, no. 4, pp. 536–539, 2008.
- [56] C. Nie, “Integrated evaporation driven microfluidic device for continuous sweat monitoring,” 2016.
- [57] S. K. Tuteja, C. Ormsby, and S. Neethirajan, “Noninvasive label-free detection of cortisol and lactate using graphene embedded screen-printed electrode,” *Nano-micro Lett.*, vol. 10, no. 3, p. 41, 2018.
- [58] Y. Yang and W. Gao, “Wearable and flexible electronics for continuous molecular monitoring,” *Chem. Soc. Rev.*, vol. 48, no. 6, pp. 1465–1491, 2019.
- [59] T. Kaya *et al.*, “Wearable sweat sensors: Background and current trends,” *Electroanalysis*, vol. 31, no. 3, pp. 411–421, 2019.
- [60] J. A. Alexander *et al.*, “Rapid Capture and Extraction of Sweat for Regional Rate and Cytokine Composition Analysis Using a Wearable Soft Microfluidic System,” *J. Invest. Dermatol.*, pp. S0022-202X, 2020.
- [61] B. Jagannath, K.-C. Lin, M. Pali, D. Sankhala, S. Muthukumar, and S. Prasad, “A Sweat-based Wearable Enabling Technology for Real-time Monitoring of IL-1 $\beta$  and CRP as Potential Markers for Inflammatory Bowel Disease,” *Inflamm. Bowel Dis.*, Jul. 2020, doi: 10.1093/ibd/izaa191.
- [62] Y. Zhang *et al.*, “Passive sweat collection and colorimetric analysis of biomarkers relevant to kidney disorders using a soft microfluidic system,” *Lab Chip*, vol. 19, no. 9, pp. 1545–1555, 2019.
- [63] L.-C. Tai *et al.*, “Wearable sweat band for noninvasive levodopa monitoring,” *Nano Lett.*, vol. 19, no. 9, pp. 6346–6351, 2019.
- [64] D. A. Sens, M. A. Simmons, and S. S. Spicer, “The analysis of human sweat proteins by isoelectric focusing. I. sweat collection utilizing the macrōduct system demonstrates the presence of previously unrecognized sex-related proteins,” *Pediatr. Res.*, 1985, doi: 10.1203/00006450-198508000-00020.
- [65] J. Tu, R. M. Torrente-Rodríguez, M. Wang, and W. Gao, “The Era of Digital Health: A Review of Portable and Wearable Affinity Biosensors,” *Adv. Funct. Mater.*, p. 1906713, 2019.
- [66] W. H. Organization, “Infectious diseases kill over 17 million people a year: WHO warns of global crisis.” WHO, 2015.
- [67] P. J. Barnes, J. M. Drazen, S. I. Rennard, and N. C. Thomson, *Asthma and COPD: basic mechanisms and clinical management*. Elsevier, 2009.

- [68] F. C. Riché *et al.*, “Inflammatory cytokines, C reactive protein, and procalcitonin as early predictors of necrosis infection in acute necrotizing pancreatitis,” *Surgery*, vol. 133, no. 3, pp. 257–262, 2003.
- [69] S. F. Pedersen and Y.-C. Ho, “SARS-CoV-2: A Storm is Raging,” *J. Clin. Invest.*, 2020, doi: 10.1172/jci137647.
- [70] K. Oved *et al.*, “A novel host-proteome signature for distinguishing between acute bacterial and viral infections,” *PLoS One*, 2015, doi: 10.1371/journal.pone.0120012.
- [71] R. W. Johnstone, A. J. Frew, and M. J. Smyth, “The TRAIL apoptotic pathway in cancer onset, progression and therapy,” *Nature Reviews Cancer*. 2008, doi: 10.1038/nrc2465.
- [72] Y. Yang *et al.*, “Exuberant elevation of IP-10, MCP-3 and IL-1ra during SARS-CoV-2 infection is associated with disease severity and fatal outcome,” *medRxiv*, 2020.
- [73] C. Huang *et al.*, “Clinical features of patients infected with 2019 novel coronavirus in Wuhan, China,” *Lancet*, vol. 395, no. 10223, pp. 497–506, 2020.
- [74] T. Okabayashi *et al.*, “Cytokine regulation in SARS coronavirus infection compared to other respiratory virus infections,” *J. Med. Virol.*, 2006, doi: 10.1002/jmv.20556.
- [75] D. W. Stuckey and K. Shah, “TRAIL on trial: Preclinical advances in cancer therapy,” *Trends in Molecular Medicine*. 2013, doi: 10.1016/j.molmed.2013.08.007.
- [76] T. Yoshikawa, T. Hill, K. Li, C. J. Peters, and C.-T. K. Tseng, “Severe Acute Respiratory Syndrome (SARS) Coronavirus-Induced Lung Epithelial Cytokines Exacerbate SARS Pathogenesis by Modulating Intrinsic Functions of Monocyte-Derived Macrophages and Dendritic Cells,” *J. Virol.*, 2009, doi: 10.1128/jvi.01792-08.
- [77] M. Liu *et al.*, “CXCL10/IP-10 in infectious diseases pathogenesis and potential therapeutic implications,” *Cytokine Growth Factor Rev.*, vol. 22, no. 3, pp. 121–130, 2011.
- [78] R. Williams, H. Yao, N. K. Dhillon, and S. J. Buch, “HIV-1 Tat co-operates with IFN- $\gamma$  and TNF- $\alpha$  to increase CXCL10 in human astrocytes,” *PLoS One*, vol. 4, no. 5, 2009.
- [79] M. Rashighi and J. E. Harris, “Interfering with the IFN- $\gamma$ /CXCL10 pathway to develop new targeted treatments for vitiligo,” *Ann. Transl. Med.*, vol. 3, no. 21, 2015.
- [80] P. A. Holoch and T. S. Griffith, “TNF-related apoptosis-inducing ligand (TRAIL): a new path to anti-cancer therapies,” *Eur. J. Pharmacol.*, vol. 625, no. 1–3, pp. 63–72, 2009.
- [81] W. D. Thomas and P. Hersey, “TNF-related apoptosis-inducing ligand (TRAIL) induces apoptosis in Fas ligand-resistant melanoma cells and mediates CD4 T cell killing of target cells,” *J. Immunol.*, 1998.
- [82] L. Lan *et al.*, “Hepatitis C Virus Infection Sensitizes Human Hepatocytes to TRAIL-Induced Apoptosis in a Caspase 9-Dependent Manner,” *J. Immunol.*, 2008, doi: 10.4049/jimmunol.181.7.4926.

- [83] K. Song *et al.*, “Tumor necrosis factor-related apoptosis-inducing ligand (TRAIL) is an inhibitor of autoimmune inflammation and cell cycle progression,” *J. Exp. Med.*, 2000, doi: 10.1084/jem.191.7.1095.
- [84] B. Jagannath, K. Lin, M. Pali, D. Sankhala, S. Muthukumar, and S. Prasad, “Temporal Profiling of Cytokines in Passively Expressed Sweat for Detection of Infection using Wearable Device,” *Bioeng. Transl. Med.*, p. e10220.
- [85] A. S. Tanak, B. Jagannath, Y. Tamrakar, S. Muthukumar, and S. Prasad, “Non-faradaic electrochemical impedimetric profiling of procalcitonin and C-reactive protein as a dual marker biosensor for early sepsis detection,” *Anal. Chim. Acta X*, 2019, doi: 10.1016/j.acax.2019.100029.
- [86] V. A. LeGrys, J. R. Yankaskas, L. M. Quittell, B. C. Marshall, and P. J. Mogayzel, “Diagnostic sweat testing: the Cystic Fibrosis Foundation guidelines,” *J. Pediatr.*, vol. 151, no. 1, pp. 85–89, 2007.
- [87] S. M. Wilhelm, “Report: impact of inflammatory bowel disease.,” *Am. J. Manag. Care*, vol. 22, no. 3 Suppl, pp. s32-8, 2016.
- [88] W. Strober and I. J. Fuss, “Proinflammatory cytokines in the pathogenesis of inflammatory bowel diseases,” *Gastroenterology*, vol. 140, no. 6, pp. 1756–1767, 2011.
- [89] I. C. Roberts-Thomson, J. Fon, W. Uylaki, A. G. Cummins, and S. Barry, “Cells, cytokines and inflammatory bowel disease: a clinical perspective,” *Expert Rev. Gastroenterol. Hepatol.*, vol. 5, no. 6, pp. 703–716, 2011.
- [90] G. Radford-Smith and D. P. Jewell, “Cytokines and inflammatory bowel disease,” *Baillieres. Clin. Gastroenterol.*, 1996, doi: 10.1016/S0950-3528(96)90045-7.
- [91] G. P. Ramos and K. A. Papadakis, “Mechanisms of disease: inflammatory bowel diseases,” in *Mayo Clinic Proceedings*, 2019, vol. 94, no. 1, pp. 155–165.
- [92] B. Khor, A. Gardet, and R. J. Xavier, “Genetics and pathogenesis of inflammatory bowel disease,” *Nature*, vol. 474, no. 7351, pp. 307–317, 2011.
- [93] S. Y. Shaw, J. F. Blanchard, and C. N. Bernstein, “Association between the use of antibiotics in the first year of life and pediatric inflammatory bowel disease,” *Am. J. Gastroenterol.*, vol. 105, no. 12, pp. 2687–2692, 2010.
- [94] W. Selby *et al.*, “Two-year combination antibiotic therapy with clarithromycin, rifabutin, and clofazimine for Crohn’s disease,” *Gastroenterology*, vol. 132, no. 7, pp. 2313–2319, 2007.
- [95] H. Khalili *et al.*, “Oral contraceptives, reproductive factors and risk of inflammatory bowel disease,” *Gut*, vol. 62, no. 8, pp. 1153–1159, 2013.

- [96] E. Liverani, E. Scaioli, R. J. Digby, M. Bellanova, and A. Belluzzi, “How to predict clinical relapse in inflammatory bowel disease patients,” *World J. Gastroenterol.*, vol. 22, no. 3, p. 1017, 2016.
- [97] M. F. Neurath, “Cytokines in inflammatory bowel disease,” *Nature Reviews Immunology*. 2014, doi: 10.1038/nri3661.
- [98] Q. Guan and J. Zhang, “Recent Advances: The Imbalance of Cytokines in the Pathogenesis of Inflammatory Bowel Disease,” *Mediators of Inflammation*. 2017, doi: 10.1155/2017/4810258.
- [99] F. Sanchez-Muñoz, A. Dominguez-Lopez, and J. K. Yamamoto-Furusho, “Role of cytokines in inflammatory bowel disease,” *World J. Gastroenterol. WJG*, vol. 14, no. 27, p. 4280, 2008.
- [100] R. L. Jump and A. D. Levine, “Mechanisms of natural tolerance in the intestine: implications for inflammatory bowel disease,” *Inflamm. Bowel Dis.*, vol. 10, no. 4, pp. 462–478, 2004.
- [101] J. M. Reimund *et al.*, “Mucosal inflammatory cytokine production by intestinal biopsies in patients with ulcerative colitis and Crohn’s disease,” *J. Clin. Immunol.*, 1996, doi: 10.1007/BF01540912.
- [102] P. Vounotrypidis *et al.*, “Interleukin-1 associations in inflammatory bowel disease and the enteropathic seronegative spondylarthritis,” *Autoimmun. Highlights*, 2013, doi: 10.1007/s13317-013-0049-4.
- [103] S. Vermeire, G. Van Assche, and P. Rutgeerts, “Laboratory markers in IBD: useful, magic, or unnecessary toys?,” *Gut*, vol. 55, no. 3, pp. 426–431, 2006.
- [104] G. V Shmarina *et al.*, “Tumor necrosis factor- $\alpha$ /interleukin-10 balance in normal and cystic fibrosis children,” *Mediators Inflamm.*, vol. 10, no. 4, pp. 191–197, 2001.
- [105] K. A. Papadakis and S. R. Targan, “Role of cytokines in the pathogenesis of inflammatory bowel disease,” *Annu. Rev. Med.*, vol. 51, no. 1, pp. 289–298, 2000.
- [106] D. Sankhala, S. Muthukumar, and S. Prasad, “A Four-Channel Electrical Impedance Spectroscopy Module for Cortisol Biosensing in Sweat-Based Wearable Applications,” *SLAS Technol. Transl. Life Sci. Innov.*, vol. 23, no. 6, pp. 529–539, 2018.
- [107] R. J. McEnroe, M. F. Burritt, and D. M. Powers, *Interference testing in clinical chemistry; approved guideline*. CLSI, 2005.
- [108] M. A. Bujang and N. Baharum, “Sample Size Guideline for Correlation Analysis,” *World J. Soc. Sci. Res.*, vol. 3, no. 1, p. 37, 2016, doi: 10.22158/wjssr.v3n1p37.
- [109] Y.-C. Chuang, V. Tyagi, R.-T. Liu, M. B. Chancellor, and P. Tyagi, “Urine and serum C-reactive protein levels as potential biomarkers of lower urinary tract symptoms,” *Urol. Sci.*, vol. 21, no. 3, pp. 132–136, 2010.

## BIOGRAPHICAL SKETCH

Badrinath Jagannath is a doctoral candidate in the department of Bioengineering at The University of Texas at Dallas. He completed his bachelor's in Electronics and Instrumentation Engineering and obtained a Master of Science degree in Biomedical Engineering from Arizona State University in 2015 before joining Dr. Shalini Prasad's lab at UT Dallas. His research interests include developing wearable and point-of-care devices for precision health. His current research focuses on developing wearable sensors for real-time monitoring of upper respiratory infections and inflammatory bowel disease non-invasively from sweat. Badri currently has 17 peer-reviewed publications among which two of the publications have been highly recognized as one of the Top 10 articles in Nature Scientific Reports and Inflammatory Bowel Diseases journals. He has received several awards and fellowships for his research work including the prestigious Baxter Young Investigator Award. Badri has given podium presentations at various conferences and has also been an invited Plenary speaker for his work on wearable diagnostics. His research work on infection monitoring wearable sensor has received a lot of recognition and was recently featured at the 2021 ACS conference.

# CURRICULUM VITAE

## Badrinath Jagannath

### PhD, Bioengineering

The University of Texas at Dallas, Richardson, USA

Jan 2016- Present

*Advisor:* Prof. Shalini Prasad, Department Head, Bioengineering

### MS, Biomedical Engineering

Arizona State University, Tempe, USA

2015

### Bachelor of Technology, Electronics & Instrumentation Engineering

Jawaharlal Nehru Technological University, Hyderabad, India

2013

## HONORS, AWARDS AND ACHIEVEMENTS

- **Plenary Speaker**, 4<sup>th</sup> Biosensors & Bioelectronics Conference 2021
- **Top 10 Best in Basic Science**, Inflammatory Bowel Diseases journal 2021
- **Bioengineering Graduate Research Productivity Award**, UT Dallas 2019
- **Tony B. Travel Award**, SLAS, (50 awardees chosen from 12 countries) 2019
- **Mary and Richard Templeton Fellowship**, University of Texas at Dallas 2018
- **Best presentation award**, ASM conference 2018
- Accolades: **Top 10 articles in Nature Scientific Reports** (Chemistry section) 2018
- **Travel Grant Award**, The Electrochemical Society 2018
- **Jonsson Family Graduate Fellowships**, University of Texas at Dallas 2017

## PUBLICATIONS

1. Sankhala, D., Pali, M., Lin, K. C., **Jagannath, B.**, Muthukumar, S., & Prasad, S. (2021). Analysis of bio-electro-chemical signals from passive sweat-based wearable electro-impedance spectroscopy (EIS) towards assessing blood glucose modulations. arXiv preprint arXiv:2104.01793.
2. Pali, M., **Jagannath, B.**, Lin, K. C., Sankhala, D., Upasham, S., Muthukumar, S., & Prasad, S. (2021). Tracking metabolic responses based on macronutrient consumption: A comprehensive study to continuously monitor and quantify dual markers (Cortisol and Glucose) in human sweat using WATCH sensor. Bioengineering & Translational Medicine, <https://doi.org/10.1002/btm2.10241>.
3. Pali, M., **Jagannath, B.**, Lin, K. C., Sankhala, D., Upasham, S., Muthukumar, S., & Prasad, S. (2021). CATCH (Cortisol Aptamer WATCH): ‘Bio-mimic alarm’ to track Anxiety, Stress, Immunity in human eccrine sweat. *Electrochimica Acta*, 138834.
4. **Jagannath, B.\***, Lin, K. C.\* , Pali, M.\* , Sankhala, D., Muthukumar, S., & Prasad, S. (2021). Temporal profiling of cytokines in passively expressed sweat for detection of infection using wearable device. *Bioengineering & Translational Medicine*, e10220.
5. Upasham, S., Banga, I. K., **Jagannath, B.**, Paul, A., Lin, K. C., Muthukumar, S., & Prasad, S. (2020). Electrochemical Impedimetric Biosensors, Featuring the Use of Room

Temperature Ionic Liquids (RTILs): Special Focus on Non-Faradaic Sensing. Biosensors and Bioelectronics, 112940

6. **Jagannath, B.**, Pali, M., Lin, K-C., Muthukumar, S., & Prasad, S. (2020). A Sweat Based Wearable Enabling Technology for Real-Time Monitoring of Inflammatory Bowel Disease Biomarkers. *Inflammatory Bowel Diseases*, 26(10), 1533-1542.
7. Bhide, A., **Jagannath, B.**, Tanak, A., Willis, R., & Prasad, S. (2020). CLIP: Carbon Dioxide testing suitable for Low power microelectronics and IOT interfaces using Room temperature Ionic Liquid Platform. *Scientific reports*, 10(1), 1-12.
8. Tanak, A. S., **Jagannath, B.**, Tamrakar, Y., Muthukumar, S., & Prasad, S. (2019). Non-faradaic electrochemical impedimetric profiling of procalcitonin and C-reactive protein as a dual marker biosensor for early sepsis detection. *Analytica Chimica Acta: X*, 3, 100029.
9. Rice, P., Upasham, S., **Jagannath, B.**, Manuel, R., Pali, M., & Prasad, S. (2019). CortiWatch: watch-based cortisol tracker. *Future science OA*, 5(9), FSO416.
10. **Jagannath, B.**, Muthukumar, S., & Prasad, S. (2018). Electrical double layer modulation of hybrid room temperature ionic liquid/aqueous buffer interface for enhanced sweat based biosensing. *Analytica chimica acta*, 1016, 29-39.
11. Kamakoti, V., Kinnamon, D., Choi, K. H., **Jagannath, B.**, & Prasad, S. (2018). Fully electronic urine dipstick probe for combinatorial detection of inflammatory biomarkers. *Future Science OA*, (0), FSO301.
12. Kamakoti, V., Shanmugam, N. R., Tanak, A. S., **Jagannath, B.**, & Prasad, S. (2018). Investigation of molybdenum-crosslinker interfaces for affinity based electrochemical biosensing applications. *Applied Surface Science*, 436, 441-450.
13. Bhide, A., **Jagannath, B.**, Graef, E., & Prasad, S. (2018). A Robust Electrochemical Humidity Sensor for the Detection of Relative Humidity Using Room Temperature Ionic Liquid (RTIL) for Integration in Semiconductor IC's. *ECS Journal of Solid State Science and Technology*, 7(7), Q3043-Q3048.
14. Graef, E. W., **Jagannath, B.**, Munje, R., & Prasad, S. (2018). Fluorinated Anionic Room Temperature Ionic Liquid-Based CO<sub>2</sub> Electrochemical Sensing. *IEEE Sensors Journal*, 18(9), 3517-3523.
15. Bhide, A., **Jagannath, B.**, Graef, E., Willis, R., & Prasad, S. (2018). Versatile Duplex Electrochemical Sensor for the Detection of CO<sub>2</sub> and Relative Humidity Using Room Temperature Ionic Liquid. *ECS Transactions*, 85(13), 751-765.
16. Upasham, S., Tanak, A., **Jagannath, B.**, & Prasad, S. (2018). Development of ultra-low volume, multi-bio fluid, cortisol sensing platform. *Scientific reports*, 8(1), 1-12.
17. Lin, K. C\*, **Jagannath, B.\***, Muthukumar, S., & Prasad, S. (2017). Sub-picomolar label-free detection of thrombin using electrochemical impedance spectroscopy of aptamer-functionalized MoS<sub>2</sub>. *Analyst*, 142(15), 2770-2780.
18. Munje, R. D., Muthukumar, S., **Jagannath, B.**, & Prasad, S. (2017). A new paradigm in sweat based wearable diagnostics biosensors using Room Temperature Ionic Liquids (RTILs). *Scientific reports*, 7(1), 1950.